A study on DNA Topoisomerases during neuronal aging *in vitro* and *in vivo*

Submitted for the award of Ph.D. degree (Biochemistry) to the University of Hyderabad

By

M. UDAY BHANU

(Enrollment No: 06LBPH03)

Department of Biochemistry

Supervisor: Prof. Anand K. Kondapi
Department of Biotechnology &
Department of Biochemistry
School of Life Sciences
University of Hyderabad
Hyderabad-46, A.P., INDIA

August 2010

University of Hyderabad
School of Life Sciences
Department of Biochemistry
Hyderabad- 500 046, (AP), INDIA

DECLARATION

I hereby declare that the work presented in my thesis is entirely original and was carried out by me in the Department of Biochemistry, University of Hyderabad, under the supervision of Prof. Anand K. Kondapi. I further declare that this has not been submitted before for the award of degree or diploma from any Institute or University.

Date:

Place: **M. UDAY BHANU**

University of Hyderabad
School of Life Sciences
Department of Biochemistry
Hyderabad- 500 046, (AP), INDIA

CERTIFICATE

This is to certify that thesis entitled "**A study on DNA Topoisomerases during neuronal aging *in vitro* and *in vivo*"** submitted to the University of Hyderabad by **Mr. M. UDAY BHANU** for the degree of Doctor of Philosophy, is based on the studies carried out by him under my supervision. This work has not been submitted before for the award of degree or diploma from any University or Institution.

Prof. Anand K. Kondapi
Supervisor

Head, Department of Biochemistry

Dean, School of Life Sciences

Date:

ACKNOWLEDGEMENTS

First and foremost I offer my sincerest gratitude to my supervisor, Prof Anand K. Kondapi, who has supported me throughout my work with his patience and knowledge whilst allowing me the room to work in my own way.

I am highly thankful to Prof M. Ramanadham Dean and Prof A. S. Raghavendra, former Dean , School of Life sciences, Prof. Ramaiah Head, Dept of Biochemistry, for giving me the opportunity and necessary facilities to carry out my work.

I thank all the faculty members of Life Sciences for cooperation and their extended help during my work.

I extend me special thanks to Prof. N. Siva Kumar whose lab has been my second working lab all through my research carrer.

I thank CIL staff members Mr. Murthy , Rama Devi, Nalini for their help in confocal microscope.

I thank non-teaching staff members Lallanji, Naik and non-teaching staff who had helped me in differentendeavors of my work.

I thank my lab mates Raj kumar, Kanna, Bhaskar, Preeti, Upendar, Kishore, Anil, Sarada, Srinivas, Satish, Farhan, Sreenu, Bhanu, Chandra for their co-operation, support and cheerful nature all through my research.

And especially my best friends Kiran and Apparao for their constant support in all fronts.
Fellowship from ICMR and UGC-CSIR during this tenure is greatly acknowledged.

I wish to express my deepest gratitude and reverence to my parents, my brother, my wife and my daughter Sumedha for helping me to choose and withstand to this career...

Lastly, I offer my regards and blessings to all of those who supported me in any respect during my work.

Uday....

ABBREVIATIONS

Mg	: Microgram
µl	: Microlitre
µM	: Micromolar
mM	: Millimolar
ATP	: Adenosine tri phosphate
ALP	: Alkaline Phosphatase
BCIP	: 5- bromo – 4 – chloro – 3 indoyl phosphate
Bis-acrylamide	: *N*,*N'*- methylene –bis –acrylamide
bp	: Base pairs
BSA	: Bovine serum albumin
cDNA	: Complementary DNA
CO_2	: Carbon dioxide
Cpt	: Camptothecin
EMEM	: Eagle's Minimum Essential Media
DMSO	: Di methyl sulphoxide
DNA	: Deoxy ribonucleic acid
DNase I	: Deoxy ribonuclease I
dNTPs	: Deoxynucleotidetriphosphates
dsDNA	: Double-stranded DNA
DSBs	: Double Strand Breaks
DTT	: Dithiothreitol
EDTA	: *N*-*N*- Ethylene di amine tetra acetic acid
ENU	: *N*-ethyl-*N*-nitrosourea
EtBr	: Ethidium bromide
FBS	: Fetal Bovine Serum
HCl	: Hydrochloric acid
IgG	: Immunoglobulin G
Kb	: Kilo basepairs
kDa	: Kilo daltons
Mab	: Monoclonal antibody

mg	: milligrams
$MgCl_2$	: Magnesium chloride
min	: Minutes
ml	: Millilitre
mRNA	: Messenger RNA
MTT	: 3-(4,5-dimethylthiozol-2-yl)-2,5-diphenyltetrazolium bromide
Na_2HPO_4	: Disodium hydrogen phosphate
NaCl	: Sodium chloride
NC	: Nitrocellulose membrane
PAGE	: Poly acrylamide gel electrophoresis
PBS	: Phosphate buffer saline
PCR	: Polymerase chain reaction.
PMSF	: Phenylmethylsulphonyl fluoride
RNA	: Ribonucleic acid
RNAi	: RNA mediated interference
RNase	: Ribonuclease
rNTPs	: Ribonucleotide tri-phosphate
rpm	: Revolutions per minute
RT	: Reverse transcriptase
SDS	: Sodium dodecyl sulphate
siRNA	: Small interference RNA
SSBs	: Single Strand Breaks
TE buffer	: Tris-ETDA buffer
TEMED	: *N'*,*N'*,*N'*,*N'*- tetra methyl ethylene diamine
TRIS	: Tris (hydroxy methyl) amino methane

Contents

CHAPTER -1

Introduction

Natural Aging:

Aging is a phenomenon that occurs in every living organism and can be defined as a diminishing of normal physiological functions, being a progressive, deleterious and irreversible process, leading ultimately to death. During aging, it has been reported to have higher level of reactive intermediates. These intermediates can cause damage to bio molecules viz., DNA, proteins, lipids, thus to cells leading to their functional variation (Bokov et al., 2004). These changes occur little by little and progress inevitably over time. However, the rate of the progression of such damage can be very different from person to person. Diseases of old age (diseases which increase in frequency with age, such as arthritis, osteoporosis, heart disease, cancer, Alzheimer's Disease, etc.) are often distinguished from aging *per se*.

Aging depends on several processes that may interact simultaneously and may operate at many levels of functional organization (Franceschi et al., 2000). Research in aging is beginning to find out the reasons for these changes and the genetic and environmental factors that control them.

Theories of aging:

It is not easy to explain the aging process, because even though aging phenomena is universal, it does not affect all living beings in the same way (Finch, 1990). Why some animals live longer than others and show fewer signs of aging is still unknown. Over the years, scientific researchers have put forth several theories of aging. Some of the most commonly applied theories of aging are the programmed and structural damage theories of aging (Brian and Poala, 2003).

Programmed theories:

Programmed theories of aging engage the concept that aging and death are the inevitable consequence of the workings of an internal biological clock, programmed

at conception that decides when cells can no longer operate and reproduce at a rate sufficient to maintain health.

Structural damage theories:

Structural damage theories of aging are concerned with the molecular damage that accumulates inside cells over time.

Wear and Tear Theory:

Posed by Weismann (1982), the theory postulates that the daily grind of life, in particular abuse or overuse, literally wears the body out, leading to disease states. The degeneration of cartilage and eventual grinding of bone on bone is an example of the aging process on body joints, as wear and tear exceeds the body's ability to repair.

Waste Accumulation Theory:

This theory proposes that, as one age, cells accumulate waste products as a consequence of normal metabolic processes in the cells (Katz et al., 1984). It is believed that this build-up of toxic "sludge" eventually compromises normal cell functions. Lipofuscin pigments or liver spots, common on aging skin, are an example of this waste material. The brownish pigments consist of oxidized rancid fats that accumulate in the skin, as well as in the internal organs of our body, as one age (Brunk and Terman 2002 ; Terman 2001).

Error Catastrophe Theory:

Orgel, (1963) proposed that maintenance of the structural integrity of DNA is critical not only for cell survival but also for the transfer of correct genetic information to daughter cells. Alterations in the fidelity of DNA polymerase alpha could result in a

progressive degradation in information transfer during DNA synthesis, which would eventually affect a wide range of cellular components during aging (Orgel, 1963 and Orgel, 1973). In other words transcription and translation introduces errors into individual proteins at a much higher rate than replication introduces mutations into DNA suggesting that cellular aging involves accumulation of error-containing enzymes as a result of an inherent inaccuracy of the transcriptional and protein synthesizing machinery. One mechanism for the introduction of such errors would be decreased fidelity of DNA polymerases during repair activity or cell division.

Immune-suppression Theory:

In 1962, Walford proposed this theory. According to the "immune-suppression theory of aging", many aging effects are due to the declining ability of the immune system to differentiate "foreign" from "self" proteins. Not only does the immune system become less capable of resisting infection & cancer, but declining cell function could be due to attacks by the immune system against native tissues. Arthritis, psoriasis and other autoimmune diseases increase with age (Walford, 1962). It is well known that the thymus gland, or gland of youth, which is located at the base of the throat, declines in size from infancy to adulthood. The thymus is known to play a role in the auto-immune system, the body’s primary defence against disease. Age-related reduction in the size of the thymus appears to correspond to reduction in our immune systems, suggesting that the thymus may play a significant role in the aging process (Burnet 1970).

DNA damage Theory:

According to this theory, the aging process is, in part, caused by damage to the genetic structure of the DNA, the genetic blueprint of our cells and that aging is a consequence of unrepaired DNA damage accumulation. Damage in this context includes chemical reactions that mutate DNA and/or interfere with DNA replication. Although both mitochondrial and nuclear DNA damage can contribute to aging,

nuclear DNA is the main subject of this analysis. Nuclear DNA damage can contribute to aging either indirectly (by increasing apoptosis or cellular senescence) or directly (by increasing cell dysfunction) (Best, 2009).

Molecular Cross-linkage Theory:

Postulated back in 1942 by Johan Bjorksten, the theory advances the thought that molecular cross-linking between protein molecules, such as the collagen found in our skin, tendons, ligaments and the glycation (cross-linking) of other structural proteins and lipids (fats) with excess glucose, disrupts the functions of these molecules, leading to acceleration of the aging process. Glycation is one of the likely reasons that diabetics, who have chronically high levels of blood sugar (glucose), exhibit accelerated aging (Bjorksten, 1955, 1971).

But, the most widely accepted structural damage theory and the one theory that encompasses all of the previous theories - is the Free Radical Theory of aging.

The Free radical Theory:

In 1956, Harman suggested that free radicals produced during respiration cause cumulative oxidative damage, resulting in aging and death (Harman, 1952, 1956, 1993, 1995 and 1998). The central nervous system (CNS) is especially sensitive to oxidative stress (Aksenova et al., 2005). One reason for this is that in humans the brain accounts for twenty percent of the body's oxygen consumption (not proportional to its size compared to other body parts). Another reason is that the brain has less capacity for cellular regeneration than other organs. Free radicals are highly reactive molecules or atoms that have an unpaired electron in an outer orbital that does not contribute to molecular bonding (Halliwell and Gutteridge, 1989). Atoms or small molecules that are free radicals tend to be the most unstable, because larger molecules can have the capacity to form resonance structures. Under normal physiological O_2 levels, 1-2% of the O_2 consumed is converted to reactive oxygen species (ROS) for

biological systems, oxygen free radicals are the most important, in particular superoxide (.O_2 -), nitric oxide (.NO) and the hydroxyl radical (.OH).

The targets of endogenous oxidants are the macromolecules such as nucleic acids, lipids, sugars, and proteins are susceptible to free radical attack (Mehlhorn, 2003). Nucleic acids can get additional base or sugar group; break in a single and double-strand fashion in the backbone and cross link to other molecules. The most prominent oxidative modification of DNA and RNA bases is formation of 8-hydroxydeoxyguanosine (Sohal et al., 1994). ROS-induced DNA damage consists primarily of single strand breaks (SSBs), double strand breaks (DSBs), at sites of base loss [apurinic/apyrimidinic (AP) sites], and base lesions (Collins et al., 1995).

Lipids form peroxides and aldehydes under oxidative stress conditions, which further affect membrane fluidity and disrupt membrane bound proteins. Protein targets for free radicals are peptide bonds or sidechains (Huggins et al., 1993). ROS are responsible for deamidation, racemization, and isomerization of protein residues as well as formation of carbonyl groups (Stadtman and Berlett 1998). These chemical modifications result in protein cleavage, aggregation and/or loss of catalytic and structural function by distorting the proteins secondary and tertiary structure (Stadtman, 1998).

At present, there is an increasing amount of evidence showing the positive correlation between oxidative stress and aging. Oxidative damage increases and lifespan decreases with oxygen concentration; indeed animals subjected to hyperoxia have higher oxidation of lipids, proteins and DNA (Agarwal and Sohal, 1994).

Brain aging:

Brain aging could be considered as process where repair mechanisms are declining in ability and efficiency, but it should be distinguished from a state of disease. It has been shown that during brain aging increased oxidative stress and the accumulation of damaged molecules promote dysfunction of different metabolic and signaling pathways (LeBel and Bondy, 1992) as well as energy deficits. Signaling mechanisms such as gene transcription (Lee et al., 2000), calcium homeostasis (Mattson, 1992), unfolded protein responses, problems in protein folding, phosphorylation and dephosphorylation (Jin and Saitoh, 1995) are some of the processes that change during brain aging. Importantly, basic processes involved in aging of the central nervous system contribute to several prevalent neurodegenerative diseases like Alzheimer's disease (AD) and Parkinson's disease (PD) (Maccioni et al., 2001). The aging brain is characterized by several age-related alterations. On the molecular and cellular level, an important aspect of the aging process of the brain is an increased production of free radicals and an accumulation of nuclear (n) and mitochondrial (mt) DNA damage (Johnson et al., 1999 and von Zglinicki et al., 2001). This is accompanied by an age-related decline in the amount of nDNA repair (Schmitz et al., 1999; von Zglinicki et al., 2001). Neuropathological studies indicate that shrinkage of the brain, loss of neurons and the presence of specific intracellular and extracellular protein aggregates, in age-related findings (Schochet, 1998). However, it has been shown over the last years that markers of these age-related alterations vary significantly between different brain regions, as well as between different types of neurons (Mandavilli and Rao, 1996; Melov et al., 1999; Lee et al., 2000; Morrison and Hof, 2002). As the brain consists of various types of neurons with different morphologic, physiologic and functional features **(Fig 1.1)**, it is of great importance to investigate the aging brain in a celltype- specific manner. There components are.

Fig 1.1

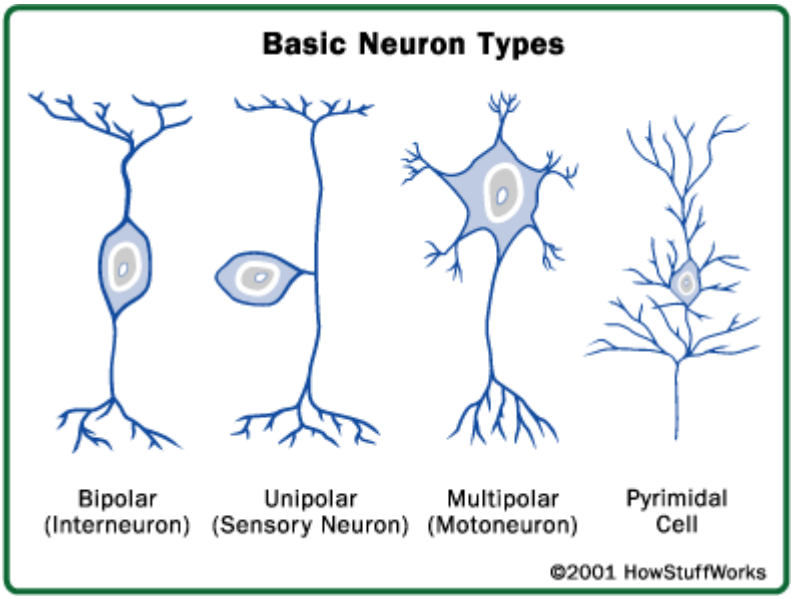

- **Sensory neurons** carry signals from the outer parts of the body (periphery) into the central nervous system.
- **Motor neurons** (motoneurons) carry signals from the central nervous system to the outer parts (muscles, skin, glands) of the body.
- **Receptors** sense the environment (chemicals, light, sound, touch) and encode this information into electrochemical messages that are transmitted by sensory neurons.
- **Interneurons** connect various neurons within the brain and spinal cord.

Age-related neurodegenerative diseases:

Neurodegenerative is a term that covers a wide range of diseases that result in the loss of nervous system function. Included are: Parkinson's Disease, Alzheimer's, Huntington's, Creutzfelt- Jakob disease, and many others. The neurodegenerative diseases are often age associated, chronic, progressive, and without known treatments. Recent investigations in medical genetics have identified specific genes for several neurodegenerative disorders. Better understanding of molecular basis of the processes involved in their pathology and their relation to aging (not absolute, but remarkable) should help in curing these diseases.

Alzheimer's disease:

Alzheimer's is the most common form of dementia. More than 12 million people worldwide have AD, and it accounts for the majority of cases of dementia diagnosed in patients over the age of 60 (Citron, 2004). The pathogenesis of this disease involves altered proteolytic processing of the β-amyloid precursor protein (APP) resulting in increased production of a long (42 amino acid) form of the amyloid β (Aβ) peptide, which in turn aggregates and forms insoluble plaques in the brain. These aggregates generate ROS which in turn disrupt cellular ion homeostasis, energy metabolism (Mattson, 1997) and neuronal synapses and makes cells more prone to apoptosis or excitotoxicity. Neurofibrillary tangles are another hallmark of AD. These tangles accumulate inside cells and have hyperphosphorylated tau protein as their main constituent. The link between tau and amyloid pathology in AD is not yet clear, nor is the link between age-related accumulation of tau or amyloid and their contribution to AD. Oxidative stress is implied as a causal factor of AD. Diets enriched in antioxidants show an improved learning and memory and a reduction of plaque load in aged canines (Milgram et al., 2004). Current therapies for patients with Alzheimer's disease only ease symptoms, providing temporary improvement and slowing the reduction rate of cognitive decline. Progress in identifying molecular mechanisms of AD should help in future to delay onset or modify the progression of this disease.

Parkinson's disease:

Parkinson's disease is a progressive neurodegenerative disorder, which is characterized by motor symptoms such as tremor, postural imbalance, and slowness in movements. As it progresses, it can lead to psychiatric and cognitive dysfunctions such as anxiety, depression and dementia. It affects at least 1% of population over 65 and 4-5% of those over 85 years of age (Lang and Lozano, 1998). The main hallmark of this disorder is a loss of dopaminergic neurons in the *substancia nigra pars compacta*, which results in depletion of dopamine in the striatum, to which these neurons project. The cellular pathological hallmarks of PD are round eosinophilic

intracytoplasmatic protein-containing inclusions – Lewy bodies and dystrophic neurites (Forno, 1996). So far, PD has been shown to be sporadic in the majority of cases and has been linked to environmental risk factors (toxins, oxidative stress, mitochondrial dysfunction). On the other hand hereditary PD has been linked to mutations in α-synuclein, parkin (Polymeropoulos et al., 1997; Kitada et al., 1998), then PINK1 (Valente et al., 2004), DJ-1 (Bonifati et al., 2002), and LRRK2 (Zimprich et al., 2004). Understanding more about the almost absolute dependence of PD on aging, the mutations that cause familial PD, and the circumstances which increase the risk of developing PD will help to provide therapeutic approaches for this serious disease.

Neuronal cell death in aging:

It has been long assumed that aging is associated with a loss of neurons throughout all regions of the brain, and that this loss of neurons would explain the functional decline of the brain during aging (Wickelgren, 1996 ; Victor, and Ropper, 2001). The death of neurons is one of the forces that shape the development of the central nervous system (CNS). Neurons establish contact with their targets during development and refine it throughout their life. In the mature nervous system, most neurons are post mitotic cells and cannot be easily replaced by cell renewal. For this reason, the death of neurons in the adult CNS is a phenomenon more severe than in other tissues: the number of mature neurons in adult is primarily dependent on the extent of neuronal survival and their decline in the old age is an important event. In addition, increasing neuronal death induced by damaging insults is also a major risk factor of neurodegenerative disorders and aging. The underlying causes of the various neurodegenerative diseases are not clear; death of neurons and loss of neuronal synapses are key pathological features.

Explaining molecular events that control neuronal cell death is critical for the development of new strategies in helping to prevent and treat neurodegenerative diseases and aging. Neuronal tissues are not proliferative and are not replaced by new

cells for the lifetime in most brain regions except in regions such as the olfactory bulb and dentate gyrus of the hippocampus, where there is a constant replacement of neurons from a pool of progenitor (stem) cells (Gage, 2000, Rao and Mattson, 2001). However, even for these cells there is clear evidence that their replacement function is unlimited. During development there is an excess number of neurons which die in order to match the number of neurons with the size of their projection areas. This process is dependent on neurotrophins and conduction of action potentials as a marker of synaptic activity (Oppenheim, 1991). Due to neurondegeneration occurring during later phases of life, for example, loss of hippocampal and cortical neurons, results in symptoms of Alzheimer´s disease; death of midbrain neurons that use dopamine as a neurotransmitter causes Parkinson´s disease; loss of striatal neurons is the hallmark of Huntington´s disease; and death of lower motor neurons cause symptoms of amyotrophic lateral sclerosis.

Neuronal cell death occurs by necrosis or apoptosis. These two pathways have distinct molecular and biochemical mechanisms. In apoptosis, a stimulus activates a cascade of events where there is orchestrated destruction of the cell. In necrosis, by contrast, the stimulus (e.g., ischemia) is itself often the direct cause of the demise of the cell (Kanduc et al., 2002; Hengartner, 2000). Necrosis is considered as a pathological process in contrast to apoptosis, which is part of normal development, but the former also occurs in a variety of diseases. The morphologic features of apoptosis include nuclear and cytoplasmic condensation, internucleosomal DNA cleavage and packaging of the cell into apoptotic bodies that are engulfed by phagocytes, preventing release of intracellular components (Hengartner, 2001). Neuronal apoptosis usually occurs because of mitochondrial damage, hypoxia, UV-rays, increased ROS, etc. and it leads to cytochrome c release into the cytosol, with subsequent formation of apoptosome and the activation of effector caspases (caspase-3, -7). This is frequently referred to as the ‘intrinsic pathway’. The ‘extrinsic pathway’ is executed by ligand binding to death receptors of the tumour necrosis factor family inducing the activation of effector caspases like caspase-8 (Micheau and Tschopp, 2003; Cryns and Yuan, 1998). Understanding the mechanism of molecular events that

control neuronal cell death is critical for design and development of new strategies that help prevention and treatment of neurodegenerative diseases and also for monitoring aging process.

DNA Damage in Aging:

The DNA, due to its central role in life, was bound to be implicated in aging. One hypothesis is that damage accumulation to the DNA causes aging, as first proposed by physicist Leo Szilard (Szilard, 1959). The theory has changed marginally over the years as new forms of DNA damage and mutation are discovered, and several theories of aging argue that DNA damage or mutation accumulation causes aging.

The stability of the genome of all organisms is constantly challenged by endogenous and exogenous agents that induce DNA lesions, genome instability, DNA recombination and other types of genotypic stress. The nuclear and mitochondrial genomes of non-replicating cells of the brain are particularly vulnerable targets of DNA damage. DNA damage may have especially deleterious consequences in post-mitotic neuronal cells, because this cell pool is not normally regenerated by cellular proliferation (Bohr et al., 2007). Recent studies of patients with Alzheimer's disease, Parkinson's disease, amyotrophic lateral sclerosis, Friedreich's ataxia, Xeroderma pigmentosum (XP) and Huntington's disease suggest that oxidative stress and neuronal DNA damage are common features associated with these diseases (Kraemer et al., 2007; Trushina et al., 2007).

It is well-established that DNA mutations/alterations and chromosomal abnormalities increase with age in mice (Martin et al., 1985; Dolle et al., 1997; Vijg, 2000; Dolle and Vijg, 2002) and humans (Esposito et al., 1989 Lu et al., 2004). It is impossible, however, to tell whether these changes are effects or causes of aging. In addition, there is no consensus as to what type, if any, of DNA changes are crucial in aging. Correlations have been found between DNA repair mechanisms and rate of aging in

some mammalian species (Hart and Setlow, 1974; Grube and Burkle, 1992; Cortopassi and Wand, 1996). The association of human syndromes (Bloom's and Werner's) of accelerated aging with inherited mutations in DNA repair genes strongly implicates DNA damage in the aging process. These disorders, known as segmental progeroid syndromes, are characterized by accelerated onset of a subset of human aging phenotypes that frequently include neurodegeneration (Hasty et al., 2003). Mutations in genes involved in single- or double-strand DNA break repair result in cerebellar degenerative syndromes known as ataxias, which are manifested by movement disorders.

Mechanisms of DNA repair:

Many different types of DNA lesions exist. Most of these lesions are repaired by the base excision repair (BER) pathway (Seeberg et al., 1995). Nucleotide excision repair (NER), mismatch repair (MMR), direct reversal of damage, homologous recombination and non-homologous end-joining are other DNA repair path- ways that may also contribute to repair of some forms of oxidative DNA damage in neural cells (Wilson et al., 2007; Brooks, 2007).

BER is primarily responsible for repairing single strand breaks (SSBs) by removing small DNA base modifications caused by alkylation, deamination and oxidation of nuclear and mitochondrial DNA (Seeberg et al., 1995). These DNA lesions accumulate over time in the genomes of experimental animals and are thought to be by-products of normal metabolic processes. Recent studies show that BER is active in neuronal cells in culture, in brain cells in experimental animal models and in human postmortem brain tissue and also been characterized in aging and/or diseased brain regions (Weissman et al., 2007). The role of DNA double-strand breaks (DSBs) in the aging of the brain is just beginning to be explored. DSBs are repaired by two major pathways: homologous recombination, which occurs during DNA replication, and nonhomologous end joining (NHEJ), the predominant pathway in postmitotic cells such as neurons. NHEJ is mediated by a number of core factors, four of which are

highly conserved from yeast to mammals, including Ku80, Ku70, Ligase IV, and XRCC4 (Lombard et al., 2005). Targeted knockouts of the NHEJ factors in mice result in embryonic lethality, genomic instability, and apoptosis of neurons in the brain soon after postmitotic differentiation. More recently even Topo II beta has been shown to be associated with the core NHEJ proteins (Bong-Gun J et al.,2006) suggesting a role of Topo II beta in NHEJ activity. Unpublished data from our lab show that there is lack of NHEJ activity in Topo II beta down regulated cells. A clear relationship has been established between increased DNA damage, defective DNA repair with aging and age-associated neurodegenerative disease (Bohr et al., 2005; Rao, 2006; de Souza-Pinto and Bohr, 2002; Vijg et al., 2005).

DNA Topoisomerases in development, brain and aging:

DNA Topoisomerases are a class of enzymes involved in the regulation of DNA supercoiling. These enzymes play a crucial role in DNA transcription, replication and recombination, though the exact mechanism still needs to be understood. During DNA replication, the two strands of the DNA must get completely delinked by Topoisomerases, and during transcription, the translocating RNA polymerase generates super coiling tension in the DNA that should get released (Wu et al., 1988; Wang 1998). DNA Topoisomerases resolve the entangled DNA intermediates by transiently cleaving one or two DNA strands and passing through the nick of another intact strand(s). Subsequently, the enzymes rejoin the DNA break and complete one round of catalytic cycle (Vosberg**,** 1985; Wang, 1987, 1996; Champoux, 2001). Based on their catalytic mechanism, Topoisomerases have been categorized into four subfamilies, type IA, IB, type IIA and IIB (Wang, 1996).

Type I Topoisomerases:

Type I enzymes are further classified into two families on the basis of their biochemical properties: type IA enzymes form a transient covalent bond to the 5’ phosphoryl of the broken strand, whereas type IB enzymes form a 3’-end covalent

bond. Members of the same family share significant sequence similarities and are structurally related (Mondragon & DiGate, 1999). The type IA family of topoisomerases, which includes topoisomerases I and III (Hanai et al., 1996) and thermophilic reverse gyrases (Confalonieri et al.,1993), are widespread in nature and not confined to prokaryotes solely.

Topoisomerase I:

All higher eukaryotes contain at least one type I Topoisomerase enzyme that plays a major role in supporting fork movement during replication and also in facilitating relaxation of transcription-related super coils. Topoisomerase I (Topo I) is indispensable during processes leading to cell development and also during cell division (Lee et al., 1993). Inactivation of Topo I affects the rate of transcription in *S. cerevisiae* **(**Di Mauro et al., 1993). Experiments with yeast Topo I mutants show that for cell growth Topo I is not indispensable (Uemura and Yanagida, 1984; Thrash et al., 1985). This is not the case with *Drosophila melanogaster*, in which Topo I is essential for development during post blastocyst stage (Lee et al., 1993).

Topo I is a crucial enzyme for cell growth and embryo development (Morham et al., 1996). Mammalian Topo I belongs to type IB subfamily. It plays key roles in DNA replication, transcription, and recombination. The members of the type IB subfamily of Topo I share no sequence or structural homology with other known Topoisomerases (Caron and Wang, 1994) and are functionally distinct from the members of the type IA subfamily. The activity and level of Topo I is age as well as gender-dependent, it increases from birth to maturity and then decreases, more significantly in males, with senescence. This shows a possible role of Topoisomerase I activity and regulation in various brain functions (Plaschkes et al., 2005).

Topoisomerase III:

Mammalian DNA topoisomerase III belongs to the type IA subfamily whose members also include bacterial DNA topoisomerases I and III, yeast DNA topoisomerase III, and the enzyme "reverse gyrase" found in hyperthermophiles (Caron and Wang, 1996).

In mammals, there are two isozymes (α and ß) of DNA topoisomerase III, which share an identity of 36% in their amino acid sequences. The two human isozymes show distinct tissue specificities, the α-isoform being predominantly expressed in the testes and the ß form in the ovaries, mice deficient in DNA topoisomerase III beta develop to maturity but show a reduced mean lifespan (Kwan and Wang, 2001). Deletion of the *top3* gene in fission yeast is lethal (Goodwin et al., 1999; Maftahi et al., 1999), which resembles a situation in higher eukaryotes, where a disruption of the gene encoding topo III*α* in mice causes embryonic lethality (Li and Wang 1998).

It has been shown in a study using *top3α*- embryos of mouse that cellular function of topoisomerase III*α* can neither be substituted by its putative variant, DNA topoisomerase III ß , nor by the three other DNA topoisomerases I, II*α*, and IIß (Li and Wang, 1998**)**. Thus, the precise cellular function of mammalian DNA topoisomerase III*α* remains enigmatic**.**

Type II Topoisomerases:

Similar to Type I Topoisomerases there are two subclasses of type II topoisomerases, type IIA and IIB. Type IIA topoisomerases include the enzymes DNA gyrase, eukaryotic topoisomerase II (topo II), and bacterial topoisomerase IV (topo IV). These enzymes span all domains of life and are essential for function. Type IIB topoisomerases are structurally and biochemically distinct, and comprise a single family member, topoisomerase VI (topo VI). Type IIB topoisomerases are found in

archaea and some higher plants. The two classes of topoisomerases share a similar strand passage mechanism and domain structure, however they also have several important differences. Type IIA topoisomerases form double-stranded breaks with four-base pair overhangs, while type IIB topoisomerases form double-stranded breaks with two base overhangs (Buhler et al., 2001). A number of studies in yeast have shown that DNA topoisomerase II is essential for chromosome condensation and disjunction during mitosis at the metaphase/anaphase transition and meiosis (Galande and Muniyappa, 1996). DNA topoisomerase II is essential in proliferating cells and is a major target for many anticancer drugs (Bakshi et al., 2001; Wang et al., 2001).

Topoisomerase II:

Mammalian cells express two genetically distinct isoforms of DNA topoisomerase II, designated as topoisomerase II*α* and topoisomerase IIß. DNA topoisomerase IIα is known to be essential for cell proliferation, since some mitotic events such as condensation and segregation of daughter chromosomes are entirely dependent on its activity (Nitiss, 2009). It is also likely to be involved in other DNA transactions like DNA replication, transcription, and recombination. The two isoforms of topo II, the 170 kD topo α and the 180 kD topo II β present in mammals have conserved catalytic activities. But the exact roles shared by these enzymes are unknown. Topoisomerase IIβ protein differs from Topoisomerase II α in many important aspects. The genes coding for the Topoisomerase II α and β proteins map to chromosomes 17q21-22 and 3p24 and are clearly distinct. Topoisomerase II β protein is less sensitive to inhibition by intercalating agents and epipodophillotoxins than the α protein.

Topoisomerase II α activity is shown to be highest during the G_2/ M phase of the cell cycle (Heck et. al., 1988). Whereas Topoisomerase II β is constant throughout the cell cycle (Woessner et. al., 1991). Topoisomerase II α is distributed in the nucleoplasm (Woessner et. al., 1990) in contrast to Topoisomerase II β, which is localized in the nucleolus during interphase, and in the cytoplasm during mitosis (Negri et. al., 1992).

Both the isoforms show different patterns of tissue distribution. Topoisomerase II α is shown to be higher in testes, spleen, bone marrow and liver. The α-isoform is present in proliferating cells, while β-isoform is predominantly present in non-proliferating cells namely neurons suggesting its role in non-replicating functions of DNA (Tsutsui et al., 2001; Kondapi et al., 2004). The decreasing activity of topoII β with aging (Kondapi et al., 2004) points out to its possible role in DNA repair activity in neurons during aging.

DNA Topoisomerases

Enzyme	Type	Organism	Subunit size (kDa) & Composition	Catalytic Activity	Function
Bacterial Topoisomerase I (ω protein)	IA	Bacteria (e.g. *E. coli*)	97 Monomer	Relax only negative supercoils (ATP-independent)	Prevent hypernegative supercoiling of DNA during transcription.
Eukaryotic Topoisomerase I	IB	Eukaryotes (e.g. human)	91 Monomer	Relax both positive and negative supercoils. (ATP-independent)	Involved in DNA replication and transcription.
Eukaryotic Topoisomerase III	IA	Eukaryotes (e.g. human Topo III α & III β)	~ 91 Monomer	Relax only negative supercoils	Involved in recombination events of DNA.
DNA gyrase	IIA	Bacteria (e.g. *E. coli*)	A:97 and B:90 A_2B_2	Introduce negative supercoils into DNA. (ATP-dependent).	Allows bacterial DNA to have free negative supercoils and help in replication.
Eukaryotic Topoisomerase II	IIA	Eukaryotes (e.g. human Topo IIα)	174 homodimer	Relax but not supercoil DNA. (ATP dependent).	Topo IIα expression is tightly regulated in a cell-cycle-dependent manner.
	IIA	Eukaryotes (e.g. human Topo II β)	180 homodimer	Relax but not supercoil DNA. (ATP dependent).	Not regulated in a cell cycle dependent manner.
Bacterial Topoisomerase IV	IIA	Bacteria (e.g. *E. coli*)	C_2:84 and E_2:70 C_2E_2	Relax but not supercoil DNA. (ATP dependent).	---------

Cell culture as a model for aging:

Animal models used in aging research are chosen partially because of their short life spans. The use of short-lived animals for aging research assumes that there is relevance to the much longer human life span and that fundamental aging processes are conserved between species. Cell culture approaches make it easier and possible to study tissue-specific and cell-specific aging rather than using animal models which are complex.

The first aging experiments using cell cultures were carried out very early in the twentieth century. Carrell (1912) performed a series of experiments, where he dissociated cells from chicks, placed them in culture, and showed by subculturing that the cells were seemingly capable of proliferating indefinitely. The conclusion was that organismal mortality (and aging) was a consequence of multicellularity. The logic behind this equivalence, however, was faulty.

Cell cultures are widely used as models to study the molecular mechanisms of aging. Numerous studies performed on cultured human fibroblasts (Wistrom and Villeponteau, 1990), T lymphocytes (Pawelec et al., 1997), and several other types of mammalian cells (Augustin Voss et al., 1993; Peterson, 1995) demonstrated that normal dividing cells have a finite proliferation capacity *in vitro*. This phenomenon is interpreted as aging at the cellular level and is known as ‘‘replicative senescence’’ (Hayflick, 1998). Replicative senescence is limited to cells that have the ability to divide *in vivo*, and hence does not apply to postmitotic cells such as mature neurons or muscle. There are other mechanisms that lead cells into senescence, such as oxidative stress, double stranded DNA breaks, expression of certain oncogenes (e.g. activated RAS or RAF), modifications in chromatin structure or changes in energy metabolism (Campisi, 2001). However, a question remains whether investigation of replicative senescence will shed insight into the senescence of postmitotic differentiated cells (Cristofalo, 1996; Rubin, 1997). Several investigators suggested that the ‘‘stationary phase’’ cell cultures (Khokhlov, 1992; Rubin, 1997) might be a more advisable model to study mechanisms of aging of postmitotic differentiated cells.

Aging of neuronal cells *in vitro* was not described until the end of the twentieth century (Aksenova et al., 1999, Lesuisse and Martin, 2002, Toescu and Verkhratsky, 2000). Providing the optimal conditions over long period of time was the biggest obstacle. Hippocampal and cortical neurons have been described as being able to survive up to 60 days in culture (Aksenova, 1999, Lesuisse and Martin, 2002).

Cerebellar granule neurons (CGNs) constitute the largest homogenous neuronal population of mammalian brain. CGNs in culture are an interesting model to study cellular and molecular correlates of mechanisms of survival/apoptosis and neurodegeneration /neuroprotection (Contestabile, 2002). Previously, long-term cultures of CGNs were shown to survive *in vitro* for a maximum of 17 days (Ishitani et al., 1996). While, CGNs could be maintained for 23 divisions (days *in vitro*) in studies on the Ca^{2+} homeostasis related to aging (Toescu et al., 2000).

Rationale & Aim of the study:

There has been abundant amount of work done in order to understand the aging phenomena and age-associated degenerative diseases. Nevertheless, the causes of aging and age associated diseases (such as Parkinson's or Alzheimer's) are still unanswered. Understanding the mechanism of molecular events that control neuronal degeneration, cell death is critical for design and development of new strategies that help prevention and treatment of neurodegenerative diseases and aging process. Aging of the brain and neurodegenerative diseases share a common predisposing factor, which poses several basic questions. First, how can a neuron survive for years and remain functionally competent? Second, do neurons possess unique mechanisms for the repair of DNA and protein damage and protection against toxic free radicals? And finally, how and when do these quality control and repair systems break down? Studying neurodegenerative diseases or creating and studying aging model systems should help towards this goal.

The aim of this study is to investigate the molecular changes that occur during neuronal aging. This is addressed through developing an *in vitro* model of aging of cerebellar granule neurons (CGNs) of rats and understanding whether CGNs *in vitro* would mimic known features of aging as *in vivo*, under prolonged period in culture. The observation that young and old neurons have different DNA repair capacity and decreased levels of DNA topoisomerases with increasing age prompted us to characterize the possible molecular mechanisms involved in causing senescence. Therefore, the DNA repair capacity of neurons and its contribution to the neuronal degeneration caused by *in vitr*o aging of CGNs was characterized. The role of Topoisomerase I in neuronal development was analyzed using siRNA mediated knockout studies.

These aims were achieved through the following objectives:

1. Establishing Cerebellar granule neurons as *in-vitro* model of aging.
2. Analysis of Topoisomerases in *in-vitro* and *in-vivo* aging.
3. DNA Repair capacity of cultured CGNs; Topo II β, a potential marker.
4. Role of Topoisomerase I in neuronal development.

CHAPTER -2

Materials & Methods

Materials

Reagents:

Eagle's minimal essential medium (EMEM), non-essential amino acids, sodium pyruvate (Invitrogen, Carlsbad, CA), Fetal Bovine Serum (FBS, Lifetech). Oligonucleotides, Taq DNA polymerase, dNTPs (deoxy Nucleotide tri phosphates) (Integrated DNA Technologies, USA). Adenosine tri phosphate (ATP), phenylmethylsulfonyl fluoride (PMSF), Bovine serum albumin (BSA), leupeptin, pepstatin, aprotinin, Triton X 100, Trizol (TRI-REAGENT), dithiothreitol (DTT), ethyl nitroso urea (ENU), dimethyl sulfoxide (DMSO), (3-(4,5-Dimethylthiazol-2-yl)-2,5-diphenyltetrazolium bromide (MTT), camptothecin (Sigma Co., USA). Nitrocellulose membrane (NC) (PALL Life Sciences, USA), all other chemicals were from Sigma and SRL unless specified.

Kits:

Caspase-3 assay kit (BD Pharmingen, San Jose, CA, USA),
Annexin V -Vybrant apoptosis assay kit#3 (Invitrogen, USA),
Enhanced avian first strand synthesis kit (eAMV-RT,SIGMA).

Animals:

Wistar rats *(Rattus novergicus)*, provided by University Animal house facility (UOH, Hyd, INDIA). All experiments were performed in accordance with Institutional animal ethics committee recommendations and guidelines were followed to minimize pain and discomfort.

Age group:

Post natal 6-8 day rat pups, young (<10 days), adult (> 6 months) and old (> 18 months).

Primary neurons:

Primary cerebellar granule neuronal cultures were prepared from post natal 6 – 8 day old rat pups cerebellum.

Antibodies:

Mouse anti-human/rat Topoisomerase IIα and mouse anti-human/rat Topoisomerase IIβ were from Pharmingen group (Becton–Dickinson biosciences). Mouse anti-human/rat Topoisomerase I, mouse anti- Glial fibrilar acidic protein (GFAP) and Rabbit anti-Neurifilament-M chain (NF) were from Sigma. Rabbit anti-Topoisomerase IIIα and Rabbit anti- Topoisomerase III β were from Corgen. Inc. The secondary antibodies were purchased from UPSTATE, USA.

Methods

2.1 Isolation and culture of cerebellar granule neurons:

The preparation of cerebellar granule cells was based on a previously described method (Cambray-Deakin, 1995). Anesthetized D7 rat pups were decapitated. Cerebella were collected and washed with phosphate-buffered saline (PBS) at 4^0C. Cerebella were minced into 500 µm or smaller sections with a no. 11 scalpel blade. Minced tissue was incubated at room temperature for 10 min in trypsin-EDTA (0.05% trypsin, 0.53 mM EDTA; GIBCO). After trypsinization, the minced tissue was resuspended in 2 mL granule cell medium (Eagle's MEM with Earle's BSS, 2 mM glutamine (0.292 g/L), 10% heat-inactivated bovine serum (Lifetech), 6 mg/mL glucose, 25 mM KCl, 10 U/mL penicillin, 10 µg/mL streptomycin containing 0.05% DNase-I (final concentrations). The suspension was placed on ice and triturated through a fire-polished glass pipette with the minimal number of strokes needed to obtain a suspension of single cells. Three pipettes of decreasing tip diameters were used and the entire suspension was moved through each pipette tip 2-4 times and triturated slowly without appearance of any bubbles. Granule cells were plated in the presence of media that contains 10% fetal bovine serum. Cultures were incubated in a humidified atmosphere of 5% CO_2/95% air at 37°C.

Seeding density:

Cells were seeded at 10^6 cells / 35 mm Poly-L- Lysine (PLL) (Sigma) coated dishes, each dish containing 2 ml of granule media. Cultures were fed every 2-3 days by

replacing half the volume of media. 1µM arabinosylcytosine (SIGMA, USA) (mitotic inhibitor) was added to cultures for 2 days, during the first week after plating, to suppress the proliferation of mitotic non neuronal cells.

2.2 CGNs as long term culture:

Cultured CGNs were kept over the period of 7 weeks in culture. In order to maintain similar conditions in the culture medium 2/3rd of the media was replaced every 2 days until the cells were in culture. Cultures were split in to 1- 7 weeks to carry out experiments.

2.3 MTT assay for Cell viability:

The viability of granule neurons under prolonged period in culture was estimated by the redox activity of mitochondria in reducing MTT (3-(4,5-Dimethylthiazol-2-yl)-2,5-diphenyl tetrazolium bromide) (Sigma) in viable cells. Cells were cultured in poly-l-lysine coated 24 well plates ($1x10^5$ cells per well). After the cultures reached required age, 500 µl of 0.5 mg/ml of MTT in fresh medium was added to each well and the cells were incubated at 37^0C for 4 h. The plates were then centrifuged at 1,500 rpm for 20 min at room temperature and the medium was carefully removed. Dimethyl sulfoxide (DMSO) (500 µl) was then added to each well to dissolve the formazan crystals. The DMSO-dissolved formazan crystals were read immediately at 540 nm with DMSO as blank on a spectrophotometer.

In case of Topo I Knockout studies, All experiments were conducted one day after plating when neurons were arborizing (dendrites and axons). At 24 hours after plating, the neurons were treated with Topo I siRNA (0.1µM - 1µM) using Lipofectamine-2000 (Invitrogen, cat. no. 11668) as tranfection agent and camptothecin (Sigma, Cat No. C9911) (1µM – 100µM), and also with 0.5 µM of non-silencing Topo I siRNA (scrambled) as control. The effect of varying

concentrations of Topo-I si RNA and camptothecin on the viability of granule neurons in culture after 16 h treatment was determined by colorimetric quantification of MTT based on assay described above and earlier by (Mosmann, 1983). Cultured CGNs in poly-l-lysine coated 24 well plates after treatment were incubated with 500 µl of 0.5 mg/ml of MTT in fresh medium at 37 °C for 4 h. The plates were then centrifuged at 1,500 rpm for 20 min at 37 °C and the medium was carefully removed. 500 µl dimethyl sulfoxide (DMSO) was then added to each well to dissolve the formazan crystals. The DMSO dissolved formazan crystals were read immediately at 540 nm with DMSO as blank on a spectrophotometer.

2.4 Caspase-3 assay:

Caspase-3 activity was measured through cleavage of a colorless substrate specific for caspase-3 (Ac-DEVD-AMC) releasing the chromophore, (7-amino-4-methylcoumarin (AMC). Assays were carried out according to manufacturer's instructions (Caspase-3 assay kit, BD Pharmingen, San Jose, CA, USA). To evaluate the activity of caspase-3, cell lysates were prepared from CGNs at different weeks in culture or after treatment with varying concentrations of Topo I siRNA and Camptothecin. Assays were performed by incubating 50 µg protein of cell lysate per sample in 1 ml protease assay buffer (1X HEPES buffer) containing 10 µl of 1 µg / µl caspase-3 substrate (Ac-DEVD-AMC, 2 mM). A caspase-3 aldehyde inhibitor 1 µg / µl (Ac-DEVD-CHO) supplied along with the kit was used as control. Lysates were incubated at 37^0C for 1 h. Samples were measured for AMC liberated from Ac-DEVD-AMC, using a spectrofluorometer with an excitation wavelength of 380 nm and an emission wavelength of 450 nm.

2.5 Western blot analysis:

Cells were harvested by scraping in 25 mM Tris–HCl, 137 mM NaCl, 3 mM KCl, pH 7.4, and centrifuged at 300g for 7 min at 4 ^{0}C. The cell pellet was homogenized in 0.2 ml protein lysis buffer (20 mM Tris–HCl pH 7.5, 0.1 mM β-mercaptoethanol, 1 mM

$MgCl_2$, 0.1 mM EDTA, 5% glycerol, 0.1% Triton X-100, 0.5 mM KCl, 0.5 mM PMSF and 1 µg/µl pepstatin and leupeptin) for 10 min on ice followed by sonication for 15–20 s. The protein concentrations in cell lysates were measured using the Bradford method (Bradford, 1976). Twenty micrograms of total protein/lane were separated on 10% sodium dodecyl sulfate (SDS) gels and then transferred to nitrocellulose membranes (Towbin et al., 1979). The membranes were blocked with 5% non-fat dry milk in Tris- buffered saline pH-7.5 (TBS) containing 0.05% Tween-20 for 1 h and then incubated overnight at 4^0C with corresponding protein specific antibodies. After washing and incubating for 1 h at 22^0C with a secondary antibody, conjugated with horseradish peroxidase or alkaline phosphatase. These membranes were then washed and immunoreactive bands were visualized either by chemiluminescence (Pierce Western Blot Chemiluminescence Reagent, USA) or by using BCIP/NBT (Bangalore Genei, India) substrate for alkaline phosphatase enzyme. Relative levels of protein in the different lanes were compared by analyzing scanned images using the NIH IMAGE J program. All studies were performed a minimum of three times using independent cultures.

2.6 Reverse Transcription PCR (RT-PCR):

Total RNA was extracted from granule neurons during the period from 1^{st} to 5^{th} week in culture or after treatments with Topo I siRNA and camptothecin using TRI-REAGENT (SIGMA, USA). Aliquots of 5 µg were then subjected to reverse transcription using oligo (dT) primer and c-DNA synthesis was carried out with enhanced avian first Strand Synthesis Kit (eAMV-RT,SIGMA). Aliquots containing an equal amout of cDNA were then used for PCR ' with primers for RAT β-actin, topo IIβ, topo IIα , topo I, topo IIIβ, topo IIIα , Pol-β, Ku 70 and Ku 80.

Primer Design:

Based on sequence homology of topo II β, topo IIα , topo I, topo IIIβ, topo IIIα , Pol-β, Ku 70 Ku 80 protein and β-actin, primer sequences were designed for Wistar rat

(*Rattus novergicus*) strains that were aligned using Primer 3 software (available Online).

The following primers were used:

Primers	Forward 5'----------3'	Reverse5'----------3'
Topo I	CTCTAGTCCACCACGAATTAAAGAC	TACTTCTTCTGCTTTGGGACTCAG
Topo IIα	AGGTGGTCGAAATGGCTATG	CCTCTCCGCTAAAGGGCTTG
Topo II β	CACATTAAAGGCCTGCTAAT	AGGTAATGGCAGCATCATCC
Topo IIIα	TGGAACAGCAGACCCAGGATCCACAC	CATGAGGGCGATGAGGTCAGCT
Topo III β	GAGTCAGCATCGGCAGTCCTGTTGA	GTCATGGCATTGCAGATGTCCGT
Ku 70	TGAA GTGCTCTGGGTCTGTG	CAGCGATGCTGATGATGTCT
Ku 80	TGCCATGGGTAACTCCTTTC	AGGAAGTCGGCTTGTTGAGA
Pol β	CACAGCTCAATGGCACCTAAC	AGTGACCAGACGCTGTGATG
β- actin	CTGACAGGATGCAGAAGGAG	GATAGAGCCACCAATCCACA

Cycling conditions were optimized for each primer, and PCR products were run on 1.2% agarose gel stained with ethidium bromide. Gels were digitally photographed, and densitometric analysis was performed. Values are expressed as ratios to β-actin.

2.7 Real time PCR:

The Applied Biosystems (ABI) Prism 7900 HT sequence detection system (Applied Biosystems, USA) was used for real-time polymerase chain reaction (RT-PCR). The synthesized c-DNA was used for quantitative RT-PCR (qRT-PCR) analysis. The real-time qRT-PCR was performed in 96- well plate (MicroAmp TM Fast optical 96-well reaction plate, Applied Biosystems.) in a 20 µl reaction volume using components of the SYBER green qPCR kit (SAF labs, USA). Relative changes in gene expression (fold change) were calculated using the 2-[delta] Ct (threshold cycle) method.

Relative gene expression was determined based on the threshold cycles (Ct) of the gene of interest (topo II β) and β-actin as an internal reference gene.

2.8 Alkaline comet assay:

Granule neurons at different stages of culture were treated with 0.5 μM N-ethyl-N-nitrosourea (ENU) for 12 h followed by 24 h recovery. Subsequently, the comet assay was carried out as in Lebailly et al. (1997). 10^5 cells were suspended in 140μl pre-warmed low melting point (LMP) agarose (0.5% PBS) and 100 μl of the suspension was rapidly spread on ice frosted microscope slides pre-coated with 80 μl of normal agarose (0.8 % in PBS) and covered with a glass coverslip. After gelling for 10 min at 0^0C, the cover slip was gently removed and a third layer of 80 μl LMP agarose was added. Slides were then put on a tank filled with lysis solution (2.5 M NaCl, 0.1 M EDTA, 10 mM Tris-HCl pH 10, 10 % dimethyl sulfoxide (DMSO) and 1 % Triton X-100 both freshly added) for one hour at room temperature. The slides were then removed from lysis solution and incubated in a fresh electrophoresis buffer (0.3 M NaOH and 1 mM EDTA, pH 13) for 40 min at room temperature to allow unwinding of DNA. Electrophoresis was then carried out at room temperature in fresh electrophoresis buffer for 24 min at 0.7 volts/cm and 300 mA. After this, the slides were gently washed twice for 5 min in fresh neutralization buffer (0.4 M Tris-HCl, pH 7.5). After drying overnight at 4^0C, slides were stained with 50μl of ethidium bromide solution (20μg/ml) and covered with a cover slip. The images were captured on a Confocal microscope (Lieca) and quantified by using Comet-IV software (Perceptive Instruments, UK). The comet moment was calculated by using the equation described in Kent et al., (1995), viz., (comet moment R_{0-n} = (intensity of DNA at distance X) (distance)/intensity of total DNA). Data is presented as an average along with the standard deviation (SD) calculated from three independent experiments (50 images for each dose of each independent experiment).

2.9 Preparation of nuclear extracts for *in vitro* NHEJ assay:

Extracts from cerebellar granule neurons in culture (CGNs) were prepared as described in Davydov et al. (2003) and Shackelford et al. (1999). Briefly, cells were homogenized in four volumes of homogenization buffer A (10 mM HEPES, pH 7.9, 0.5 mM dithiothreitol (DTT), 10 mM KCl, 1.5 mM $MgCl_2$, and protease inhibitor cocktail) on ice. The final concentration of protease inhibitors in the buffers was 0.2 mM phenylmethylsulfonyl fluoride (PMSF), 5 mM benzamidine, 0.05 mg/ml leupeptin, 0.025 mg/ml pepstatin A, and 0.05 mg/ml aprotinin. Homogenates were centrifuged at 5000×*g* for 15 min at 4^0C. The supernatants were considered as the cytosolic fraction. Pellets were resuspended in an equal volume of high salt buffer C (20 mM HEPES, pH 7.9, 25% glycerol, 1.5 mM $MgCl_2$, 1 M NaCl, 0.2 mM EDTA, 0.5 mM DTT, and protease inhibitor cocktail), extracted for 30 min at 4^0C with continuous gentle mixing, and centrifuged at 70,000×*g* for 30 min at 4^0C. This supernatant is the nuclear protein extract. This was dialyzed for 6 h at 4^0C against 20 mM HEPES, pH 7.9, 20% glycerol, 100 mM KCl, 0.2 mM EDTA, 0.5 mM dithiothreitol, and 0.2 mM PMSF, centrifuged at 16,000×*g* for 30 min at 4^0C aliquoted and frozen at -70^0C. Protein concentrations were determined by the Bradford method (Bradford, 1976) using bovine gamma-globulin as the standard protein.

2.10 DNA end joining assay:

DNA end joining assay was performed as described previously (Pfeiffer, 1988; Baumann and West, 1998). pUC19 plasmid DNA was isolated using standard protocol. For creating a specific double strand break, plasmid DNA was subjected to restriction digestion generating cohesive (*Eco*RI) ends. Completion of digestion was monitored by agarose gel electrophoresis and around 95% of the plasmid DNA was digested while generating the monomer. Linear pUC 19 obtained by *Eco*RI digestion was labeled with γ^{32}P dCTP using RediprimeTM II kit (Amersham Pharmacia Biotech) for random priming and the labeled product, after purification, was used as a probe for Southern detection of end joined products.

A standard end joining assay mixture contained final concentrations of 45 mM HEPES–KOH buffer pH 7.9, 50 mM KCl, 7.4 mM $MgCl_2$, 0.4 mM EDTA, 0.9 mM DTT, 2 mM ATP, 20 µM dNTPs, 3.4% glycerol, 18 µM BSA, 400 ng of substrate DNA (pUC 19 plasmid DNA digested with indicated restriction enzyme) and 40µg of extract proteins. The reaction mixture was incubated for 2 h at 25^0C. DNA products were purified by phenol/chloroform extraction and ethanol precipitation. Products were loaded on 0.8% Agarose gel and electrophorosed in 0.5× TBE buffer at 60 volts for 5 h. The gel was stained by EtBr (ethidium bromide) and documented for results. For Southern analysis, the gel was depurinated and blotted onto a nylon membrane (Hybond N+, Amersham) in denaturating buffer (alkaline transfer) and the membrane hybridized with the ^{32}P-labeled plasmid probe prepared as mentioned above. The end joined products were visualized as dimers and multimers on the autoradiogram.

2.11 Senescence-Associated ß-Galactosidase (SA-β-gal) assay:

Cultured neurons grown on glass cover slips were fixed with 4% paraformaldehyde at room temperature for 3-5 min, cells were washed three times with PBS and incubated in the dark in X-gal staining solution pH-6 (100 mM sodium phosphate, 2 mM $MgCl_2$, 150 mM NaCl, 0.01% sodium deoxycholate, 0.02% NP-40, 5 mM potassium ferricyanide, 5 mM potassium ferrocyanide, and 1 mg/ml X-gal). Cells were incubated in the dark for 10 hrs at 37°C. The cells were then washed in PBS, mounted and viewed under a bright field microscope. The positive percentages were determined by counting stained and unstained cells under a microscope at 400X magnification in 4 random fields. A minimum of 200 cells were counted and results were presented as the mean (SEM) for a given number of observations (n) along with mean standard errors.

2.12 Imaging of Intracellular Ca^{2+} using Fura 2-AM:

For measurement of intracellular Ca^{2+} levels we followed the method described in Barreto-Chang et al. (2009). CGNs cultured on poly- d- lysine coated glass cover slips

were transferred into 35mm dishes containing Fura 2-AM loading solution in Hanks' balanced salt solution-bovine serum albumin containing 2.5 mM probenecid, pH 7.45 (HBSS-BSA-probenecid, pH 7.45) with a concentration of 1µM Fura 2-AM. The cells were incubated in the dark at room temperature for 30 min and were then washed twice with pre-warmed HBSS-BSA-probenecid buffer. Immediately the cells were incubated in a 37^0C incubator (no CO_2 required as the HBSS BSA probenecid is not bicarbonate buffered), for 30 min in the dark. These cells on the coverslips were mounted on an inverted microscope (Leica Fluorescence confocal microscope) setting the excitation/emission wavelengths for fura-2, (set fluorimeter optics for dual excitation at 340 and 380 nm and emission at 510 nm). The fluorescence ratio images were captured using 20x fluor objective and were digitized. To measure the calcium, the region of interest tool (ROI) was used to define the areas of the image and the intensity of fluorescence was quantified using J-image software (NIH). Several images of cells (minimum 50 cells) in different random fields were selected and the fluorescence intensity was averaged and quantified.

2.13 siRNA synthesis:

We have used double strand siRNA oligos for transient down regulation of Topo I in rat CGNs. Lipofectamine 2000 (Invitrogen) was used for transfecting the double strand siRNA oligos. One day cultured cells were used for transfection as standardized in our lab (Mandraju 2008)**.** Double strand siRNA oligos were synthesized as described earlier (Donze and Picard, 2002). For this, desalted DNA oligonucleotides were obtained from Sigma (India). The oligonucleotide-directed production of small RNA transcripts with T7 RNA polymerase has been implemented as described (Milligan and Uhlenbeck, 1989). For each transcription reaction, 1 nM of each oligonucleotide was annealed in 50 µl of TE buffer (10 mM Tris–HCl, pH 8.0, and 1 mM EDTA) by heating at 95 ºC; after 2 min, the heating block was switched off and allowed to cool down slowly to obtain double stranded DNA. Transcription was performed in 50 µl of transcription mix: T7 transcription buffer (40 mM Tris–HCl, pH 7.9, 6 mM $MgCl_2$, 10 mM Dithiothreitol (DTT), 10 mM NaCl and 2 mM

spermidine) 1 mM NTPs, 0.1 U yeast pyrophosphatase (Sigma), 40 U Rnase OUT (Life Technologies) and 100 U T7 RNA polymerase (Invitrogen) containing 200 pM of the dsDNA as template. After incubation at 37 ºC for 2 h, 1 U RNase-free DNase (Genetix) was added at 37 ºC for 15 min. Sense and antisense 21-nt RNAs generated in separate reactions were annealed by mixing both crude transcription reactions, heating at 95 ºC for 5 min followed by 1 h at 37 ºC to obtain 'T7 RNA polymerase synthesized small interfering double-stranded RNA' (T7 siRNA). The mixture (100 µl) was then adjusted to 0.2 M sodium acetate, pH 5.2, and precipitated with 2.5 volume of ethanol. After centrifugation, the pellet was washed once with 70% ethanol, dried and resuspended in 50 µl of water.

2.13.1 si RNA oligos:

The following oligos were used to synthesize siRNA, Topo I sense strand-5`GCGGATTTCCGATTGAATGTT3', Topo I anti-sense strand-5'CATTCAAT CGGAAATCCGCTT3'. Scrambled sense-5'TTCGCGGATCGATTGAATGTT3', Scrambled anti-sense-5'CATTCAATCGATCCGCGAATT3'.

Figure 2.1

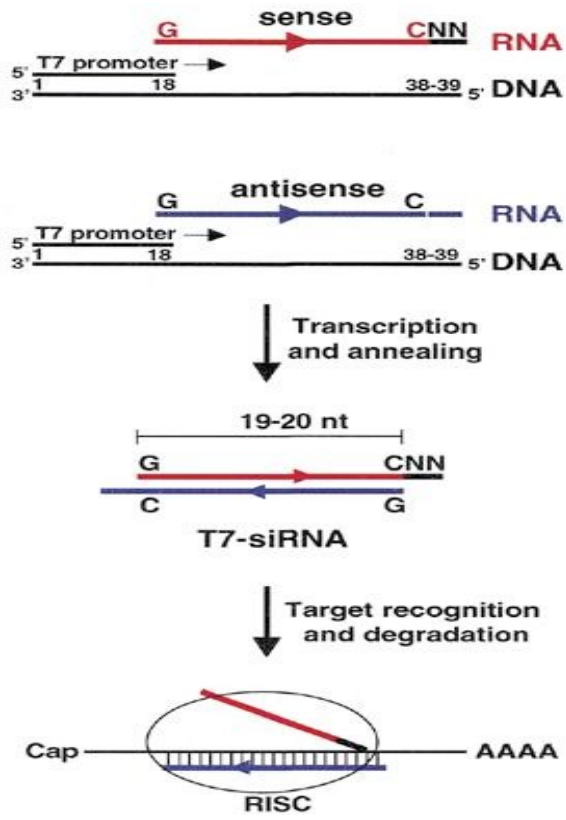

Fig. 2.1. Strategy to generate T7 siRNAs: The sequence of the gene of interest is shown in red (sense) or blue (antisense), while the two unrelated nucleotides are in black. RISC stands for the RNA-induced silencing complex that targets the mRNA for cleavage (Taken from Donzé and Picard, 2002).

2.13.2 siRNA transfection:

Cultured granule neuron Cells (2 x10^6 million) were transfected by using Lipofectamine-2000 (Invitrogen) with 0.5 µM of non-silencing Topo I siRNA (scrambled) and silencing Topo-I siRNA separately. In case of immunoflurosence studies the CGNs were co-transfected with green fluoresent expressing pEGFP-N2 plasmid along with siRNA.

2.14 S^{35}-methionine in vitro labeling:

S^{35-} methionine is a commonly used isotope for radio labeling of proteins. Topo-I si RNA transfected in CGNs for 16 hrs or camptothecin treated CGNs for 16 hrs (2 × 10^6 cells) were incubated with 10 µCi S^{35}-methionine in methionine-free DMEM medium (Gibco) for 4 h in 5% CO_2 incubator, later the cells were suspended in protein lysis buffer (20mM Tris–HCl pH 7.5, 0.1 mM ß-mercaptoethanol, 1mM $MgCl_2$, 0.1 mM EDTA, 5% glycerol, 0.1% Triton X-100, 0.5 mM KCl, 0.5 mM PMSF and 1 µg/µl pepstatin and leupeptin) and 100 µg total protein extract was subjected to 10% polyacrylamide gel electrophoresis (PAGE) and stained with Coomassie. The dried gels were exposed to X-ray film for 4 days and developed. Protein equivalent S35 methionine incorporation into proteins was measured using 25µg of treated cell extracts, aliquoted on filter, dried followed by counting in toluene containing scintillation liquid using LKB Beta counter. The data is represented as counts per minute (cpm).

2.15 Annexin-V assay by FACS:

16 hours after transfection with appropriate siRNA constructs and camptothecin concentrations, apoptosis was measured in terms of annexin-V staining (Vybrant Apoptosis Assay Kit#3, Invitrogen, USA) followed by FACS analysis (BD biosciences). For the cytotoxicity assay 2×10^6 freshly-trypsinized 0.5µM Topo I siRNA transfected or 10µM camptothecin treated granule neurons were used. The collected target cells were then washed in PBS, resuspended in 1× annexin binding

buffer and stained with annexin V-FITC for 5 min at room temperature in the dark. The staining solution was removed and the cells were resuspended in cold PBS on ice for FACS. Quantification of cytotoxicity was determined by the percentage of apoptotic target cells scored by FACS analysis.

2.16 Immunofluorescence:

CGNs were dissociated and cultured, as described above in 6-well plates containing poly-L lysine coated cover slips at a density of $2x10^6$ cells/well. After 24 hr in culture the cells were co-transfected with siRNA and pEGFP-N2 plasmid (a gift from Prof. N. Siva kumar, University of Hyderabad, India) using Lipofectamine 2000, or treatment with 10μM camptothecin separately as required. After 16 hr treatment, the neurons were fixed with 4% para formaldehyde containing 0.025% triton X-100, for 15 min at room temperature, blocked with PBS containing 5% bovine serum, and incubated with monoclonal anti-Topo I (1:100 dilution) (Sigma USA) and polyclonal anti-neurofilament (NF) (1: 100 dilution). Subsequently the cells were washed 3-4 times with PBS and incubated with fluorescent-tagged anti-mouse IgG-Cy3, anti-rabbit IgG-Cy5 (Chem Bio) at 1:250 dilutions. These cultures on cover slips were mounted on to glass slide and viewed under Fluorescence confocal microscope Lieca (Leach Instruments, Heidelberg, Germany). The excitation/emission wavelengths employed were 400 nm/510 nm for GFP (green), 548nm/ 562 nm for Cy3 (blue) and 650/700 for Cy5 (red).

2.17 Morphometric analysis:

To evaluate neurite length, cells were co-transfected with 0.5 μM Topo I siRNA + pEGFP-N2 plasmid, transfected cells were cultured for 16 hrs. In a separate dish cells were treated with 10μM camptothecin for 16 hrs. After 16 hours, cells were fixed and immunolabeled with anti-Topo I and anti- neurofilament (NF) antibodies as described in Immunofluoresence (2.8). Based on the GFP (green) and NF (red) positive cells individual processes were traced manually and measured with Image J, a java-based

image analysis program (NIH,USA) available on the internet. The total neurite length per neuron was determined and measured as the sum of the lengths of all neurites of neurons in culture. The average total neurite length was determined from a sample of at least 50 neurons per group from two independent experiments. The neurite lengths were compared to Topo I siRNA and control cells. Values are expressed as mean ± standard error. Statistical differences were evaluated with independent parametric *t*-test.

2.18 Data analysis:

All experiments were repeated three times individually unless otherwise specified. Differences between groups were assessed by One Way Anova followed by student-Newman-Keuls test, p- value less than 0.05 ($p < 0.05$) were considered statistically significant. Data are expressed as the mean ± SD.

CHAPTER -3

Establishing Cerebellar granule neurons as *in-vitro* model of aging

Introduction:

The precise relationship between the processes of aging in different tissues *in vivo* and in experimental models of cellular aging remains unclear. Reactive oxygen species (ROS) and many other DNA-damaging agents can cause cells to enter a state of irreversible cell cycle arrest, accompanied by characteristic morphological and functional alterations, referred to as senescence (Ben-Porath and Weinberg, 2004). Evidence for the role of cellular senescence in aging is based mainly on correlations. In mammals, the cells programmed for senescence accumulate with increasing age and at sites of pathogenesis (Itahana et al., 2004). Several mouse and human models of premature aging are also reported to show premature cellular senescence *in vitro* (Weidenheim et al., 2009). Typically senescent cells become enlarged and express a pH-dependent β-galactosidase activity (Dimri et al., 1995) and the corresponding assay has become one of the most commonly used markers of cell aging. Altered Ca^{2+} regulation might play a role in brain aging and also in Alzheimer's disease (AD) (Landfield, 1983; Disterhoft et al., 1994). Increased levels of intracellular calcium ($[Ca^{2+}]i$) are implicated in the neuronal losses associated with aging related disorders. Recent evidence demonstrates increased expression of voltage gated Ca^{2+} channel proteins and associated Ca^{2+} currents with aging (Thibault, 2001; Veng, 2002). Middle-age neurons in comparison to young neurons exhibit significant elevations in basal $[Ca^{2+}]_i$ levels in culture (Raza, 2007).

In the present investigation, our primary objective is to examine and characterize cultured CGNs *in vitro* as an aging model.

Results:

Cerebellar granule neurons (CGNs) in culture.

Cerebellar granule neurons (CGNs) isolated from 6-day-old rat pups were cultured *in vitro* on PLL-coated plates or cover slips following the procedure as detailed in Materials and Methods. 2 x 10^6 cells/60mm dish were seeded for carrying out the experiments under the same media conditions. A mitotic inhibitor, arabinosylcytosine, was used to inhibit the growth of non-neuronal cells like glia. Over 95% of the cells cultured in this way were granule cells as identified by both from their small size (diameter 8–12 μm) and their rounded body shape with bipolar neurites **(Fig3.1.).** Immunoblot analysis was performed for neurofilament (NF) and glial fibrilar acidic protein (GFAP) **(Fig 3.2.A, B)** to confirm the purity of CGNs at different weeks in culture. The results clearly show the purity of CGNs at different weeks in culture, evident by immunoblot analysis for NF and GFAP. The minimal amount of GFAP present in the 1^{st} week might be due to the presence of mitotic astroglial cells.

Viability of CGNs under prolonged period in culture.

The viability of cerebellar granule neurons (CGNs) over prolonged periods in culture was measured using the MTT assay. The results showed no changes in viability until 5 weeks in culture, while a consistent viability decrease with increasing age was seen only after the 5^{th} week, and this decrease amounts to almost 50% by the 7^{th} week **(Fig 3.3)**. These results clearly suggest that granule neurons can indeed survive at least for 5 weeks in culture under stable media conditions, a duration much longer than that reported earlier. Previously, long-term cultures of cerebellar granule neurons were shown to survive *in vitro* for a maximum of 17 days (Ishitani et al., 1996). While CGNs could be maintained for 23 divisions (days *in vitro*) in studies on the Ca^{2+} homeostasis related to aging (Toescu et al., 2000).

The Analysis of results on the caspase 3 activity (a pro-apoptotic marker) in aging CGNs in culture at 1st and 2nd weeks showed no significant elevation of its level except for a slightly higher expression of activity in the neurons in culture **(Fig 3.4)**, which may be due to apoptotic death of un-established neurons in culture. This also points out that the observed depletion of neurons after 5 weeks **(Fig 3.3)** did not involve any elevation of caspase-3 activity **(Fig 3.4)**, suggesting that the process responsible for depletion be ascribed to pathways other than the apoptosis. For a control study, Caspase-3 aldehyde (Ac-DEVD-CHO) was used as inhibitor for caspase-3 activity.

Figure 3.1

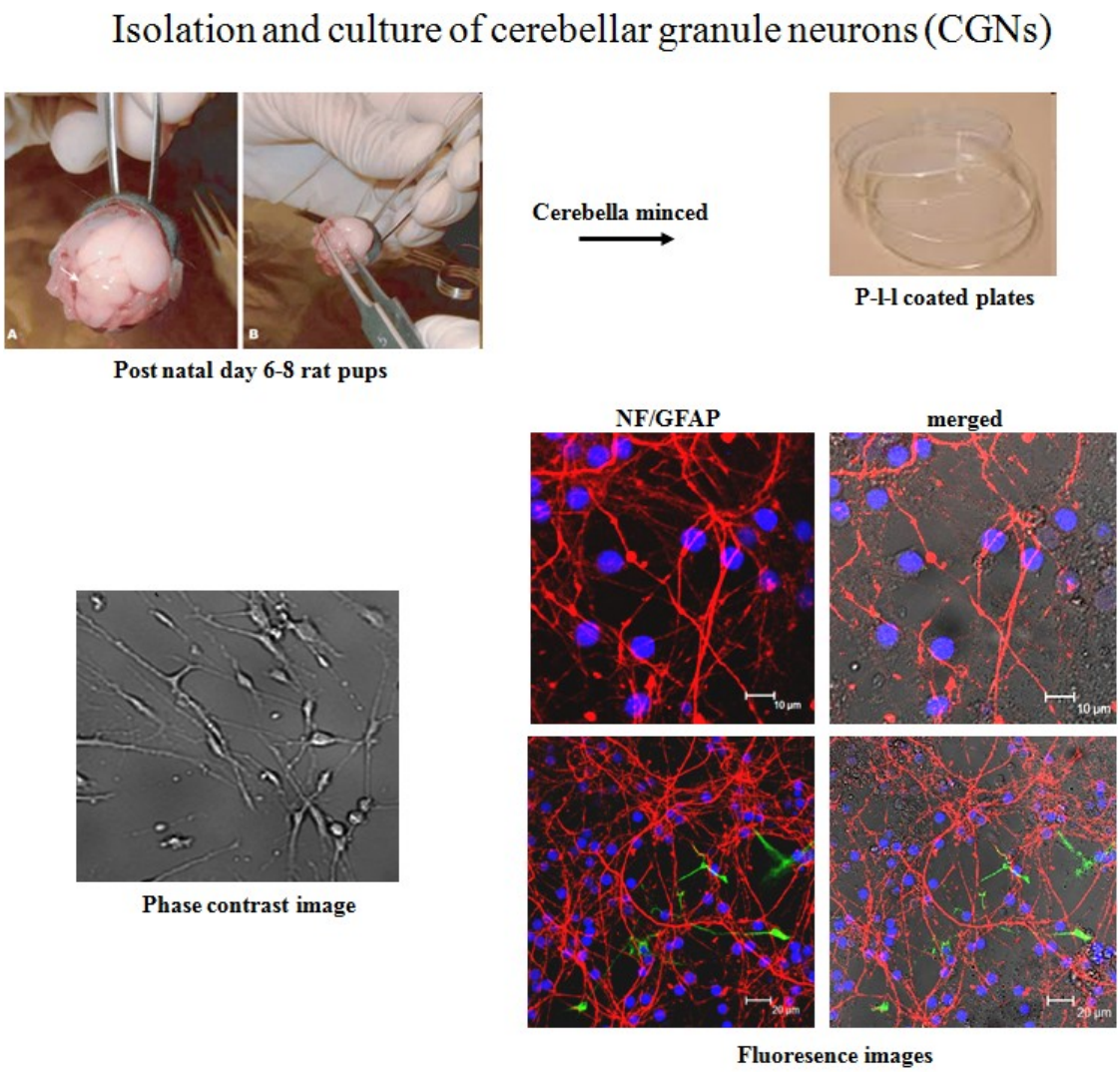

Fig 3.1. Granule neurons from cerebellum were isolated by following procedure of Martin A. Cambray-Deakin, (1995). Neurons were cultured in EMEM with 18mM KCl, 30mM Glucose, 2mM glutamine and 10% FBS on poly-L-lysine coated plates. Cells prepared were stained with (GFAP/NF/Dapi). Neurofilament (NF) for neurons, glial fibrilar acidic protein (GFAP) for astrocytes and DAPi for nuclear staining.

Figure 3.2

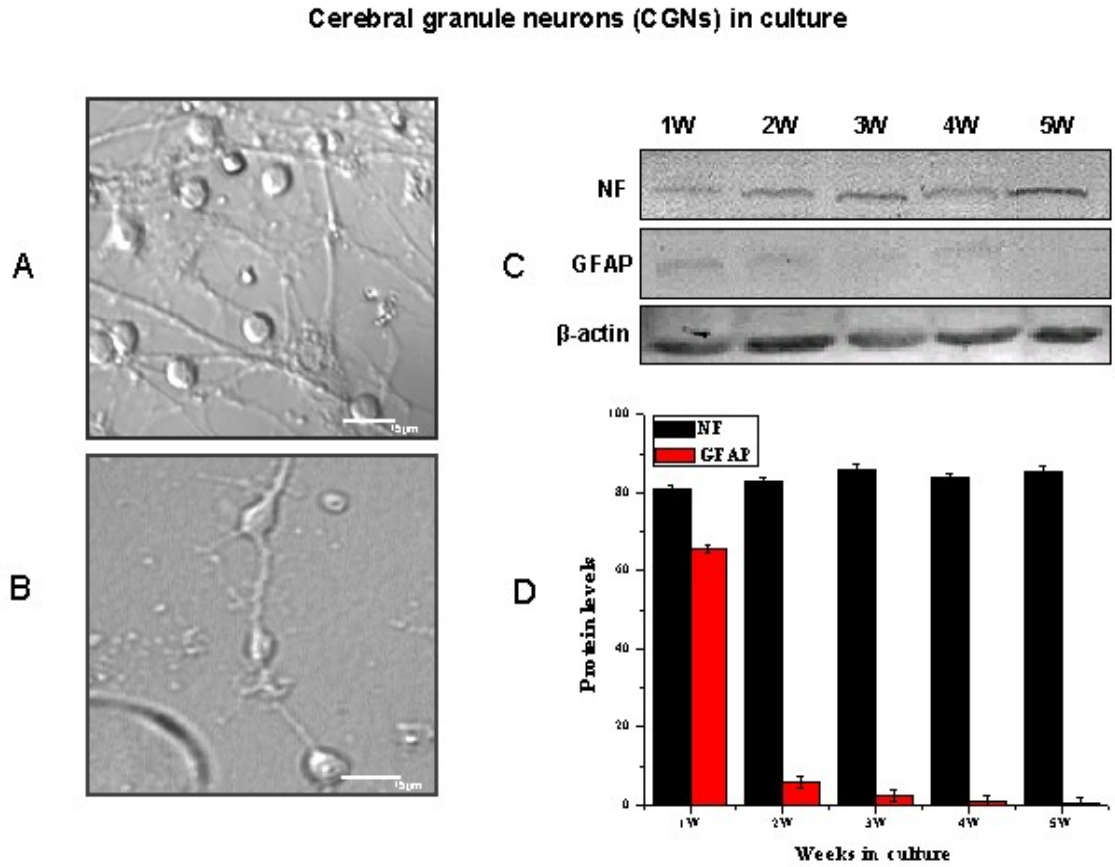

Fig 3.2. Purity of isolated cerebellar granule neurons (CGNs) in Culture. Granule neurons were isolated from 6-8 day old rat pups as described in the text. Immunoblot analysis for neurofilament (NF) and glial fibrillary acidic protein (GFAP) was done to confirm the purity of CGNs at different weeks in culture. Pictures represented in Panel A and B are transmission images showing CGNs at 1st week in culture as identified by both their small size (diameter 8–12 μm) and rounded body shape with bipolar neuritis. Panel C represents the immunoblot for NF and GFAP of CGNs at different weeks in culture, with β-actin as internal control. (D) Shows the representative bar graph of (C) normalized with β-actin, analysed using Image J software (USA).

Figure 3.3

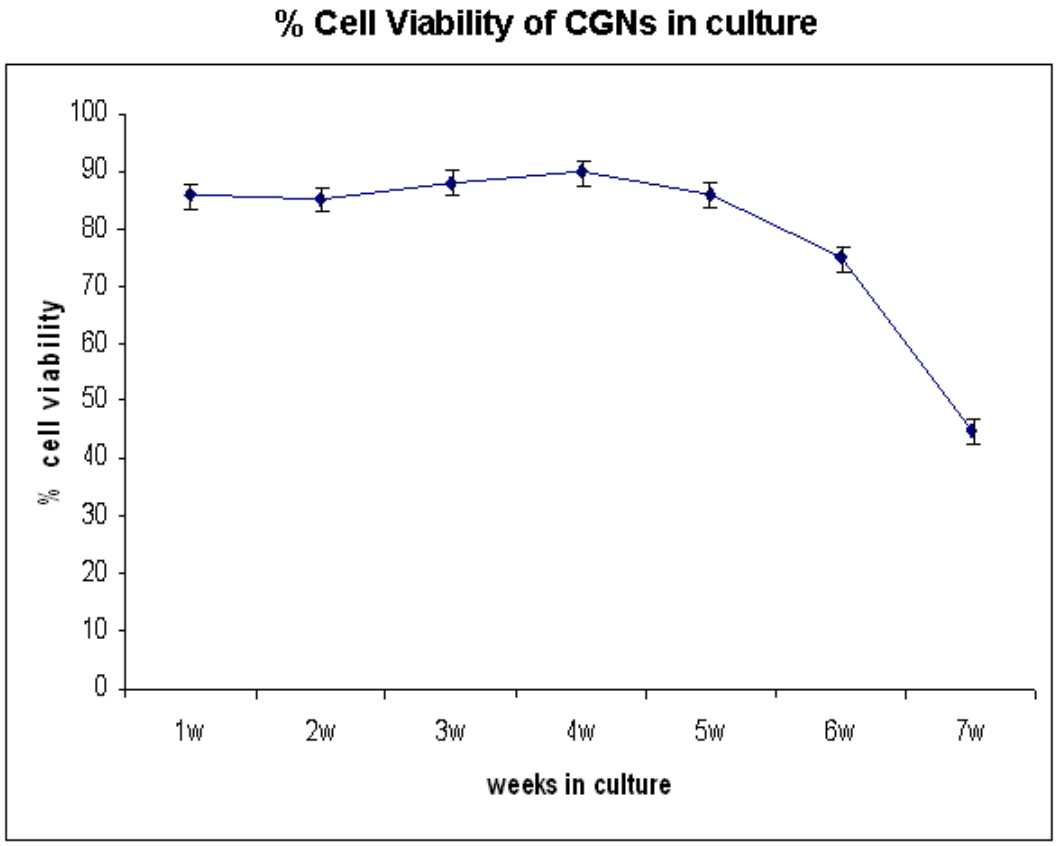

Fig 3.3. Cell viability of aging cerebellar granule neurons (CGNs) in culture. CGNs isolated from 6-8 days rat pups were cultured under standard conditions for up to 7 weeks. The viability of granule neurons at each week was determined by an MTT assay. The data represented in line graph shows a stable viability up to 4th week and starts showing a decrease in cell viability only after 4th week, decreasing to less than 50% by 7thweek. Experiments have been performed in triplicate and repeated independently three times.

Figure 3.4

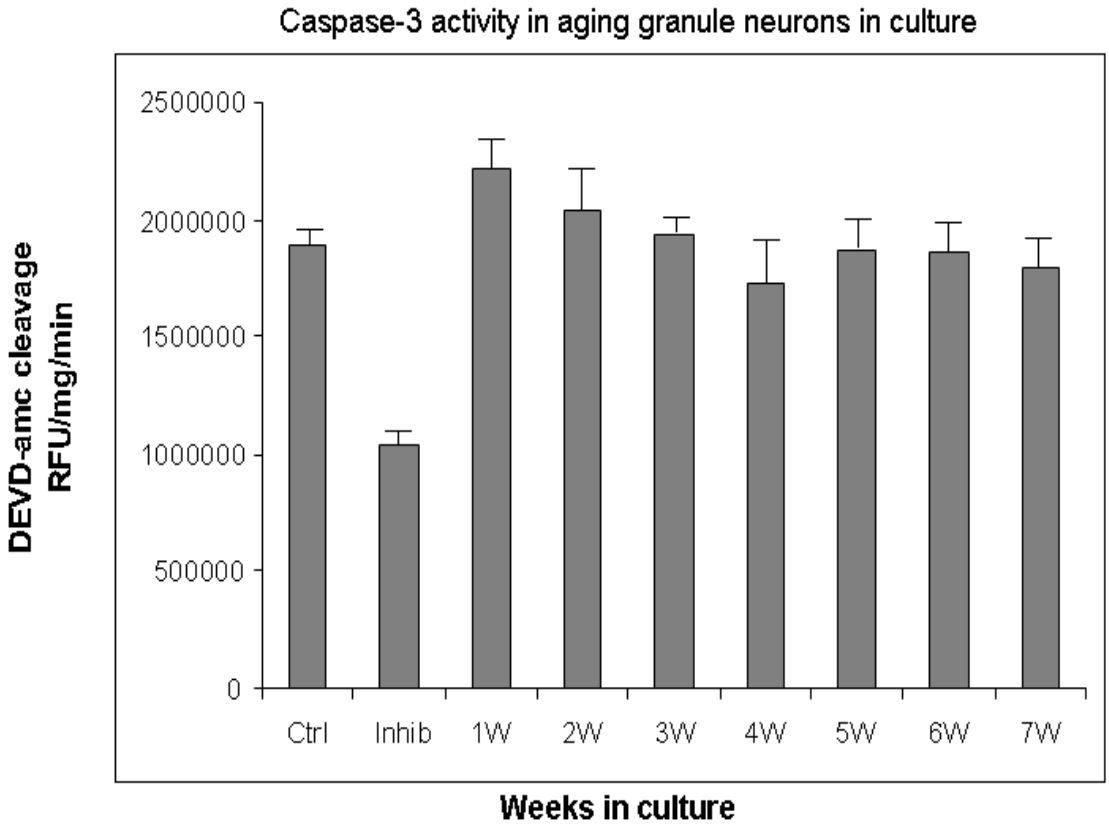

Fig. 3.4. Caspase activity in aging CGNs in culture. To assess apoptotic induction in aging CGNs in culture, caspase-3 activity was measured using fluorogenic (Ac-DEVD-AMC) substrate using extracts of CGNs at different weeks in culture, caspase-3 aldehyde (Ac-DEVD-CHO) was used as inhibitor for caspase-3 activity. There was no significant elevation of caspase-3 activity in the aging CGNs in culture as shown in bar graph. This suggests the depletion of neurons after 4th week is due to pathways other than apoptosis. Experiments have been performed in triplicate and repeated independently three times.

Senescence associated ß-gal (SA-β-gal) in aging cerebellar granule neurons *in vitro*.

The role of SA-beta gal with respect to replicative senescence has been well established (Itahana et al., 2004; Weidenheim et al., 2009). Studies on post mitotic cells like neurons are very few. In one of the recent studies on rat models, elevated activity of SA-β-gal in hippocampal neurons, characterized by dependence on age and duration of neuron culture periods, has been reported (Geng, et al., 2008). The results of this study presented in **Figure 3.5** show that the average proportion of SA-β-Gal-positive cells increases with the increase of the culture period, from 7.5 ± 2 % in the first week to 99.5 ± 2% ($p < .05$) in the 5th week. This increase in SA-β-gal may be due to stress accumulation under the prolonged culture period. Such a significant enhancement in the SA-ß gal in cultured CGNs shows *in vitro* aging similar to physiological aging.

Intracellular Ca^{2+} in CGNs *in vitro*.

Increased levels of intracellular calcium ($[Ca^{2+}]_i$) are often implicated in the neuronal loss associated with aging related disorders (Thibault et al., 2001). Mid-age neurons in comparison to younger neurons are characterized by significant elevation of basal $[Ca^{2+}]i$ levels in culture (Raza 2007; Thibault et al., 2001). To further examine this aspect and validate that the cultured CGNs indeed mimic aging *in vitro*, we have estimated intracellular Ca^{2+} in cultured CGNs using Fura 2-AM, a cell-associated Ca^{2+} binding dye. The results presented in **Figure 3.6** show that intracellular Ca^{2+} levels increased over time, maximizing at the 4th week and thus suggest dysregulation in calcium homeostasis.

Figure 3.5

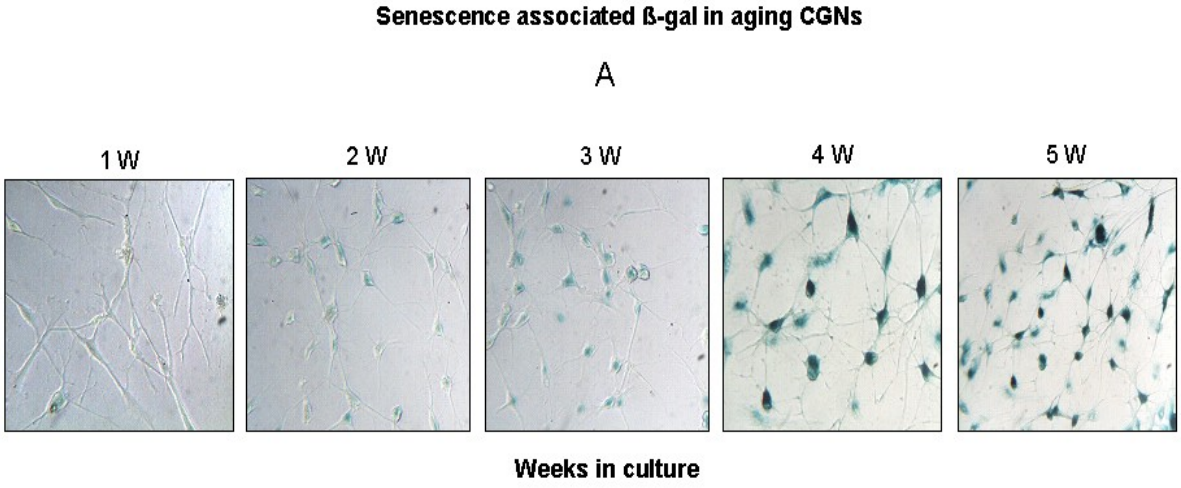

B

Days in culture	%of SA-β-gal + cells	No of observations (n)
6	7.5± 2	4
12	25± 5	4
18	55±7 *	4
24	97± 5 **	4
30	99.5±2 **	4

*p< 0.05; * * p< 0.001

Fig 3.5. SA-β-gal activity in aging CGN cultures. Aging CGNs were stained with X-gal for the determination of senescence associated β gal (SA-β-gal) at pH 6 in neurons at different weeks from 1st to 5th week, in culture. Representative pictures are shown in (A). The number of SA-β-Gal-positive cells was tabulated in (B). Experiments have been performed in triplicate and repeated independently three times, (* $p<0.05$; **$p< 0.001$) according to Student's t-test.

Figure 3.6

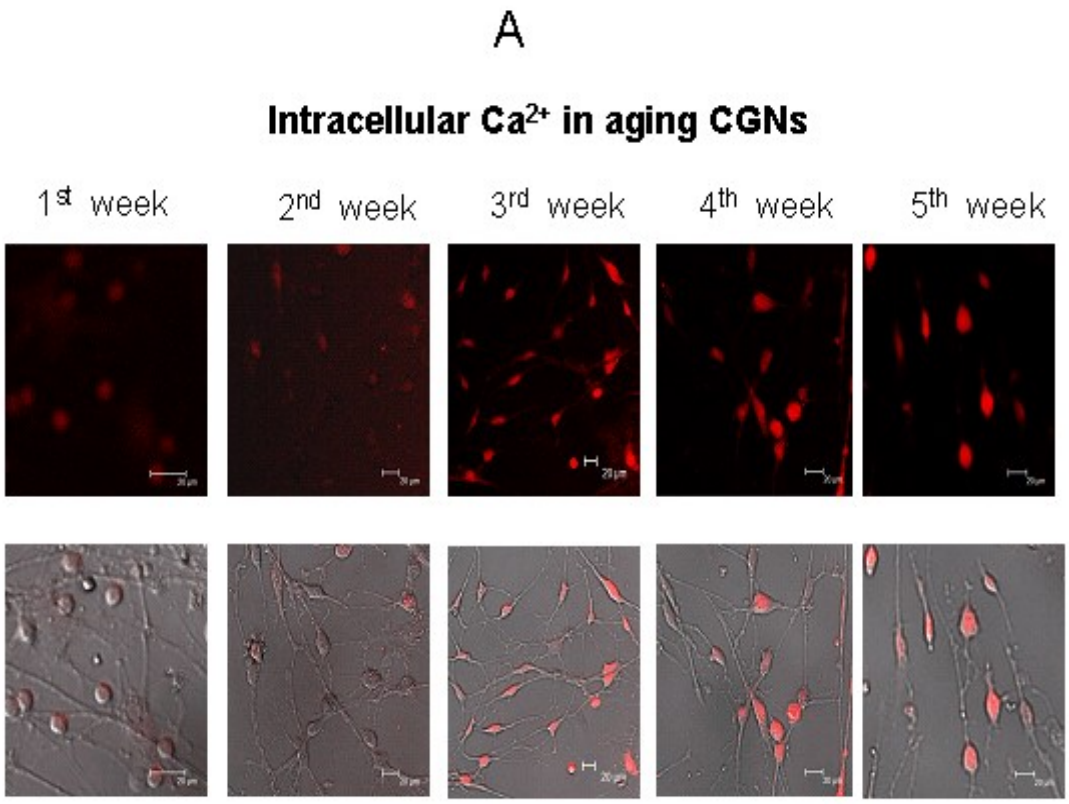
A
Intracellular Ca2+ in aging CGNs
1st week
2nd week
3rd week
4th week
5th week

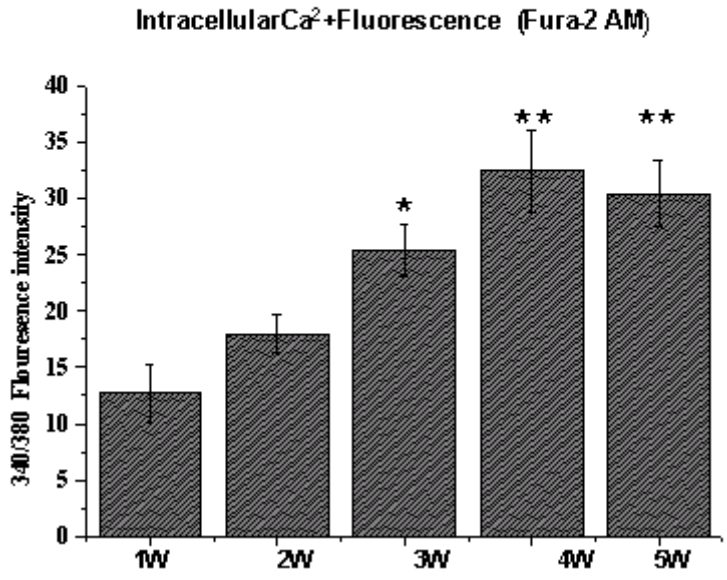
B
IntracellularCa2+Fluorescence (Fura-2 AM)
340/380 Flouresence intensity
0
5
10
15
20
25
30
35
40
*
**
**
1W
2W
3W
4W
5W

Fig 3.6. Intracellular Ca^{2+} in aging CGN cultures. Intracellular Ca^{2+} in cultured CGNs was determined using Fura 2-AM, a cell associated Ca^{2+} binding dye. Images were captured using inverted microscope (Leica Fluorescence confocal microscope) setting excitation/emission wavelengths (for fura-2) using fluorimeter optics for dual excitation at 340 and 380 nm and emission at 510 nm. The fluorescence ratio images were captured using 20x Fluor objective and then digitized, using the region of interest tool (ROI) to define the areas of the image for measuring calcium fluorescence, the intensity of fluorescence is quantified using J-image software (NIH). Several images of cells (minimum 50 cells) in different random fields were selected and the fluorescence intensity was averaged and quantified. A gradual increase in intracellular Ca^{2+} levels is observed from 1^{st} week to 5^{th} week in culture as may be seen in bar graph (B). Representative cell pictures are shown in (A). (* $p<0.05$; ** $p< 0.01$) according to Student's t-test. Experiments have been performed in triplicate and repeated independently three times.

Discussion:

The present results clearly show that CGNs in culture can survive for 5 weeks *in vitro* without significant change in the viability. The viability is shown to fall <50% by 7th week under similar media conditions through out the period of cultures. No significant elevation of caspase-3 activity was found, with increase in the age of the cultures and it is inferred that the depletion of CGNs after 5th week may be due to pathways other than apoptosis. Further a significant increase in the SA-ß gal positive cells was observed with increase in the age of the CGNs in culture, with the number of stained cells maximizing at 3rd week. This increase in the SA-ß gal suggests an enhancement of senescence of neurons, establishing aging of CGNs in culture *in vitro*.

Cerebellar granule neurons (CGNs) have been reported to show characteristics of apoptosis after 17 days in culture (DV). Further, CGNs in culture (after 17day culture) are also shown to exhibit several characteristics of apoptosis like ultrastructural changes and inter-nucleosomal DNA fragmentations, which may be effectively arrested by pretreatment with actinomycin-D and cycloheximide (Ishitani et al., 1996). In several of the studies (Tajes Orduña et al., 2009; Tajes et al., 2009; Bénard et al., 2004; Sunaga et al., 2002; Yao et al., 1999; Copani et al., 1998; Skaper et al., 1998; Ishitani et al., 1996), CGNs in Culture were used as aging associated apoptotic model based on an elevated DNA damage, as demonstrated by increase in the activation of ataxia telangiectasia muted (ATM). Recent studies (Tajes Orduña et al., 2009) showed that melatonin causes increase in the activation levels of prosurvival Akt, p53, p-FOXO1 phosphorylation, and a decrease in the levels of DNA damage indicators, viz. cyclin D, GSK3beta and E2F-1, thus suggesting the role of bioactive molecules acting on pro-survival pathways in protecting cell survival. Similar results were obtained in a study carried out on lithium (Tajes et al 2009). Consistent with these observations, our results in the present study clearly demonstrate the survival of CGNs in culture for 5 weeks followed by cell death. The results further establish that CGNs serve as an effective *in vitro* aging model and bring out their potential use for understanding and evaluation of pro- and anti-survival activities of various bioactive

agents and further elucidation of the mechanisms of the associated biological processes (Tajes Orduña et al., 2009; Tajes et al 2009; Sunaga et al., 2002; Copani et al., 1998).

Studies on the relationship between cytosolic $[Ca^{2+}](i)$ and mitochondrial membrane potential showed that neuronal stimulation (KCl-evoked depolarisation) induces a mitochondrial depolarisation response (Xiong et al., 2004). But in young CGN cultures (10 DIV), the mitochondrial membrane potential is shown to recover fully within 30s from the start of the stimulation, despite the continuous presence of the depolarisation stimulus and sustained cytosolic $[Ca^{2+}](i)$ signal. On the other hand in older CGNs (DIV 22), the mitochondrial response is reported to be of smaller amplitude and displayed a much longer repolarization period with a 50% increase in threshold $[Ca^{2+}](i)$ level for the initiation of the mitochondrial depolarisation response (Xiong et al., 2004). The enhancement of calcium homeostasis and the age-dependent increase in intracellular calcium along with enhanced senescence-dependent beta galoctosidase observed in the results of the present study are consistent with the above reports, and point out to possible mitochondrial membrane changes during aging of granule neurons (Xiong et al., 2004; Kirischuk et al., 1996; Kirischuk and Verkhratsky, 1996).

Calcium dysregulation hypothesis of brain aging and Alzheimer's disease, initially proposed in mid-1980s (Landfield and Pitler 1984; Gibson & Peterson, 1987), suggests that aging alters brain Ca^{2+} regulation, resulting in impaired neuronal function that eventually leads to neurodegeneration. Several studies have implicated increased levels of intracellular calcium ($[Ca^{2+}]_i$) in the neuronal loss associated with age related disorders. The increase of intracellular Ca^{+2} with the progress of time as observed in the present study establishes that cultured CGNs can serve as an effective aging model *in vitro*.

The results of the study on prolonged CGNs in culture clearly demonstrate the significant similarities between physiological aging and *in vitro* aging and provide new directions towards understanding of normalytic ageing processes in human brain. Understanding the molecular basis of aging processes at the cellular level should provide clues to gain insights into the pathology of various neurological diseases for eg., Alzheimer's and Parkinson's diseases, which are considered to be associated with high risk factors with increasing age.

CHAPTER -4

Analysis of Topoisomerases in *in-vitro* and *in-vivo* aging

Introduction:

DNA topoisomerases solve the topological problems associated with DNA manipulation by introducing a transient break in the DNA and resolving the DNA structure (Wang, 2002). They have been implicated in such critical cellular functions as transcription, DNA replication, repair and recombination. Type I topoisomerases are monomeric, cleave one strand of duplex DNA, and require no energy cofactor. In contrast, the type II enzymes function as dimers, cleave both strands of the DNA, and pass an intact DNA duplex through the transient double-stranded break in an ATP-dependent manner (Wang, 1996).

Cellular aging appears to be accompanied by a reduced ability to respond to certain stresses that might lead to such DNA damage. Several studies have indicated that the cell defense mechanism against DNA damage may involve altered molecular events involving the transcriptional activation of a number of genes that may change during the aging process (Richardson, 1985; Pandey and Wang ,1995; Sarkar and Bolander, 1995).

An important role for Topo I in DNA repair has been clearly indicated from a number of studies, but they involve only actively proliferating cultured cells (Beck and Danks, 1991; Henningfeld and Hecht , 1995). There is an increasing evidence to suggest that DNA topoisomerases may act in concert with certain repair associated proteins like RecQ helicases to preserve genomic integrity. Previous studies in bacteria and yeast have identified an interaction between Topoisomerases and members of the RecQ helicase family. In Escherichia coli, RecQ and topo III together catalyze the linking and unlinking of covalently closed circular DNA molecules (Harmon et al., 1999). The yeast homologue of RecQ helicases, SGS1, interacts both physically and genetically with a type I topo, topo III. Mutations in SGS1 partially suppress the pleiotropic effects of TOP3 mutations, suggesting that Sgs1p and Top3p act in the same pathway (Gangloff et al., 1994; Onodera et al., 2002). Wu et al., (2000) have shown that the Bloom protein (BLM) also interacts with human topo III and have

reported recently that BLM stimulates the ability of topo III to relax supercoiled DNA (Wu and Hickson, 2002). Furthermore, a previous study found that topo I was coimmunoprecipitated with an antibody against WRN from human colon carcinoma SW480 cell extracts (Lebel et al., 1999). Topo IIα is only present in proliferating tissues, tumors, while TopoIIβ is present in all tissues, including terminally differentiated tissues (Bauman et al., 1997; Hsiang et al., 1988; Tsutsui et al., 2001a). A number of recent studies have suggested that TopoIIβ plays a role in neuronal differentiation. In TopoIIβ knockout mice, motor neuron axons fail to innervate the diaphragm muscles and sensory neuron axons fail to enter the spinal cord, suggesting a role of TopoIIβ in axon growth and/or guidance (Yang et al., 2000). Studies of brain-specific TopoIIβ knockout mice have also revealed a major defect in corticogenesis during brain development (Lyu and Wang, 2003). Also topo II beta is shown to be associated with the core NHEJ proteins (Bong-Gun et al., 2006). Both the levels of Type I (Topo I) and Type II (Topo IIα & IIβ) Topoisomerases have been shown to be decreasing with age in catalytic activity and levels (Kondapi et al., 2004; Plaschkes, 2005). The association of DNA toposiomerases with certain repair genes WRN and BLM helicases, the mutations of these genes are known to cause premature aging disorders (Karow et al., 2000), characterized by the early onset of age-related clinical features.

In the present study, we have analyzed the levels of Type I and Type II Topoisomerases in aging CGNs *in vitro* and aging whole brain of rat *in vivo*.

Results:

Type I Topoisomerase levels in aging CGNs *in vitro* and aging whole brain of rat *in vivo*:

Analysis of the gene expression (mRNA) levels of Topo I, Topo IIIα and Topo IIIβ during 1-5 weeks of CGNs in culture showed that Topo I, III α and IIIβ are significantly present during 1st - 3rd weeks of CGNs in culture, while levels of Topo I

and IIIβ decrease at 4th-5th week (Fig 4.1 A) suggesting that the levels of Topo I and IIIβ decrease during aging. Further, Topo IIIα increased marginally from 1st - 4th week of CGNs in culture, while remains the same at 5th week (Fig 4.1 A). Consistent with these observations, the expressed protein and mRNA levels of Topo I and IIIβ indeed remained high in young and adult rat brain extracts, while their levels decrease in old rat brain extracts (Fig 4.1 B, 4.3). These results suggest that Topo I and Topo III β are present till adult stages both in CGNs (3rd week) and rat brain (adult), while the levels decrease during aging in CGNs (5th week) and rat brain (old).

Type II Topoisomerase levels in aging CGNs *in vitro* and aging whole brain of rat in *vivo*:

Topo IIα and Topo IIβ levels were analyzed in aging CGNs in culture and aging rat whole brain extracts. The Analysis of gene expression levels of Topo IIα and Topo IIβ during 1-5 weeks of CGNs in culture showed that Topo IIα and β levels were high at 1st week, followed by marginal decrease at 2nd week and 3rd week, while the levels of these enzymes significantly decreased by 4th week and become very low by 5th week in culture (Fig 4.2 A). Consistent with these observations the Topo IIβ is high in young, decreased in adult and become very low in old rat brain extracts (Fig 4.2 B, 4.3). These results suggest that the level of Topo IIβ decreases during aging of CGNs as well as in rat whole brain extracts. The expression of Topo IIα in 1st week in CGNs and young rat brain extracts could be due to the presence of undifferentiated neuronal stem cells. There was a significant decrease in Topo IIα in 2nd week and 3rd week of CGNs, which become negligible in 4th and 5th week.

In case of rat whole brain extracts, Topo IIα observed at young showed a significant decrease in old both in m-RNA as well as of protein levels. The above results clearly establish that the levels of Topoisomerases in CGNs are in close comparison with aging *in vitro* (in culture) and *in vivo* (in whole brain), where the observed levels in 1st week culture are comparable to young, while 3rd week in culture to adult and 5th week of culture to that of old.

Figure 4.1

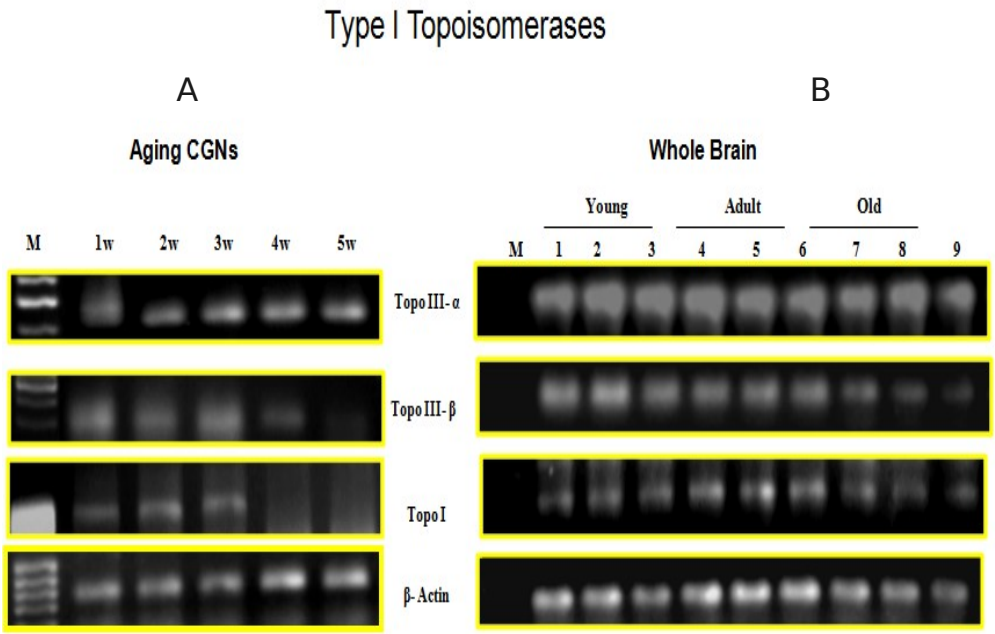

Fig 4.1 Semi quantitative RT- PCR analysis of Topo I, III (α & β) in aging CGNs *in vitro* (1-5 weeks) in Panel A and aging rat whole brain eaxtracts, young (< 10days) (lanes 1-3), adult (> 6 months) (lanes 4-6) and old (> 18 months) (lanes 7-9) in Panel B. β- actin was used as internal control.

Figure 4.2

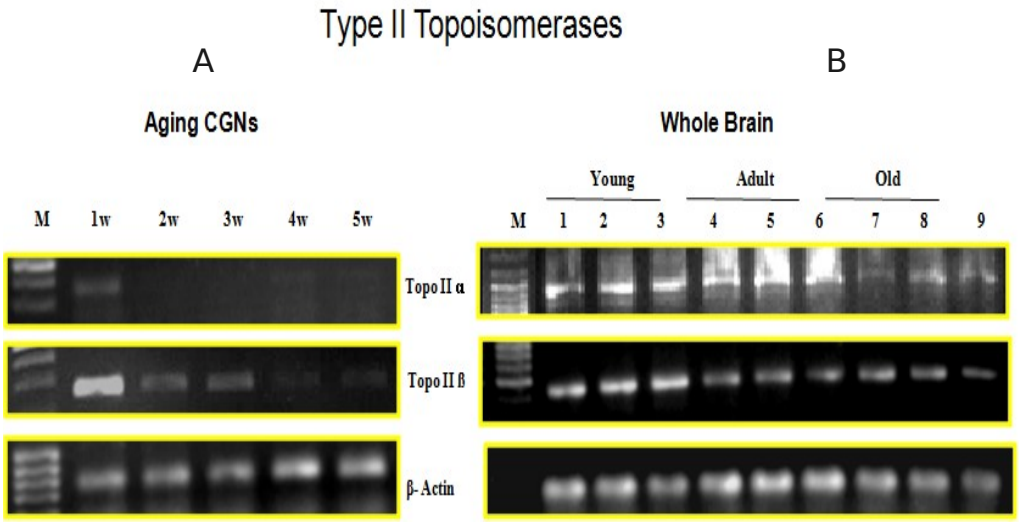

Fig 4.2 Semi quantitative RT- PCR analysis of Topo, II (α & β) in aging CGNs *in vitro* (1-5 weeks) in Panel A and aging rat whole brain extracts, young (< 10days) (lanes 1-3), adult (> 6 months) (lanes 4-6) and old (> 18 months) (lanes 7-9) in Panel B. β- actin was used as internal control.

Figure 4.3

Age dependent changes of Topoisomerases in rat whole brain.

A

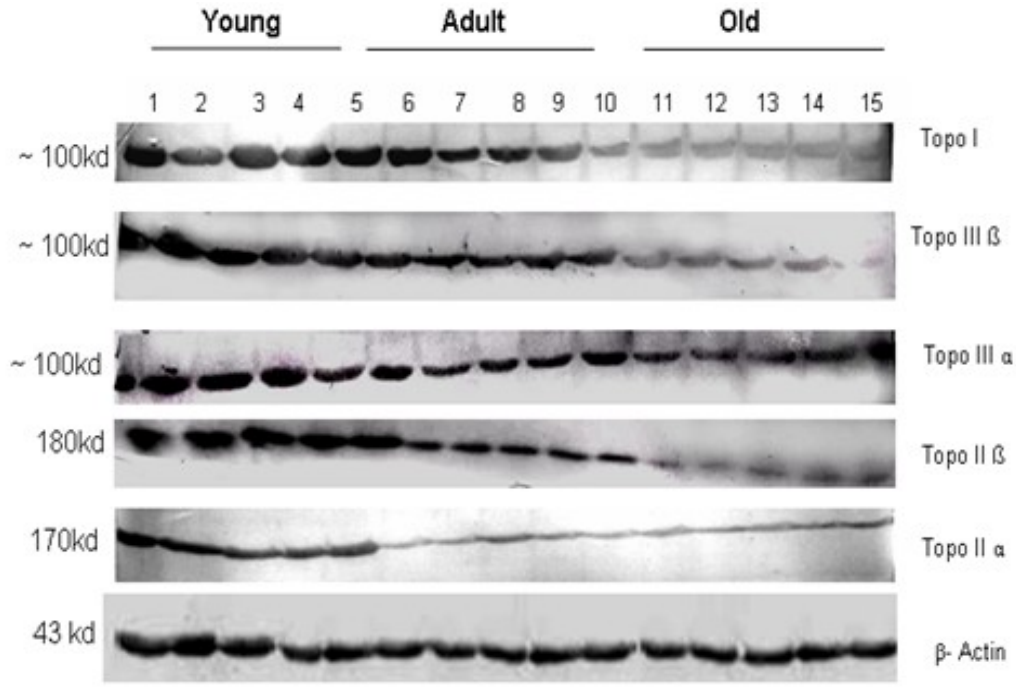

B

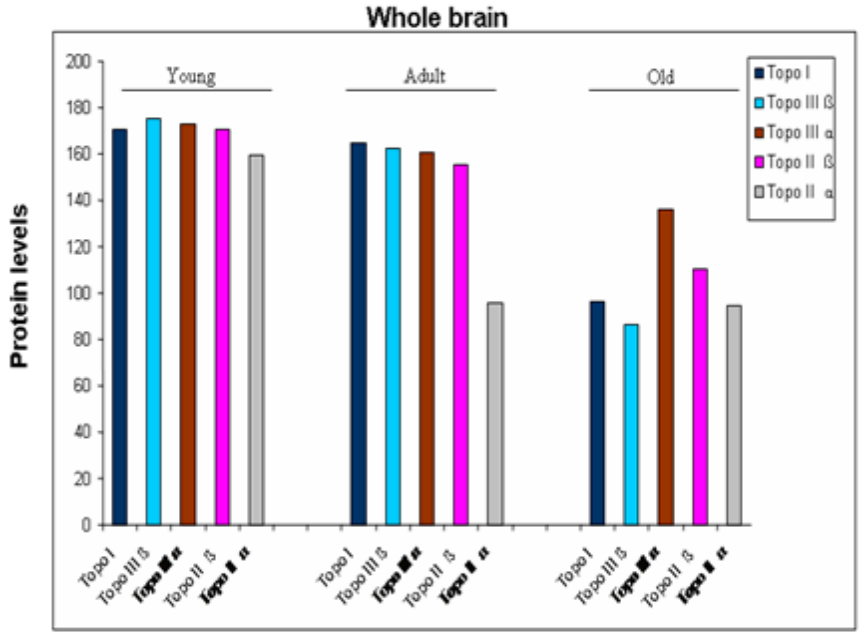

Fig 4.3 Immunoblotting analysis of age dependant changes of Topo I, III (α & β), II(α & β) in rat whole brain; young (< 10 days) (lanes 1-5), adult (> 6 months) (lanes 6-10) and old (> 18 months) (lanes 11-15) in Panel A. β- actin was used as internal control. Panel B represents the densitometricaly quantified protein levels of Topo I, III (α & β), II(α & β) normalized with β- actin using Image J software *(NIH, USA).*

Discussion:

The results of Type I (Topo I, IIIα and β) and Type II (Topo II α and β) Topoisomerases in aging CGNs (1- 5 weeks) *in vitro* and aging rat whole brain (young (<10 days), adult (> 6 months) and old (> 18 months) shows that, the different types of topoisomerases are predominant in brain and CGNs *in vitro.* Earlier studies from our lab have shown higher catalytic activity and protein levels of the topo II β isoforms in rat cerebellar extracts (Kondapi et al., 2004). The studies of Tsutsui et al. (1993, 2001) on localization of Topo II isoforms in developing rat brain also showed that developing rat cerebellar region possess high levels of Topo II β during the early post-natal period suggesting the importance of Topo II β in rat cerebellum in its development and growth. Results also suggest age-dependent changes of Topo II α and β suggested that α isoform remains low and unaltered with age, while the activity of β isoform is higher in young, moderate in adult and low in old rat cerebellar region suggesting an age-dependent decline in Topo II β protein and activity(Kondapi et al., 2004). Consistent with these above findings, the present studies shown an decrease in expression levels of Topo II β isoforms both in aging CGNs *in vitro* and *in vivo* (Fig 4.2, 4.3). While Topo II α isoform is absent in aging CGNs from 2nd week onwards further confirming the absence of Topo IIα isoform in post mitotic cells like neurons. The initial expression of Topo II α isoform in the 1st week of CGNs in culture may be due to mitotic astroglial cells (Fig 4.2 A). The present results also suggest that neurons possess significant Topo II β. Studies of Woessner et al., (1991) showed that in developing rat neurons Topo II β is present is Purkinjee and granule neurons during development suggesting that Topo IIβ is expressed in cerebellar neurons during cerebellar development and growth. Since Topoisomerases are reported to be involved in promiscuous recombination, and cellular response to radiation damage of DNA (Asami et al., 2002; Kohji et al., 1998; Ishii and Ikushima, 2002; Pastor and Cortes, 2002; Franchitto et al., 2000; Wu et al., 1999), the above results on the decreased expression of Topo II β in aging CGNs *in vitro* may be correlated as one of the factors contributing towards decrease in repair activity in aging neurons as Topo II β may be required for resolving certain topological restrictions formed during DNA rearrangements that take place in DNA repair.

Topoisomerase I is known to predominantly participate in transcription (Gilmour et al., 1986; Elgin and Gilmour, 1987; Kretzschmar et al., 1993; Merino et al., 1993). Since neurons are fully differentiated, nonmitotic, but metabolically active cells, it may be associated with certain regulators. Recent studies demonstrated the high topo I activity in various brain regions with a specific distribution pattern in neurons and also show that the activity and level of topo I is age- and gender-dependent which increases from birth to maturity and decreases, more significantly in males, with senescence. (Plaschkes, et al., 2005). Moreover, the heterogeneous distribution of topo I suggests that topo I has an important, if as yet undefined, role in neuronal function, especially in post mitotic cells like neurons. In the above studies we show the predominant expression of Topo I, IIIα and IIIβ in the aging CGNs *in vitro* and rat whole brain. The Topo I and Topo III β show an age-dependant decline both in aging CGNs *in vitro* and rat whole brain extracts (Fig 4.1, 4.3). While Topo III α show a consistent expression not changing significantly both in aging CGNs *in vitro* and rat whole brain (Fig 4.1 A). This suggests Topo III α may have a role in neuronal survival. This observation is supported by the results of studies on the gene encoding Topo III*α* in mice, where a disruption of it causes embryonic lethality (Li and Wang 1998), while mice lacking DNA topoisomerase III ß develop to maturity but show a reduced mean lifespan (Kwan and Wang, 2001).

The varied expression of different Topoisomerases and their isoforms in rat brain and CGNs *in vitro* suggest distinct roles shared by these enzymes in development and functioning of brain and suggest a possible role in brain aging. Further, the close comparison of CGNs in culture and rat brain extracts *in vivo* demonstrate that CGNs represent a best model to elucidate the functions of Topoisomerases in aging.

CHAPTER -5

DNA Repair capacity of cultured CGNs; Topo II β, a potential senescence marker

Introduction:

Aging is a multifactorial phenomenon, and of the many theories that have been proposed to explain the process of aging, those that explain the process at the genetic level, e.g., DNA damage and repair theory (Hart and Setlow, 1974; Gensler and Bernstein, 1981), have attracted much attention. Accumulation of DNA damage as a function of age was reported by some workers. Single-strand breaks (SSBs) (Price et al., 1971; Chetsanga et al., 1977) and Double strand breaks (DSBs) (Bhaskar and Rao, 1994) were reported to accumulate in aging neurons.

The error-free maintenance of nuclear DNA is critical to cellular and organismal function. The maintenance of the efficiency of cellular DNA repair machinery is an important facet for cellular stability, which itself may become deficient with age. In neurons double strand breaks (DSBs) in DNA are predominantly repaired via the nonhomologous end-joining (NHEJ) and homologous recombination (HR) pathways, whereas lesions on a single strand of DNA are repaired via base excision repair (BER) and nucleotide excision repair (NER) mechanisms. NHEJ is the predominant pathway in post mitotic cells such as neurons. NHEJ is mediated by at least six core factors, four of these proteins are, Ku80, Ku70, Ligase IV, and XRCC4. These proteins are conserved from yeast to mammals (Jeggo, 1998; Lewis and Resnick, 2000). They are indispensable for all NHEJ reactions, in mammalian cells and loss of NHEJ by mutations in Ku70, Ku80, or DNA ligase IV lead to hypersensitivity to ionizing radiation (Adachi et al., 2001; Critchlow and Jackson, 1998). More recently even topo II beta is shown to be associated with the core NHEJ proteins (Bong-Gun et al., 2006), suggesting a role for topo II beta in NHEJ activity. The decreasing activity of topoII β with aging (Kondapi et al., 2004) points out to its possible role in DNA repair activity in neurons during aging.

The aim of the present study is to estimate the DNA repair capacity of CGNs, when SSBs and DSBs were induced and to further analyze the role of Topo IIβ in aging, cultured CGNs *in vitro*.

Results:

Repair efficiency of aging CGNs *in vitro*:

Efficiency of Base excision repair:

Ethylnitrosourea (ENU) is an alkylating agent that causes alkylation of bases that leads to formation of single strand breaks (SSBs). Cultured CGNs at indicated weeks in culture were challenged with ENU for 12 hours (Damage) and washed and recultured (Recovery) for 24 hours (see Materials and Methods). The extent of single strand cleavage was estimated by alkaline comet assay. The results (**Figure 5. 1)** show that the sensitivity of CGNs to ENU increases with increase in age of the cultures, reaching a maximum by 4^{th} week, while the recovery efficiency of CGNs reaches a minimum by 4^{th} week, suggesting a reduced single strand break repair capacity (probably BER repair) in aging CGNs in culture.

Double strand break repair of CGNs:

Double strand breaks (DSBs), generally believed to play an important role in aging process, are frequently occuring events in mammalian somatic cells, where they are commonly repaired by NHEJ. NHEJ activity of CGNs at different ages was analyzed by *in vitro* NHEJ activity assay. The results presented in Fig 5.A and B show that the NHEJ activity in terms of plasmid multimerization was higher at 1^{st} week of CGNs in culture, which decreased significantly at 3^{rd} week, that further decreased by 4^{th} week of CGNs in culture and becomes negligible at 5^{th} week. Thus suggesting that DSB repair activity of the cultures was higher in young (1^{st} week), decreases in adult (3^{rd} week) and becomes negligible in old (5^{th} week). A similar observation has been reported in rat brain extracts, where in the repair activity is higher in young, followed by a decrease in adult and low in old rats **(**Vyjayanti and Rao, 2006**).**

Genes involved in DNA repair:

To investigate whether the decreased efficiency of neurons in supporting NHEJ activity is due to corresponding decrease in NHEJ proteins, semi quantitative RT-PCR was conducted. The topo II β m-RNA levels were found to show a significant decrease from 2nd week of CGNs in culture, reaching negligible levels by 4th week of CGNs in culture, similar to that observed in the case of Ku70 and Ku 80. In contrast, polymerase β (Pol-β) levels were found to be stable till the 3rd week and decreased to a negligible level by the 4th week **(Fig 5.3)**. These results point out that the NHEJ proteins especially Ku 70, Ku 80 and topo IIβ have decreased with age **(Fig 5.3)** along the line of NHEJ activity **(Fig 5.2)**. To further confirm the important role played by topo IIβ, the protein levels of topo IIβ were quantified. The results presented in **Figure 5.4 A,B** clearly show a age-dependent decrease of topo IIβ levels in CGNs, which is further confirmed by quantitative RT-PCR **(Fig 5.4 C).** The decrease in NHEJ activity is thus strongly correlated with the corresponding decrease in Ku 70, Ku 80 and topo IIβ.

Figure 5.1

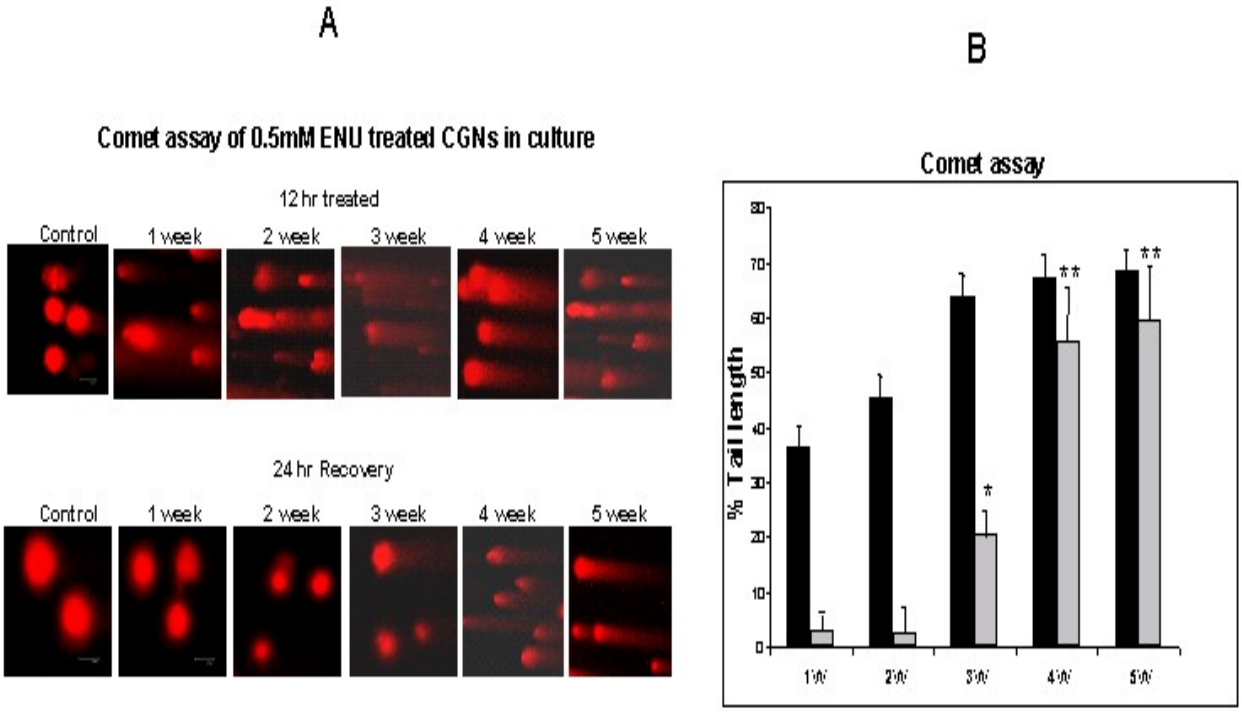

Fig 5.1. Efficiency of Base excision repair in aging CGN cultures. DNA repair efficiency of SSBs (single strand breaks) in the aging cerebellar granule neurons (CGNs) *in vitro* was assessed using alkaline comet assay. CGNs *in vitro* showed age-dependent decrease in recovery after 12 hour of treatment with 0.5 □M ENU, the DNA damaging agent used, followed by 24 hr recovery. Representative pictures are presented in (A). The degree of damage is assessed through measurement of the extent of tail movement, which is the product of tail length and fraction of DNA in the comet tail as presented in the Bar graph (B). (*$p<0.05$; **$p< 0.01$) according to Student's t-test.

Figure 5.2

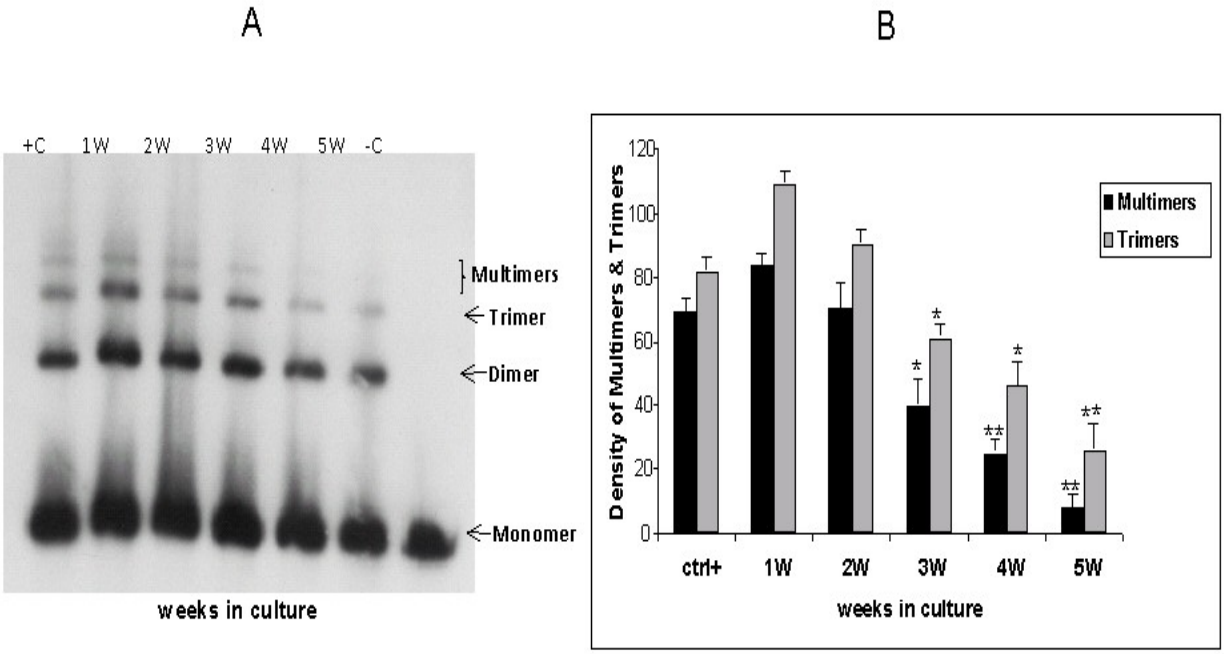

Fig 5.2. Efficiency of double strand repair in aging CGN cultures. This was assessed by *in vitro* functional NHEJ assay using protein extracts from aging CGNs in culture, NHEJ activity was analyzed in terms of plasmid multimer and trimer formation as shown in the represented autoradiogram (A). The amount of multimer and trimer formation was measured densitometricaly using J-Image software (NIH, USA) and the values are represented as bar graph (B). Experiments have been performed in triplicate and repeated independently three times. (* $p<0.05$; ** $p< 0.01$) according to Student's t-test.

Figure 5.3

A

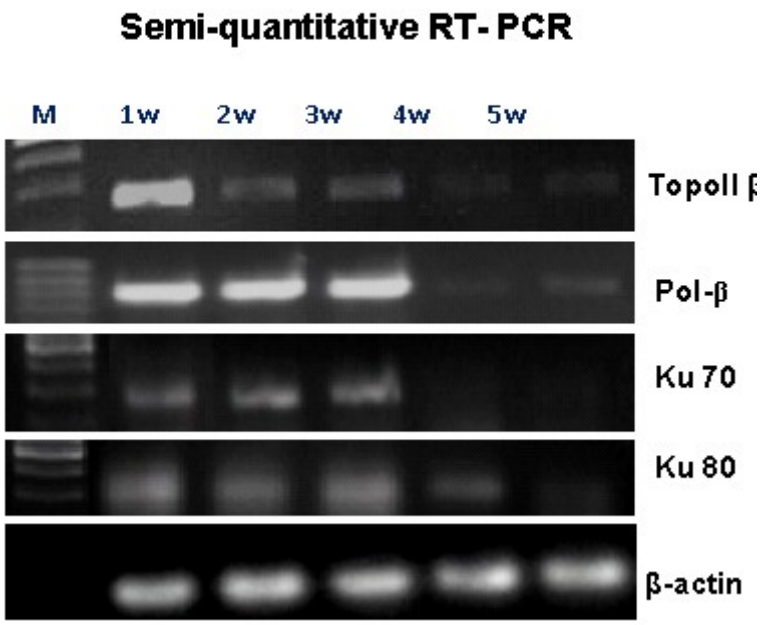
Semi-quantitative RT- PCR
M
1w
2w
3w
4w
5w
Topoll β
Pol-β
Ku 70
Ku 80
β-actin

B

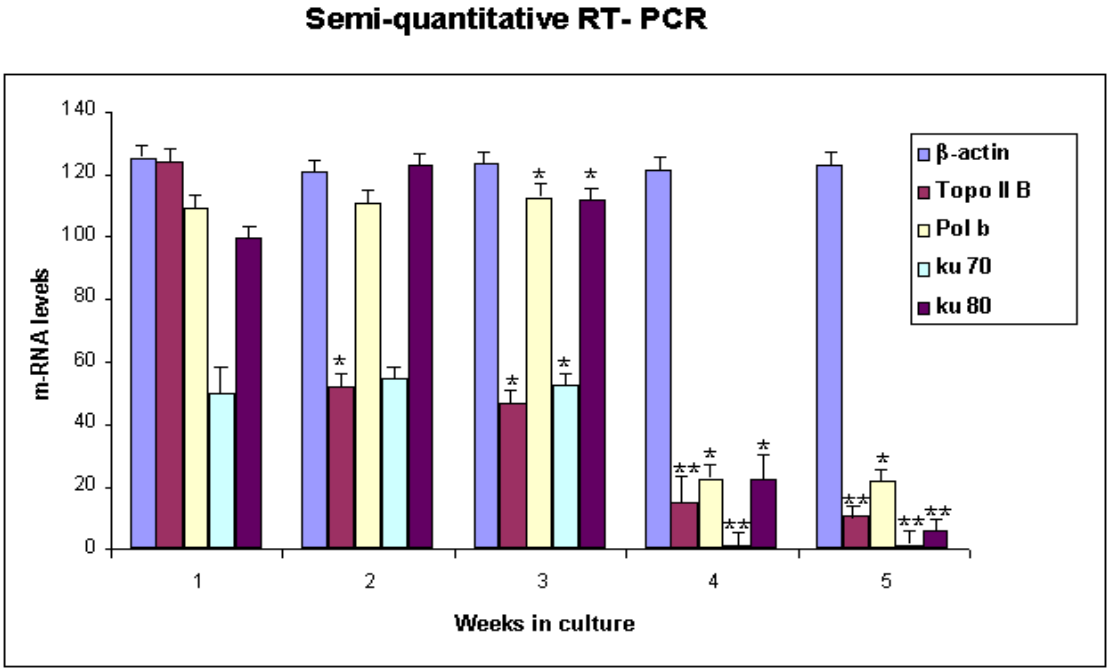
Semi-quantitative RT- PCR
m-RNA levels
Weeks in culture
β-actin
Topo II B
Pol b
ku 70
ku 80

Fig 5.3. Semi-quantitative RT-PCR of proteins associated with NHEJ pathway. Semi quantitative RT- PCR analysis of mRNA of DNA Polymerase-β, Ku-70, Ku-80 and topo II β in extracts of cultured CGNs. (A) Agarose gel electrophoretic analysis of PCR products Pol-β, Ku-70, Ku-80 and topo II β. ß-actin is included as internal control. (B) Bar graph representing the densitometricaly measured agarose gel in (A). Experiments have been performed in triplicate and repeated independently three times (* $p<0.05$; ** $p< 0.01$) according to Student's t-test.

Figure 5.4

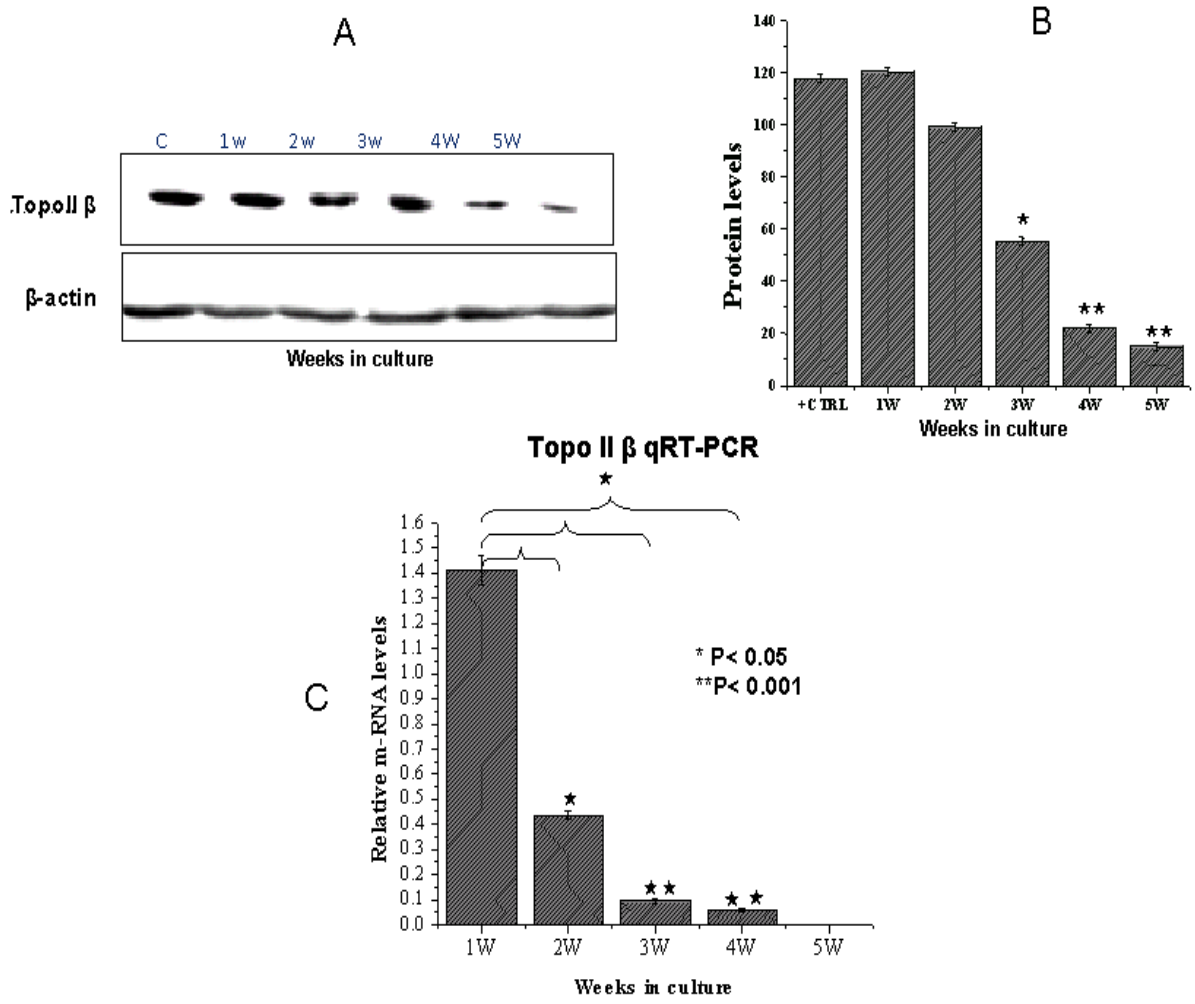

Fig 5.4. Topo IIβ in aging CGN cultures. (A) Results of immunoblot analysis of topo IIβ with ß-actin as loading control, in cultured CGNs at indicated time of cultures, (B) Results based on the densitometricaly measured immunoblot (A) using J-Image software (NIH, USA), which is normalized with β-actin (* $p<0.05$; **$p< 0.01$) according to Student's t-test.. (C) Bar Graph representation of the topo II β levels measured at m-RNA levels by quantitative RT-PCR. Relative gene expression was determined based on the threshold cycles (Ct) of topo II β and of internal reference gene β-actin. Statistical comparisons were made using one-way ANOVA followed by Bonferroni's multiple comparison test. *$p<0.05$, **$p< 0.001$. Experiments have been performed in triplicate and repeated independently three times.

Discussion:

The present results clearly bring-out that aging granule neurons become deficient in topo IIβ leading to near cessation of NHEJ activity from the 5th week of culture and topo IIβ has thus emerged as an additional marker for NHEJ pathway and aging. The major factors contributing to the aging and degeneracy of functional activity of brain are due to decreased DNA repair potential (e.g., Rao et al., 1997; 2003). It was indeed shown in the case of rat neurons that both single (SSB) and double strand breaks (DSB) in nuclear DNA, accumulate with age (Mandavilli et al., 1996). Ganoderiol F (GoIF), a ganoderma triterpene, an inhibitor of topoisomerases *in vitro*, is reported to induce senescence in hepatoma HepG2 cells (Chang et al., 2006). Short-term exposure of HepG2 cells to GolF temporarily arrested the progression of the cell cycle and the cell growth recovered when the drug was withdrawn after a 24-h exposure. After 18 days of continuous treatment of HepG2 cells with 30 mM GolF, over 50% of cells were found to be enlarged and flattened, and were found to be beta-galactosidase positive phenotypes of senescent cells. Activation of the mitogen-activated protein kinase EKR and up-regulation of cyclin-dependent kinase inhibitor p16 were found in early stages of GolF treatment and were presumed to cause cell-cycle arrest and trigger premature senescence of HepG2 cells (Chang et al., 2006).

In normal human fibroblasts, senescence induced by oncogenic H-ras displays a cellular phenotype nearly identical to that of replicative senescence, suggesting the activation of common senescence mechanisms in replicative and terminally replicative senescence. Topoisomerase IIα and HDAC9 gene expression were specifically altered under different conditions associated with senescence in H-ras-induced senescent cells. These cells exhibited specific down regulation of genes involved in G2/M checkpoint control and contained tetraploid cells that were arrested in a G1 state (Mason et al., 2004) suggesting that topo IIα could serve as one of the markers for senescence.

Topo IIα gene expression levels are known to be high in proliferating tissues, such as bone marrow and spleen, and are undetectable or low in 17 other tissues. In contrast, high or intermediate levels of expression of topo IIβ gene were found in a variety of tissues of adult mice, including those with non proliferating cells. These isoforms were differentially regulated in the post-natal period, and a tissue-specific role is suggested for the two isoenzymes in the development of differentiated tissues such as the brain and the liver (Capranico et al., 1992). Between the two isoforms of topo IIβ isoform is predominantly found in brain tissue, while topo IIα is found in embryos up to post-natal day 1. Beta isoform showed highest activity in cerebellar region as well as in neuronal cell fraction (Kondapi et al., 2004). Strong signals pointing out to presence of topo IIα mRNA were detected in the ventricular zone of brain region at embryonic day 13-15 (E13-E15), and in the external granular layer of the cerebellum at postnatal day 7-14 (P7-P14) followed by a steep decrease in signal levels (Watanabe et al., 1994).A significant age-dependent decrease in activity of topo IIβ has been observed in brain specifically in cerebellum (Kondapi et al., 2004). Further, topo IIβ knock-down neurobalstoma cells were shown to be sensitive to DNA damaging agents due to decreased repair capacity of neurons (Mandraju et al., 2008). These observations suggest that the low levels of topo IIβ activity in aging cerebellum may contribute to the genomic instability in cerebellar region of aging brain.

The NHEJ activity of the whole cell extracts in the present study was measured through plasmid end-joining based multimerization assay. The NHEJ activity is generally known to be mediated by four conserved core factors. Four of these proteins, Ku80, Ku70, Ligase IV, and XRCC4, are conserved from yeast to mammals; they are indispensable for all NHEJ reactions. Recently another protein topo II beta was shown to be associated with the core NHEJ proteins (Bong-Gun Ju et al., 2006) suggesting a role for topo II beta in controlling NHEJ activity. Earlier studies showed a deficiency in DSB repair in topo IIβ siRNA mediated down regulated cells implying, the significance of Topo II β for NHEJ activity (Mandraju et al., 2008). The present results (**Figure 5.2)** also show a higher NHEJ activity of cultured CGNs at 1st

week, with the activity significantly decreasing by 3rd week and reaching a minimum by 5th week. NHEJ and BER repair activities which are shown to be predominant in the initial phase of cellular aging decrease during the later phases and, in the present study such a decrease was observed from 3rd week of cultured CGNs. This decrease in the repair activities results in enhancement of the vulnerability of neurons to damaging agents and, thus introduce errors in certain genes causing senescence which in turn leads to neuronal depletion with aging. These results point out that topo IIβ could serve as an additional biomarker for evaluating senescence and DNA repair efficiency especially in respect of NHEJ activity in aging neurons.

CHAPTER -6

Role of Topoisomerase I in neuronal development

Introduction:

DNA Topoisomerase I (Topo I), is an enzyme involved in DNA rearrangements, transcription and replication. Topo I is indispensable during processes leading to cell development and also during cell division (Lee et al., 1993). Inactivation of Topo I affects the rate of transcription in *S. cerevisiae* **(**Di Mauro et al., 1993). Experiments with yeast Topo I mutants show that for cell growth Topo I is not indispensable (Thrash et al., 1985) and (Uemura and Yanagida, 1984). This is not the case with *Drosophila melanogaster*, in which Topo I is essential for development during post blastocyst stage (Lee et al., 1993).

Topo I is a crucial enzyme for cell growth and embryo development (Morham et al., 1996). Mammalian Topo I belongs to type IB subfamily. It plays key roles in DNA replication, transcription, and recombination. The members of the type IB subfamily of Topo I share no sequence or structural homology with other known Topoisomerases (Caron and Wang, 1994) and are functionally distinct from the members of the type IA subfamily. The activity and level of Topo I is age as well as gender-dependent, it increases from birth to maturity and then decreases, more significantly in males, with senescence. This shows a possible role of Topoisomerase I activity and regulation in various brain functions (Plaschkes et. al., 2005).

Camptothecin is one of the chemotherapeutic agents poisoning the catalytic activity of Topo I through formation of single strand protein-DNA crosslinks. Irreversible DNA double- strand breaks are produced during DNA synthesis in the presence of camptothecin, suggesting that this agent should not be toxic to non-dividing cells, such as neurons. Unexpectedly, camptothecin is found to induce significant, dose-dependent cell death of post mitotic rat cortical neurons in vitro, while astrocytes are more resistant (Morris and Geller, 1996). Although many studies link Topo I to important cellular functions, the precise role of the enzyme in these processes remains obscure.

Granule neurons are the most abundant type of neurons in the brain. The granule neurons, in addition to their sheer volume and homogeneity of their population together with the fact that they can be transfected with ease render them ideal for neurotoxic studies.

In the present study, we have analyzed the neurotoxic activity of Topo I inhibitor, camptothecin, in cultured CGNs and analyzed the role of Topo I in drug-mediated neurotoxicity versus siRNA mediated down-regulation of enzyme.

Results:

siRNA mediated Transient down regulation of Topoisomerase I.

siRNA-mediated transient downregulation of Topoisomerase-I CGNs transfected with Topo-I siRNA and camptothecin for 16 h were analyzed to determine protein and mRNA levels with immunoblotting and semi-quantitative RT-PCR, respectively, using Topo-I-specific monoclonal antibodies and PCR primers, as described above (Chapter 2 Methods). The immunoblotting analysis and RT-PCR studies show a nearly 80% decrease in Topo-I in 0.5 mM Topo-I siRNA-transfected CGNs. Camptothecin (10 mM) showed no marked effect on the Topo-I mRNA and protein levels **(Fig.6.1).** Fluorescence confocal images **(Fig. 6.6)** confirm the efficient downregulation of Topo-I with siRNA, whereas no significant change was observed in control and camptothecin treated CGNs.

Effect of Topo-I-siRNA and Camptothecin on viability of CGNs.

The effect of Topo-I-siRNA and camptothecin on the viability of CGNs in culture was tested using MTT assay as described in (Chapter 2 Methods). Increasing concentrations of camptothecin and Topo-I-siRNA was used to test the viability of

CGNs **(Fig 6.2).** Camptothecin showed cytotoxicity starting at 1µM decreasing the viability to more than 50% at 10µM. Topo-I-siRNA showed only a 20% decrease in viability at 0.5 µM at a concentration corresponding to more than 80% downregulation of Topo-I **(Fig. 6.1)** and there was no change even at higher concentrations of siRNA. These results show that siRNA mediated down regulation of Topo-I was achieved under these conditions.

Figure 6.1

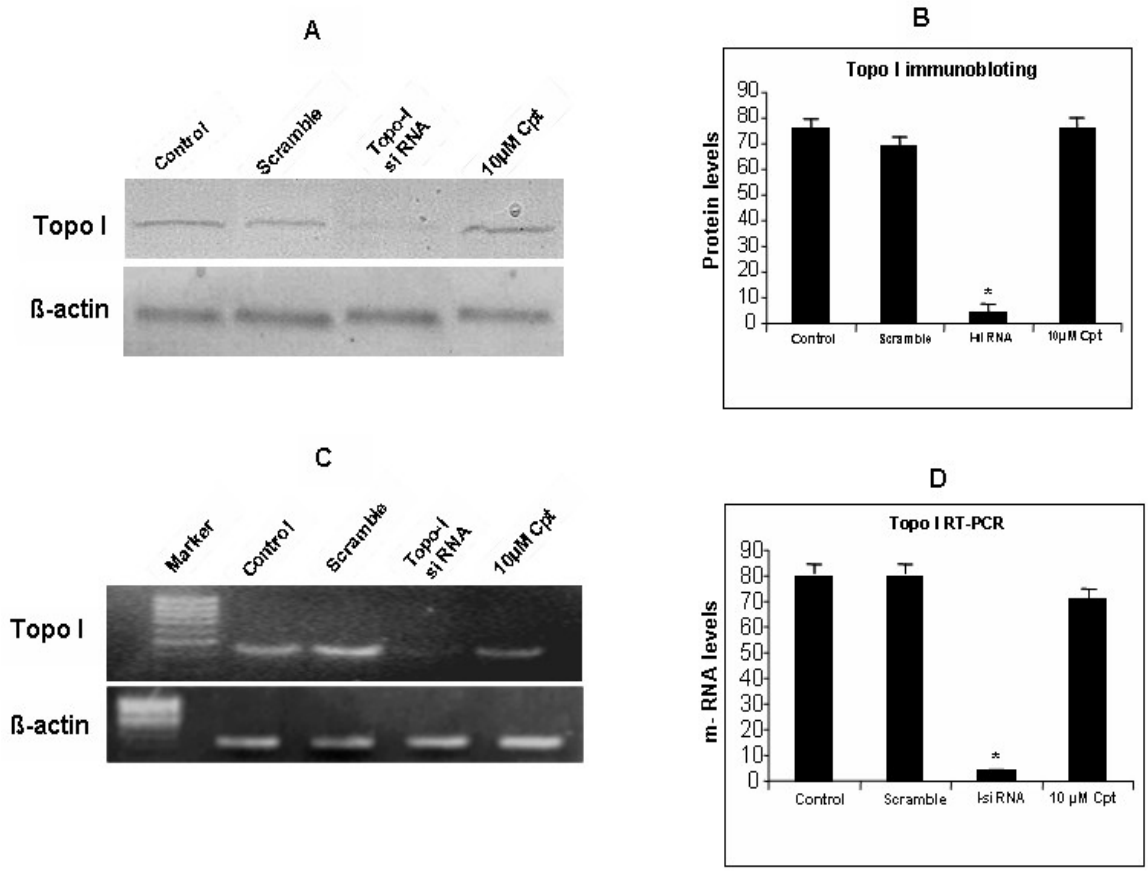

Fig 6.1. Protein and mRNA levels of Topo-I in siRNA-transfected and camptothecin-treated CGNs. Following 16 h of siRNA transfection or camptothecin (Cpt, 10 mM) treatment, cultured CGNs were used for protein and RNA isolation and were subjected to immunoblotting and semi-quantitative RT-PCR. Panel A shows the immunoblot of a ~100 kD Topo-I protein with a 43 kD b-actin as an endogenous control; Panel B represents the corresponding densitometric graph. Panel C shows the amplification of Topo-I and bactin m-RNA by PCR followed by separation on a 1% agarose gel with the corresponding densitometric data in Panel D. The results clearly show a significant decrease in Topo-I protein and mRNA levels (_80%), which suggests there was efficient downregulation of Topo-I using siRNA, while camptothecin induced no significant decrease in these levels. Data are presented as the mean ± SD in three independent experiments; *$p < 0.05$.

Figure 6.2

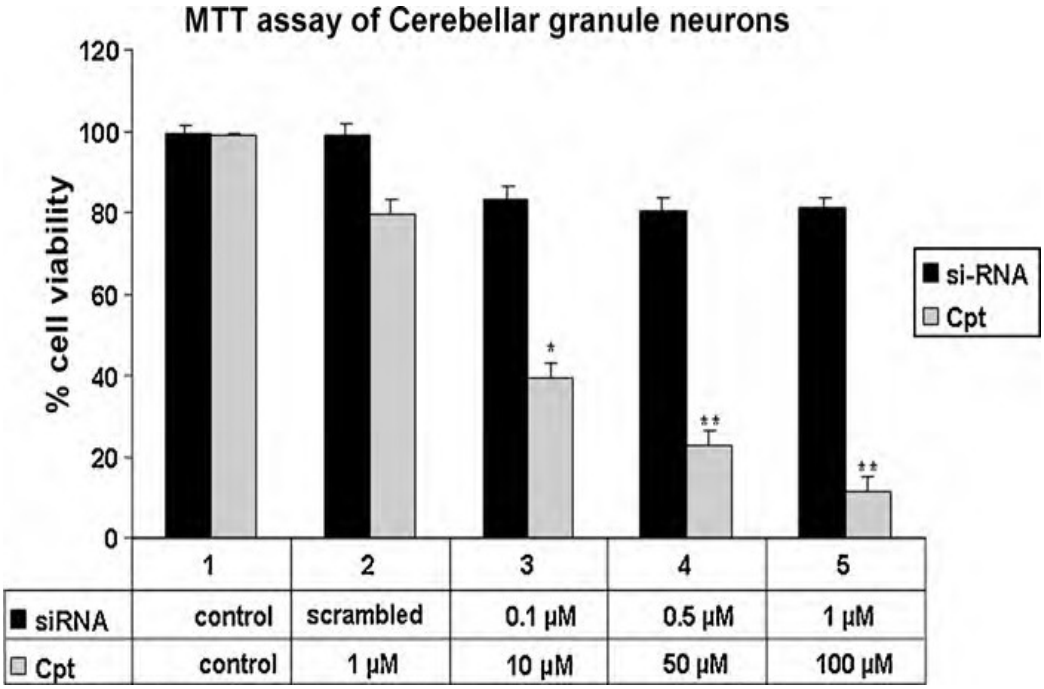

Fig 6.2. MTT assay for viability of CGNs. Acolorimetric-basedMTTassaywas performed to examinethesurvival ofCGNsunder siRNAtransfectionorcamptothecin treatments using 1-day-old CGNs in culture. The data are represented in termsof % cell viability of CGNs at the indicated concentrations of siRNA or camptothecin. The bar graph clearly shows a decrease in CGN viability with increasing camptothecin concentrations, whereas there was no significant change with increasing concentrations of Topo-I siRNA. Data are presented as the mean ± SD in three independent experiments; *$p < 0.05$ and **$p < 0.01$ as compared to the normal control.

Comparison of apoptosis in Topo I siRNA transfected and Camptothecin treated CGNs .

Camptothecin is known to induce caspase-3 dependant death of cortical neurons (Stefanis et al.,1999) and (Keramaris et al., 2000), which plays a central role in the execution-phase of cellular apoptosis. As a measure of apoptosis, caspase-3-activity was assessed by extent of cleavage of the fluorogenic substrate Ac-DEVD-AMC by neuronal lysates prepared after transfection with Topo I siRNA and camptothecin treatments. As shown in **Figure 6.3**, there is elevation in caspase-3 activity in camptothecin treated cell extracts while Topo I siRNA transfected extracts did not show any marked increase. Further we have used FACS analysis of Annexin V as an additional measure of apoptosis. As one of the earliest indications of apoptosis is the translocation of the membrane phospholipid phosphatidylserine (PS) from the inner to the outer leaflet of the plasma membrane to which Annexin V binds (Vermes et al., 1995).

FACS analysis of FITC- apoptotic cell population showed a marked increase of about 20% in 10µM Cpt while 0.5 µM Topo I siRNA transfected CGNs didn't show any significant increase (~ 5%) in Annexin-V positive cells (FITC) **(Fig 6.4).** This further confirms that it is camptothecin, not Topo I siRNA that induces a high degree of apoptosis in CGNs. These results suggest that the increase in apoptosis is not due to the cells devoid of Topo I, but rather due to the induction of pro-apoptotic factors by the protein-DNA- camptothecin cross link mediated signaling or single stranded DNA break intermediates.

Comparison of overall protein expression in Topo I siRNA transfected and Camptothecin treated CGNs.

Action of Topo I down regulation on overall protein expression in siRNA and camptothecin treated granule neurons was studied using *in vitro* S^{35} methionine incorporation assay as outlined in materials and methods. The autoradiogram **(Fig 6.5**

B) and S^{35} radiolabel counts **(Fig 6.5 C)** show decreased S^{35} methionine incorporation in the protein extracts of Camptothecin but not in Topo I siRNA transfected samples. This suggests Topo I has no significant role in regulation of protein expression. This effect induced by camptothecin may be due to factors like DNA strand breaks that may be involved in induction of apoptosis, proteolysis and DNA fragmentation.

Figure 6.3

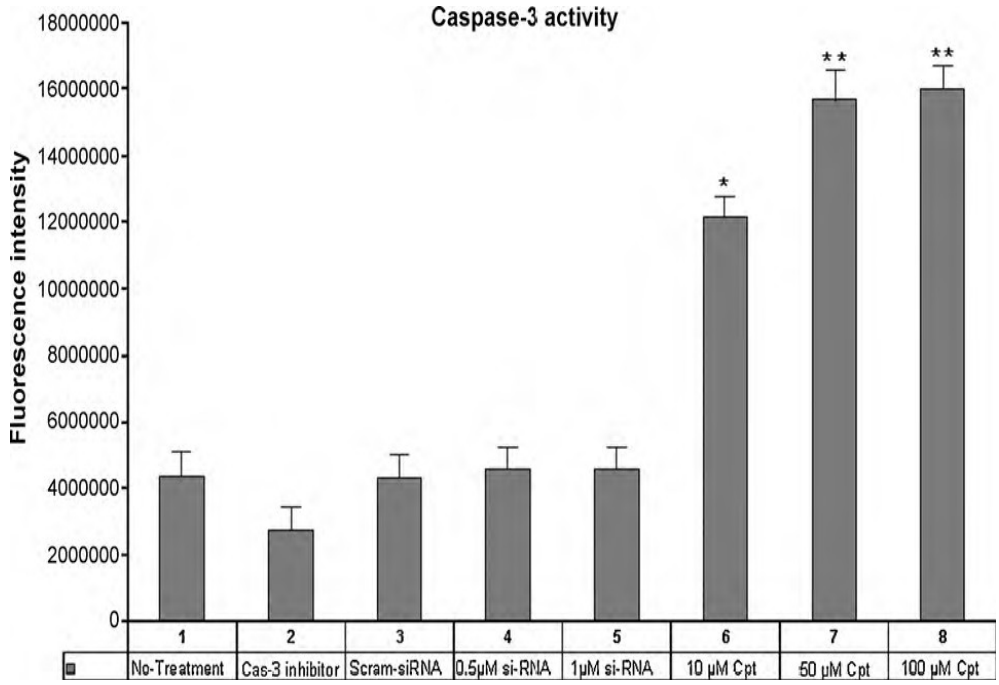

Fig 6.3. Caspase-3 activity in CGN extracts. Caspase-3 activity was measured using a fluorogenic (Ac-DEVD-AMC) substrate in the extracts of siRNA-transfected or camptothecin-treated CGNs. The data are presented in terms of caspase-3 activity in different siRNA transfected or camptothecin-treated CGN extracts. The bar graph clearly shows elevation of caspase-3 activity with increasing concentrations of camptothecin, while Topo-I siRNA showed no significant elevation of caspase-3 activity. Data are represented as the mean ±SD in three independent experiments; *$p < 0.05$ and **$p < 0.01$ as compared to the normal control.

Figure 6.4

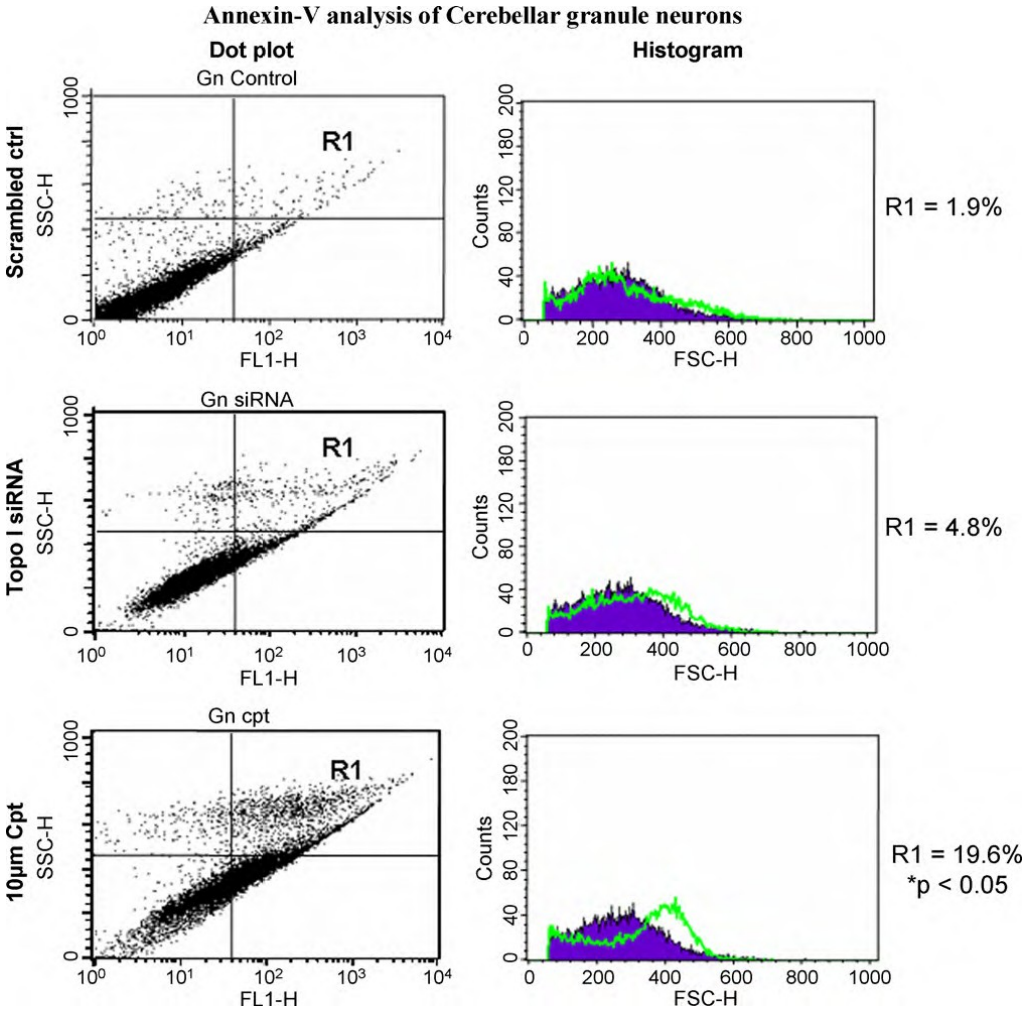

Fig 6.4. Flow cytometric analysis of FITC Annexin-V staining. Cultured CGNs were subjected to 16 h of transfection with 0.5 mMsilencing and non-silencing (scrambled) Topo-I siRNA or treatment with 10 mM camptothecin. CGNs were then incubated with FITC Annexin-V (Vybrant Apoptosis Assay Kit#3, Invitrogen, USA) and were analyzed for Annexin-V positive cells using a flow cytometer (BD biosciences). Data are presented in the contour diagram of Annexin-V-labeled cells. The upper right quadrant in the dot plot shows a significant increase (~20%) in Annexin-V positive cells in camptothecin-treated CGNs, while Topo-I siRNA-transfected CGNs only showed a small increase (~5%) in annexin-V positive cells. Data are the mean ± SD in three independent experiments; *$p < 0.05$ as compared to the control.

Figure 6.5

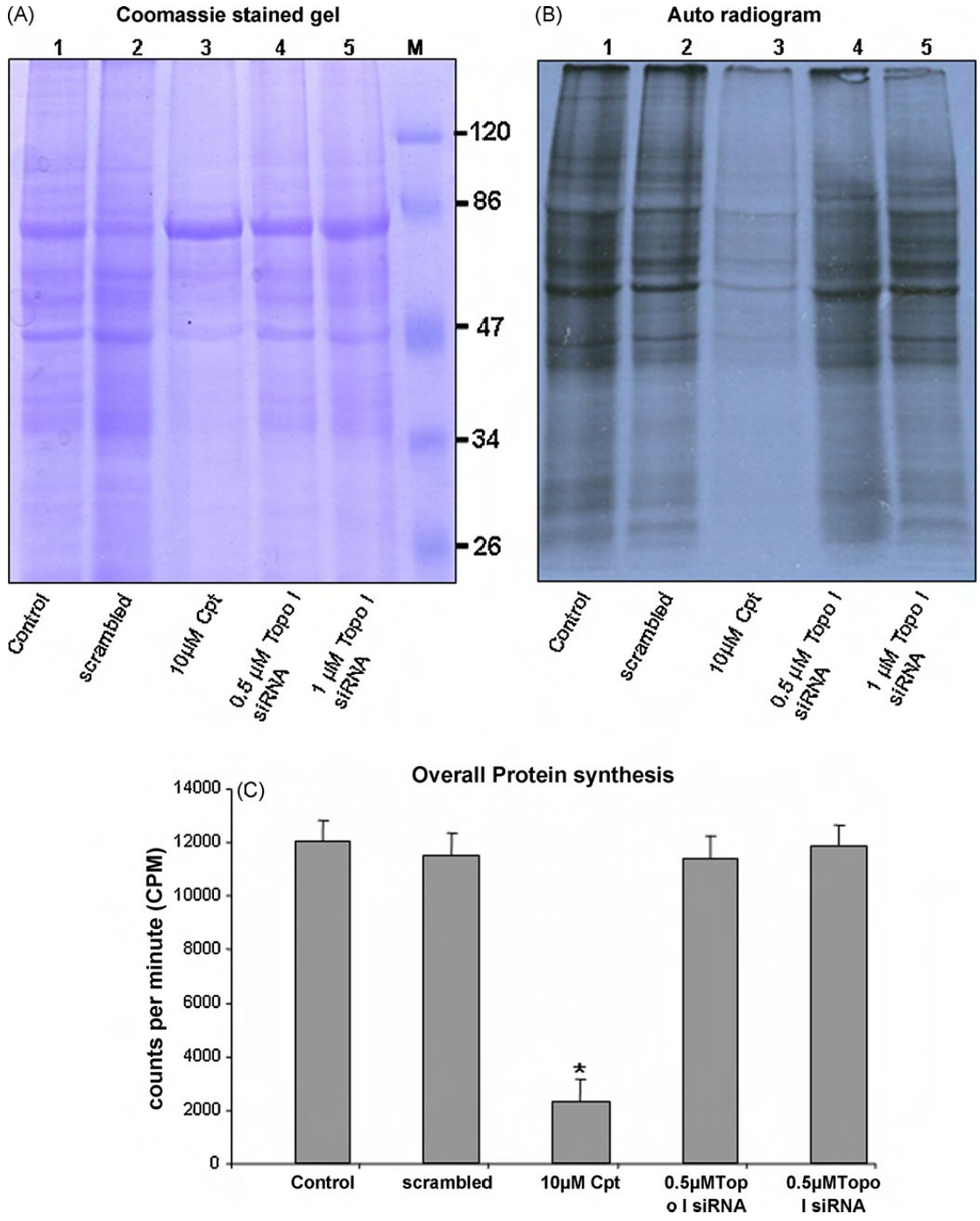
(A)
Coomassie stained gel
1
2
3
4
5
M
120
86
47
34
26
Control
scrambled
10μM Cpt
0.5 μM Topo I siRNA
1 μM Topo I siRNA
(B)
Auto radiogram
1
2
3
4
5
Control
scrambled
10μM Cpt
0.5 μM Topo I siRNA
1 μM Topo I siRNA
(C)
Overall Protein synthesis
counts per minute (CPM)
14000
12000
10000
8000
6000
4000
2000
0
*
Control
scrambled
10μM Cpt
0.5μMTopo I siRNA
0.5μMTopo I siRNA

Fig 6.5. S35-methionine incorporation. Protein synthesis in siRNA- or camptothecin-treated CGNs was assayed by incorporation of radiolabeled S35-methionine. Panel A represents Coomassie-stained 100 mg total protein extracts separated on 10% SDS PAGE, as detailed. Panel B represents the autoradiogram of the corresponding Coomassie gel. Panel C represents the bar graph of the S35-methionine incorporation that was measured using a liquid scintillation counter; 25 mg of siRNA- and camptothecin-treated CGN cell extracts were assayed for S35 methionine incorporation using a toluene-based liquid scintillation counter as radiation counts per minute (CPM). The data clearly show a significant decrease in S35-methionine incorporation into 10 mMcamptothecin-treated CGNs, whereas Topo-I siRNA showed no significant change in comparison with control cells. Data are presented as the mean ± SD in three independent experiments; *$p < 0.05$ as compared to the normal control.

Neurite outgrowth in Topo-I-siRNA transfected and Camptothecin treated CGNs.

The degree of maturation of neurite growth was examined (arborization status of neurons) and traced based on the pEGFP-N2 (GFP-green) and anti-neurofilament (NF-red) positive cells in Topo-I- siRNA tranfected CGNs and NF (red) positive in case of camptothecin treated cultures, as described above. The results show that 0.5μM Topo I siRNA+pEGFP-N2 transfected CGNs failed to arborize normally, when compared to control and scrambled siRNA treated cells. While 10μM camptothecin treated granule neurons showed an enhanced aggregation followed by clumping and altered morphological features of apoptosis without any extended processes **(Supplementary Fig 6) (Fig 6. 6 A)**. Further analysis of the length of neurite using Image J software showed a significant decrease in neurite outgrowth **(Fig 6.6 B)** in both siRNA downregulated cells or camptothecin treated cells. The observed affect in the presence of camptothecin could be due to clumping of cells **(Fig 6.6 A)** or death of cells due to apoptosis. While in the case of siRNA downregulated cells, the observed effect on the neurite out growth could be due to deficiency of Topo I enzymatic activity, which implicates the role of Topo I in neurite out growth, though the exact mechanism needs to be elucidated.

Figure 6.6

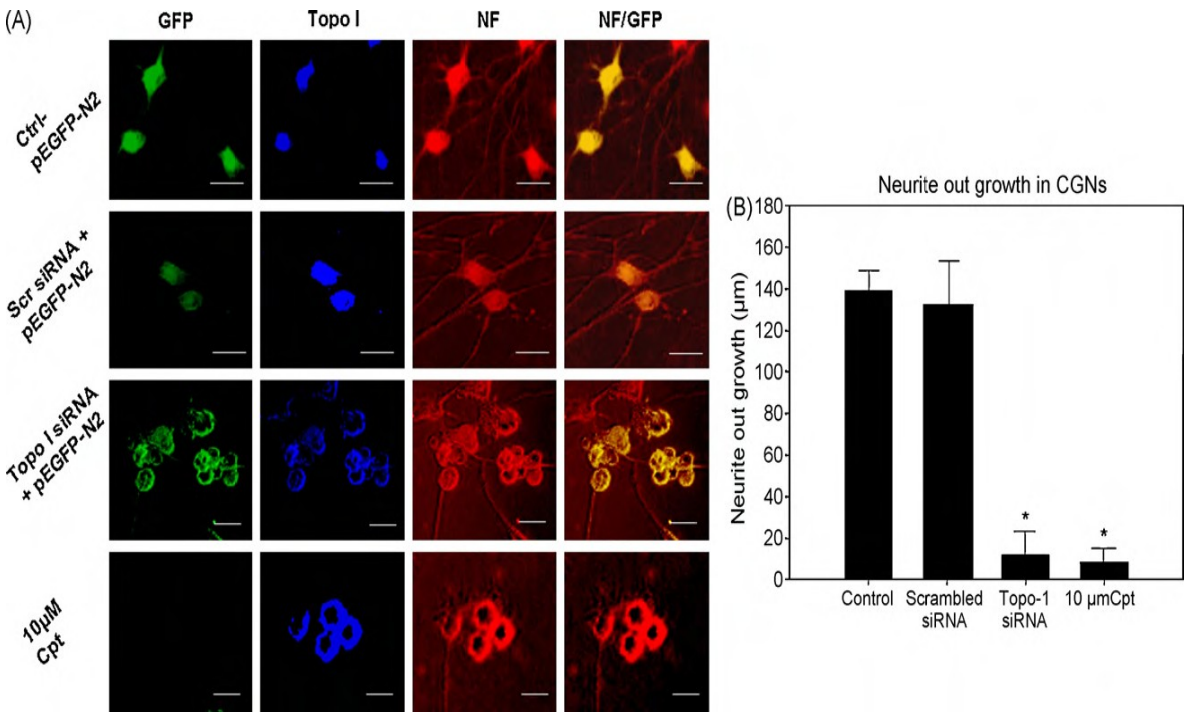

Fig. 6.6. Morphometric analysis of CGNs. Figure represents fluorescent confocal images of pEGFP-N2 (GFP-green), Topo-I (Cy3-blue) and neurofilament (NF) (Cy5-red) staining in treated CGNs as indicated. Individual neuritic processes were traced manually and measured with Image J, a java-based image analysis program (NIH, USA); GFP-green and anti-neurofilament (NF-red) positive cells were traced in Topo-I siRNA + pEGFP-N2-transfected CGNs, and NF (red) positive cells were traced in camptothecin-treated cultures. Panel A represents the confocal images, and Panel B represents the bar graph of the average total neurite length, which was determined from a sample of at least 50 neurons per dish from two independent experiments. The results clearly demonstrate a significant change in neuronal arborization in Topo-I siRNA-transfected CGNs. Data are presented as the mean ± SD;

*$p < 0.05$ as compared to control. Scale bar-15 mm.

Supplementary Figure 6

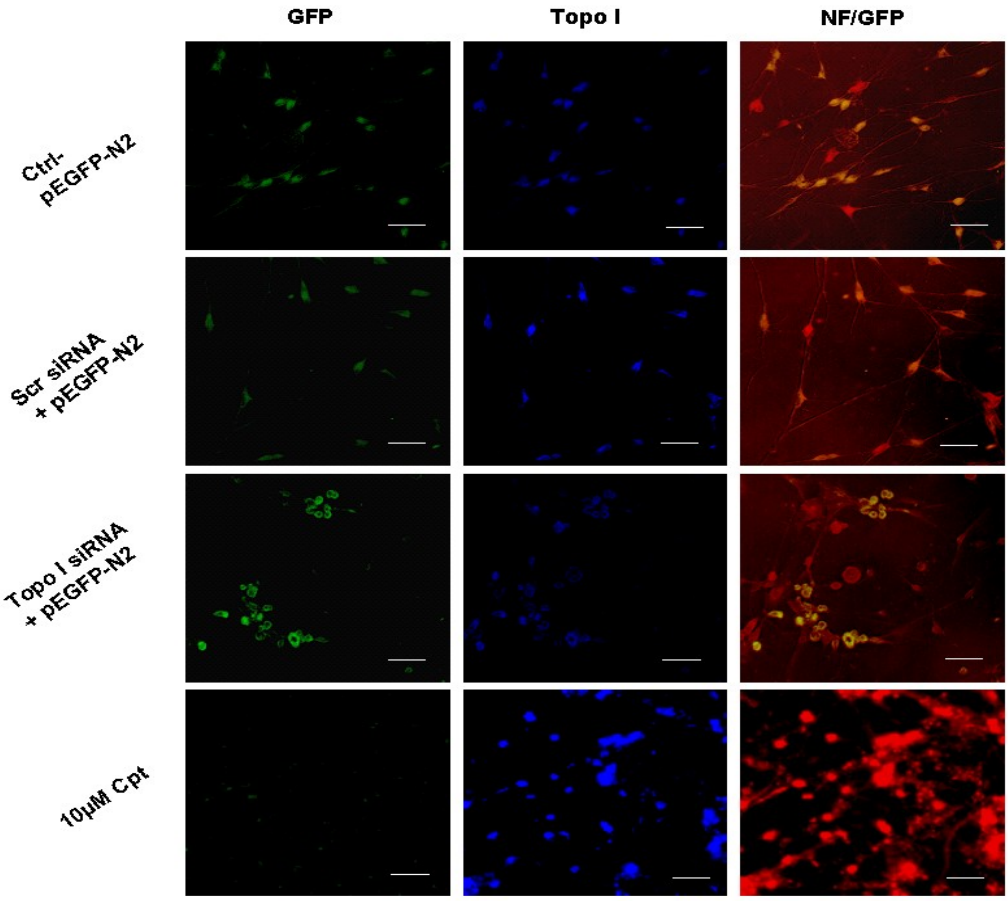

Supplementary Fig 6. Fluorescence confocal imaging of CGNs. Cerebellar granule neurons after co tranfection with pEGFP-N2 plasmid + Topo I siRNA and camptothecin treatments were fixed and subjected to immuno cytochemical analysis for Topo I and neurofilament. Fig 6 represents Fluorescent confocal images of pEGFP-N2 (GFP- green), Topo I (Cy 3-blue) and neurofilament (NF) (Cy 5- red) staining in treated CGNs as indicated. The results clearly show a markable decrease in Topo I levels in Topo I siRNA treated CGNs corresponding to GFP positive cells. scale bar-40μm.

Discussion.

The present study shows that Topo-I downregulation alone does not induce any apoptotic factors; however, camptothecin, a Topo-I specific inhibitor, promotes the formation of Topo-I DNA cleavage complexes, which may induce apoptosis in cells. The viability of CGNs in 0.5 mM Topo-I siRNA-transfected neurons showed only a ~20% decrease, whereas camptothecin showed more than a 50% decrease in viability at 10 mM. The observed marginal decrease in ~20% of Topo-I siRNA-treated granule neurons was not associated with elevated levels of caspase 3 and Annexin-V positive cells. However, camptothecin-treated neurons had elevated levels of pro-apoptotic markers. This result suggests that camptothecin induces apoptotic death, whereas the downregulation of Topo-I marginally decreases neuronal survival (<20%) in a non-apoptotic pathway. Our results thus demonstrate that camptothecin is neurotoxic, affecting neuronal survival through induction of a pro-apoptotic pathway, whereas transient downregulation of Topo-I with siRNA showed no significant effect on cell viability and activation of pro-apoptotic markers. Neuronal development includes the birth and differentiation of neurons from stem cell precursors. High rates of transcription and protein synthesis are required for neuronal development, differentiation and information processing. Neurons are metabolically very active and hence carry out a high level of protein synthesis. We have used the incorporation of radiolabeled S35-methionine to assess the effect of camptothecin and Topo-I siRNA on overall protein synthesis. Topo-I siRNA-transfected CGNs showed no significant effect on total protein synthesis compared to camptothecin- treated neurons. However, the decrease in protein synthesis in camptothecin-treated cerebellar granule neurons might be attributed to its apoptotic induction and DNA damage (data not shown here). This result establishes that Topo-I itself has no significant role in DNA transcription and translation. Directional neurite extension from the soma depends on precise cytoskeletal and adhesion dynamics that are induced by sensing attractive and extracellular cues, such as chemokines and extracellular matrix proteins (ECMs) (Dityatev and Schachner, 2003; Kleene and Schachner, 2004). Although a large amount of information is available on the extracellular mechanisms, the intracellular mechanisms have only recently been addressed. The camptothecin and Topo-I siRNA-transfected CGNs failed to extend their neuritic processes; this result suggests

a role for Topo-I in neuritogenesis. There is a significant effect on the arborization status of neurons related to neuritic growth in Topo-I siRNAtransfected and camptothecin-treated granule neurons. This effect of camptothecin on neuritic growth can be attributed to neurotoxicity and protein depletion, whereas the Topo-I siRNAmediated downregulation suggests a significant role for Topo-I in processes related to neuritic growth and development, including controlling the genes involved at the transcriptional level. Present observation is similar to that of Topoisomerase-II, which shows no effect on expression of housekeeping genes but has a role in neuronal development and maturation (neuritic growth and cone formation) (Tsutsui et al., 2001; Nur-E-Kamala et al., 2007).

Conclusions

Conclusions:

The results of the present study on prolonged CGNs in culture clearly demonstrate the significant similarities between physiological aging i*n vivo* and of prolonged culture of CGNs *in vitro.* This will provide new directions towards understanding of normal aging processes in brain. Understanding the molecular basis of aging processes at the cellular level should provide clues to gain insights into the pathology of various neurological diseases e.g. Alzheimer's and Parkinson's diseases, which are considered to be associated with high risk factors with increasing age.

- Earlier studies from our lab showed a significant age-dependent decrease in activity of topo IIβ in brain specifically in cerebellum (Kondapi et al., 2004). Further, topo IIβ knock-down neurobalstoma cells were shown to be sensitive to DNA damaging agents due to decreased repair capacity (Mandraju et al., 2008).

- These observations suggest that the low levels of topo IIβ activity in aging cerebellum may contribute to the genomic instability in cerebellar region of aging brain.

- The above studies also show a age-dependant decrease in Topo I, Topo III along with Topo IIβ both in aging rat brain extracts as well as in aging CGNs in culture.

- Topo III α show age-dependant increase both at protein and m-RNA levels till 4^{th} week (adult rats), while remains same till 5^{th} week (old rats), suggesting its significance in aged condition. This is similar to earlier reports which show that, disruption of gene encoding Topo IIIα in mice causes embryonic lethality (Li and Wang 1998).

- This varied expression of Topoisomerases in aging brain and aging CGNs *in vitro* suggest distinctive roles shared by these enzymes in development and functioning of brain.

- NHEJ and BER repair activities are shown to be predominant in the initial phase of life, decrease during the later phases of aging. This strongly correlates with Topo IIβ levels, an enzyme that can be used as additional biomarker for senesense and aging.

Further, our study shows that Topo I down regulation alone does not induce any apoptotic factors, while camptothecin though a Topo I specific inhibitor, causes Topo I DNA cleavage complexes inducing apoptosis in cells. This clearly suggests that camptothecin induces apoptotic death, while the knock-down of Topo I affects neuronal differentiation in a non-apoptotic pathway.

- Si RNA mediated downregulation of Topo I in CGNs show no significant effect on total protein synthesis as compared to camptothecin treated neurons. This establishes that Topo I itself has no significant role in DNA transcription affecting an active translation.

- Topo I depleted neurons failed to extend their neuritic processes pointing out to a possible role of Topo I in neuritogenesis.

In summary, the results bring out the importance of DNA topoisomerases viz., Type I (Topo I, III α and IIIβ) and Type II (Topo II α and IIβ) in neuronal development, and aging, whose actual mechanisms needs to be elucidated.

References:

- Adachi N, Ishino T, Ishii Y, Takeda S, Koyama H., (2001). DNA ligase IV deficient cells are more resistant to ionizing radiation in the absence of Ku70: implications for DNA double-strand break repair. *Proc Natl Acad Sci, USA*. **98**, 12109–13.

- Agarwal and R.S. Sohal., (1994). DNA oxidative damage and life expectancy in houseflies. *Proc. Natl. Acad. Sci. USA.* **91**, 12332–12335.

- Alex Bokova, Asish Chaudhurib, Arlan Richardson., (2004). The role of oxidative damage and stress in aging. *Mechanisms of Ageing and Development*. **125**, 811–826.

- Artal-Sanz M, Tavernarakis N., (2005). Proteolytic mechanisms in necrotic cell death and neurodegeneration. *FEBS Lett*. **579**, 3287-96.

- Asami, Y., Jia, D.W., Tatebayashi, K., Yamagata, K., Tanokura, M., Ikeda, H., (2002). Effect of the DNA Topoisomerase II inhibitor VP-16 on illegitimate recombination in yeast chromosomes. Gene. **291**, 251–257.

- Augustin-Voss HG, Voss AK, Pauli BU., (1993). Senescence of aortic endothelial cells in culture: effects of basic fibroblast growth factor expression on cell phenotype, migration, and proliferation. *J Cell Physiol*. **157**, 279–288.

- Bakshi, R.P., S. Galande, and K. Muniyappa., (2001). Functional and regulatory characteristics of eukaryotic type II DNA topoisomerase. *Crit. Rev. Biochem. Mol. Biol.* **36**, 1–37.

- Barreto-Chang O.L., Dolmetsch R.E., (2009). Calcium Imaging of Cortical Neurons using Fura-2 AM. *JoVE*., **23**.

- Baumann, P., West, S. C., (1998). DNA end-joining catalyzed by human cell-free extracts, *Proc. Natl. Acad. Sci.* USA. **95**, 14066–14070.

- Beck, W.T. and M.K. Danks., (1991). Mechanisms of resistance to drugs that inhibit DNA topoisomerases, Semin. *Cancer Biol*. **2,** 235–244.

- Bénard M, Gonzalez BJ, Schouft MT, Falluel-Morel A, Vaudry D, Chan P, Vaudry H., (2004). Fontaine M. Characterization of C3a and C5a receptors in rat cerebellar granule neurons during maturation. Neuroprotective effect of C5a against apoptotic cell death. *J Biol Chem*. **279 (42)**, 43487-96.

- Ben-Porath, I.,Weinberg., (2004). R. A. When cells get stressed: an integrative view of cellular senescence. *J. Clin. Invest*. **113**, 8–13.

- Best BP., (2009). "Nuclear DNA damage as a direct cause of aging". *Rejuvenation Research* **12 (3),** 199–208.

- Bjorksten J., (1955). Crosslinking—key to aging. Chem and Engin News. **33**, 1967.

- Bjorksten, Johan., (1971). The crosslinkage theory of aging, *Finska Kemists Medd*. **80**, 23-38.

- Bohr VA, Sander M, Kraemer KH., (2005). Rare diseases provide rare insights into DNA repair pathways, TFIIH, aging and cancer center. *DNA Repair (Amst).* **4(2)**, 293–302.

- Bohr, Ottersen O.P and Tonjum T., (2007). Genome instability and DNA Repair in Brain, Ageing and Neurological Disease. *Neuroscience.* **145**, 1183–1186.

- Bong-Gun J. U., Lunyak V. V., Perissi V., Garcia-Bassets I., Rose D. W., Glass C. K., (2006). Rosenfeld M. G. A Topoisomerase IIß-Mediated dsDNA Break Required for Regulated Transcription. *Science.* **312**, 1798.

- Bonifati V, Rizzu P, van Baren MJ, Schaap O, Breedveld GJ, Krieger E, Dekker MC, Squitieri F, Ibanez P, Joosse M, van Dongen JW, Vanacore N, van Swieten JC, Brice A, Meco G, van Duijn CM, Oostra BA, Heutink P., (2003). Mutations in the DJ-1 gene associated with autosomal recessive early-onset parkinsonism. *Science*. **299**, 256-9.

- Bradford M. M., (1976). A rapid and sensitive method for quantitation of microgram quantities of protein utilizing the principle of protein-dye-binding. *Anal Biochem*, **72**, 248-54.

- Brian T. Weinert and Poala S., (2003). Timiras Invited Review: Theories of aging. *J Appl Physiol*. **95**. 1706-1716.

- Brooks PJ., (2007). The case for 8,5=-cyclopurine-2=-deoxynucleosides as endogenous DNA lesions that cause neurodegeneration in xeroderma pigmentosum. Neuroscience, **145** (4), 1407-17.

- Brunk UT and Terman A., (2002). Lipofuscin: mechanisms of age-related accumulation and influence on cell functions. *Free Radic Biol Med.* **33**. 611–619

- Buhler C; Lebbink J H; Bocs C; Ladenstein R; Forterre P., (2001). DNA topoisomerase VI generates ATP-dependent double-strand breaks with two-nucleotide overhangs. *The Journal of biological chemistry*, **276(40)**, 37215-22.

- Burnet F.M., (1970). An Immunological approach to ageing. THE LANCET. **296**, 358-360.

- Cambray-Deakin M.A., (1995). Cerebellar Granule cells. In Neural Cell Culture A Practical Approach, (James Cohen, Graham P. Wilkin, ed), OIRL Press, 3-14.

- Camins Espuny A. An evaluation of the neuroprotective effects of melatonin in an in vitro experimental model of age-induced neuronal apoptosis. *J Pineal Res.*, **46** (2009), pp. 262-7.

- Campisi, J.,(2001). Cancer, aging and cellular senescence. *In Vivo* **14**, 183–188.

- Capranico G., Tinelli S., Austin C. A., Fisher M. L., Zunino F., (1992). Different patterns of gene expression of topoisomerase II isoforms in differentiated tissues during murine development. *Biochim Biophys Acta*., **1132**, 43-8.

- Caron P.R and Wang J.C, (1994). Alignment of primary sequences of DNA topoisomerases. *Adv. Pharmacol.* **29**, 271–97.

- Carrell, A., (1912). On the permanent life of tissues outside of the organism. *J. Exp. Med* 15, 516-528.

- Champoux J.J, (2001). DNA topoisomerases: structure, function, and mechanism. *Annu Rev Biochem* 70pp. 369–413.

- Chang U. M., Li C. H., Lin L. I., Huang C. P., Kan L. S., Lin S. B., (2006) Ganoderiol F. A ganoderma triterpene, induces senescence in hepatoma HepG2 cells. *Life Sci.*, **79**, 1129-39.

- Choi DW., (1992) Excitotoxic cell death. *J Neurobiol*, **23**, 1261-76.

- Citron M. Strategies for disease modification in Alzheimer's disease., (2004), *Nat Rev Neurosci*, **5**, 677-85.

- Collins AR, Ma AG, Duthie SJ., (1995). The kinetics of repair of oxidative DNA damage (strand breaks and oxidised pyrimidines) in human cells. *Mutat Res* **336**, 69-72.

- Confalonieri F, Elie C, Nadal M, de La Tour C, Forterre P, and Duguet M., (1993). Reverse gyrase: a helicase-like domain and a type I topoisomerase in the same polypeptide. *PNAS*. **90(10)**, 4753–4757.

- Contestabile A., (2002). Cerebellar granule cells as a model to study mechanisms of neuronal apoptosis or survival *in vivo* and *in vitro*. *Cerebellum.* **1**, 41-55.

- Copani A., Casabona G., Bruno V., Caruso A., Condorelli D. F., Messina A., Di Giorgi Gerevini V., Pin J. P., Kuhn R., Knöpfel T., Nicoletti F., (1998). The metabotropic glutamate receptor mGlu5 controls the onset of developmental apoptosis in cultured cerebellar neurons. *Eur J Neurosci.*, **10**, 2173-84.

- Cortopassi, G. A., and Wang, E., (1996). "There is substantial agreement among interspecies estimates of DNA repair activity." *Mech Ageing Dev* **91(3)**, 211-218.

- Cristofalo VJ., (1996). Ten years later: what have we learned about human aging from studies of cell cultures? *Gerontologist*. **36**, 737–741.

- Critchlow SE and Jackson SP., (1998). DNA end-joining: from yeast to man. *Trends Biochem Sci*. **23**, 394–398.

- Cryns V, Yuan J., (1998) Proteases to die for. *Genes Dev*. **12**, 1551-70.

- Davydov, L., Hansen, A and D. A. Shackelford D. A., (2003). Is DNA repair compromised in Alzheimer's disease? *Neurobiol. Aging* **24**, 953–968.

- de Souza-Pinto NC, Bohr VA., (2002). The mitochondrial theory of aging: involvement of mitochondrial DNA damage and repair. *Int Rev Neurobiol*. **53**, 519–534.

- Di Mauro E, Camilloni G, Verdone L and Caserta M., (1993). DNA Topoisomerase I controls the kinetics of promoter activation and DNA topology in Saccharomyces cerevisiae. *Mol. Cell. Biol* 13, 6702–6710.

- Dimri G. P., Lee X., Basile G, Acosta M, Scott G., Roskelley C, Medrano E. E., Linskens M., Rubelj I., Pereira-Smith O., Peacocke M., Campisi J., (1995). A biomarker that identifies senescent human cells in culture and in aging skin in vivo, *Proc. Natl. Acad. Sci. U.S.A.* **92**, 9363–9367.

- Disterhoft J. F., Moyer J. R. Jr, Thompson L. T., (1994). The calcium rationale in aging and Alzheimer's disease. Evidence from an animal model of normal aging. *Ann. N. Y. Acad. Sci.* **747**, 382–406.

- Dityatev and Schachner M., (2003). Extracellular matrix molecules and synaptic plasticity, *Nature Reviews Neuroscience*. **4**, 456–468.

- Dolle, M. E., and Vijg, J., (2002). "Genome dynamics in aging mice." *Genome Res.* **12(11)**, 1732-1738.

- Dolle, M. E., Giese, H., Hopkins, C. L., Martus, H. J., Hausdorff, J. M., and Vijg, J.,(1997). "Rapid accumulation of genome rearrangements in liver but not in brain of old mice." *Nat Genet* **17(4)**, 431-434.

- Donze O and Picard D., (2002). RNA interference in mammalian cells using siRNAs synthesized with T7 RNA polymerase, Nucl. Acids Res. **30**, 46.

- Duguet, M., (1997). When helicase and topoisomerase meet. *J. Cell Sci*, **110**, pp. 1345–1350.

- Earl R. Stadtman and Barbara S. Berlett., (1998). Reactive Oxygen-Mediated Protein Oxidation in Aging and Disease. *Drug Metabolism Reviews,* **30**, 2.

- Earl R. Stadtman., (1998). Protein modification in aging. *J. Gerontol*. **43**, 112–120.

- Elgin SCR, Gilmour DS., (1987). Localisation of specific topoisomerase I interactions within the transcribed region of active heat shock genes byusing the inhibitor camptothecin. Mol Cell Biol. **7**, 141–148.

- Esposito, D., Fassina, G., Szabo, P., De Angelis, P., Rodgers, L., Weksler, M., and Siniscalco, M. (1989). "Chromosomes of older humans are more prone to aminopterine-induced breakage." *Proc Natl Acad Sci U S* . **86** (4), 1302-1306.

- Finch, C. E., (1990). *Longevity, Senescence, and the Genome*. The University of Chicago Press, Chicago and London.

- Forno LS. (1996). Neuropathology of Parkinson's disease. *J Neuropathol Exp Neurol*, **55**, 259-72.

- Franceschi C, Valensin S, Bonafe M, Paolisso G, Yashin AI, Monti D, and De Benedictis G., (2000). The network and the remodeling theories of aging: historical background and new perspectives. *Exp Gerontol*. **35**, 879-896.

- Franchitto, A., Pichierri, P., Mosesso, P., Palitti, F., (2000). Catalytic inhibition of topoisomerase II in Werner’s syndrome cell lines enhances chromosomal damage induced by X-rays in the G2 phase of the cell cycle. Int. J. Radiat. Biol. **76**, 913–922.

- Gage FH., (2000). Mammalian neural stem cells. *Science*, **287**, 1433-8.

- Galande S, Muniyappa K., (1996) Purification and functional characterization of type II DNA topoisomerase from rat testis and comparison with topoisomerase II from liver. *Biochem Biophy Acta*. **1308**, 58–66.

- Gangloff, S., McDonald, J. P., Bendixen, C., Arthur, L., and Rothstein, R., (1994). The yeast type I topoisomerase Top3 interacts with Sgs1, a DNA helicase homolog: a potential eukaryotic reverse gyrase. *Mol. Cell. Biol*. **14**, 8391–8398.

- Geng, Y., Guan, J. T., Wang, B., Xu, X., Fu, Y., (2008). Senescence-Associated β-Galactosidase as a Senescence Biomarker Showed in Rat Hippocampus. *BMEI* **1**,173-177.

- German J, Bloom's syndrome., (1995). *Dermatol Clin.* **13**, 7–18.

- Gibson G. E., Peterson C., (1987). Calcium and the aging nervous system. *Neurobiol. Aging.* **8**, 329–343.

- Gilmour DS, Pflugfelder G, Wang JC, Lis JT., (1986). Topoisomerase I interacts with transcribed regions in Drosophila cells. Cell, **44**, 401–407.

- Goll DE, Thompson VF, Li H, Wei W, Cong J., (2003). The calpain system. *Physiol Rev,* **83**, 731-801.

- Goodwin A, Wang SW, Toda T, Norbury C, Hickson ID., (1999). Topoisomerase III is essential for accurate nuclear division in *Schizosaccharomyces pombe*. *Nucleic Acids Res*. **27**, 4050–4058.

- Grube, K., and Burkle, A., (1992). "Poly(ADP-ribose) polymerase activity in mononuclear leukocytes of 13 mammalian species correlates with species-specific life span." *Proc Natl Acad Sci U S* . **89**(24), 11759-11763.

- Halliwell B and Gutteridge J.M., (1989). *Free Radicals in Biology and Medicine* (second ed.),, *Oxford University Press*, Oxford.

- Hanai R, Caron P R, and Wang J C., (1996). Human TOP3: a single-copy gene encoding DNA topoisomerase III *PNAS*, **93**(8), 3653-3657.

- Harman, D., (1956). Aging: A theory based on free radical and radiation chemistry. *J. Gerontol.* **11**, 298–300.

- Harman, D., (1998). Extending functional life span. *Exp. Gerontol.* **33**, 95–112.

- Harman, D., (1993). Free radicals and age-related diseases. In: Yu, B.P. Editor. *Free Radicals in Aging* CRC Press, Boca Raton, FL, 205–222.

- Harman, D., (1995). Free radical theory of aging: Alzheimer's disease pathogenisis. *Age* **18**, 97–119.

- Harmon, F. G., DiGate, R. J., and Kowalczykowski, S. C., (1999). RecQ helicase and topoisomerase III comprise a novel DNA strand passage function: a conserved mechanism for control of DNA recombination. *Mol. Cell*, **3**, 611–620.

- Hart R.W. and Setlow R.B., (1974). Correlation between deoxyribonucleic acid excision repair and life span in a number of mammalian species. *Proc. Natl. Acad. Sci. USA* 71, 2169-2173 .

- Hasty P, Campisi J, Hoeijmakers J, van Steeg H, Vijg J., (2003). Aging and genome maintenance: lessons from the mouse? *Science.* **299**, 1355–5

- Hayflick L. A., (1998). brief history of the mortality and immortality of cultured cells. *Keio J Med* 47, 174–182.

- Hengartner MO., (2001). Apoptosis: corralling the corpses. *Cell.* **104**, 325-8.

- Hengartner MO., (2000). The biochemistry of apoptosis. *Nature*, **407**, 770-6.

- Henningfeld, K.A. and S.M. Hecht., (1995). A model for topoisomerase I-mediated insertions and deletions with duplex DNA substrates containing branches, nicks, and gaps. *Biochemistry*, **34**, 6120–6129.

- Hickson I.D., (2003). RecQ helicases: caretakers of the genome, *Nat Rev Cancer*. **3**, 169–177.

- Hsiang Y.H, Hertzberg R, Hecht S and Liu L. F., (1985). Camptothecin induces protein-linked DNA breaks via mammalian DNA Topoisomerase-I, *J. Biol. Chem.* 260, 14873–14878.

- Huang, S., Li, B., Gray, M. D., Oshima, J., Mian, I. S., and Campisi, J., (1998). The premature ageing syndrome protein, WRN, is a exonuclease. *Nat. Genet*. **20**, 114–116.

- Huggins, T.G., Wellsknecht, M.C., Detorie, N.A., Baynes, J.W., Thorpe, S.R., (1993). Formation of O-tyrosine and dityrosine in proteins during radiolytic and metal-catalyzed oxidation. *J. Biol. Chem*. **268**, 12341– 12347.

- Ishii, Y., Ikushima, T., (2002). Post treatment effects of DNA Topoisomerase inhibitors on UVB and X-ray induced chromosomal aberration formation. *Mutat. Res.* **25**, 67–74.

- Ishitani R, Sunaga K, Hirano A, Saunders P, Katsube N, Chuang D. M., (1996). Evidence that glyceraldehyde-3-phosphate dehydrogenase is involved in age-induced apoptosis in mature cerebellar neurons in culture. *J Neurochem.* **66**, 928-35.

- István Vermes Clemens Haanen, Helga Steffens-Nakken and Chris Reutellingsperger., (1995). A novel assay for apoptosis Flow cytometric detection of phosphatidylserine expression on early apoptotic cells using fluorescein labelled Annexin V, *Journal of Immunological Methods.* **184**, 39-51.

- Itahana, K., Campisi, J, Dimri, G. P., (2004). Mechanisms of cellular senescence in human and mouse cells. *Biogerontology.* **5**, 1–10.

- Jeggo PA., (1998). Identification of genes involved in repair of DNA doublestrand breaks in mammalian cells. *Radiat Res*.**150**, 80–91.

- Jin LW, Saitoh T., (1995). Changes in protein kinases in brain aging and Alzheimer's disease. Implications for drug therapy. *Drugs Aging*. 6, 136-49.

- John L. Nitiss., (2009). DNA Topoisomerase II and Its Growing Repertoire of Biological Functions. *Nat Rev Cancer*. **9** (5), pp. 327-337.

- Johnson, F.B., Sinclair, D.A., (1999). Guarente, L. Molecular biology of aging. *Cell* **96** (2), 291- 302.

- Kanduc D, Mittelman A, Serpico R, Sinigaglia E, Sinha AA, Natale C, Santacroce R, Di Corcia MG, Lucchese A, Dini L, Pani P, Santacroce S, Simone S, Bucci R, Farber E., (2002). Cell death: apoptosis versus necrosis (review). *Int J Oncol*, **21**, 165-70.

- Kang M.R, Muller M.T and Chung I.K., (2004). Telomeric DNA damage by topoisomerase I. A possible mechanism for cell killing by camptothecin, *J Biol Chem.* **279**, 12535-12541.

- Karow, J. K., Wu, L., and Hickson, I. D., (2000). RecQ family helicases: roles in cancer and aging. *Curr. Opin. Genet. Dev*, **10**, 32–38.

- Ken Tsutsui, Kimiko Tsutsui, Kuniaki Sano, Akihiko Kikuchi and Akira Tokunaga., (2001). Involvement of DNA Topoisomerase IIβ in Neuronal Differentiation. *J. Biol. Chem*, **276**, 5769-5778.

- Kent C. R., Eady J. J., Ross G. M., Steel G. G., (1995). The comet moment as a measure of DNA damage in the comet assay. *Int. J. Radiat. Biol*. **67**, 655–660.

- Keramaris E, Stefanis L, MacLaurin J, Harada N, Takaku K and Ishikawa T et al., (2000). Involvement of caspase 3 in apoptotic death of cortical neurons evoked by DNA damage. *Mol Cell Neurosci*. **(4)**, 368-79.

- Khokhlov AN., (1992). Stationary cell cultures as a tool for gerontological studies. *Ann NYAcad Sci.* **663**, 475–476.

- Kirischuk S., Verkhratsky A., (1996). Calcium homeostasis in aged neurones. *Life Sci.* **59**, 451-9.

- Kirischuk S., Voitenko N., Kostyuk P., Verkhratsky A., (1996). Age-associated changes of cytoplasmic calcium homeostasis in cerebellar granule neurons in situ: investigation on thin cerebellar slices. *Exp Gerontol.*, **31**, 475-87.

- Kitada T, Asakawa S, Hattori N, Matsumine H, Yamamura Y, Minoshima S, Yokochi M, Mizuno Y, Shimizu N., (1998). Mutations in the parkin gene cause autosomal recessive juvenile parkinsonism. *Nature*. **392**, 605-8.

- Kleene R and Schachner M., (2004). Glycans and neural cell interactions, *Nature Reviews Neuroscience.* **5**, 195–208.

- Kohji, T., Hayashi, M., Shioda, K., Minagaw, M., Morimatsu, Y., Tamagawa, K.O.M., (1998). Cerebellar neurodegeneration in human hereditary DNA repair disorders. *Neurosci. Lett*. 243, 133–136.

- Kondapi, A. K., Mulpuri, N., Mandraju, R. K., Sasikaran, B., Subba Rao, K., (2004). Analysis of age dependent changes of topoisomerase II β and α in rat brain. *Int. J. Dev. Neurosci.* **22**, 19–30.

- Kraemer KH, Patronas NJ, Schiffmann R, Brooks BP, Tamura D, Digiovanna JJ., (2007). Xeroderma pigmentosum, trichothiodystrophy and Cockayne syndrome: A complex genotype-pheno- type relationship. *Neuroscience*. **145**(4), 1388-96.

- Kretzschmar M, Meisterernst M., (1993). Roeder RG. Identification of human DNA topoisomerase I as a cofactor for activator-dependent transcription by RNA polymerase II. *Proc Natl Acad Sci USA*. **90**, 11508–11512.

- Kwan K.Y and Wang J.C., (2001). Mice lacking DNA topoisomerase III beta develop to maturity but show a reduced mean lifespan, *Proc. Natl. Acad. Sci. U.S.A.* **98**, 5717–5721

- Landfield P. W., (1983). Mechanisms of altered neural function during aging. Aging of the Brain, Ed. Gipsen W. H., Traber J, Amsterdam, *The Netherlands: Elsevier*, 51–57.

- Lang AE, Lozano AM., (1998) Parkinson's disease. First of two parts. *N Engl J Med*, **339**, 1044-53.

- Lebailly P., Vigreux C., Godard T., Sichel F., Bar E., LeTalaer J. Y., Henry-Amar M., (1997). Gauduchon P. Assessment of DNA damage induced *in vitro* by etoposide and two fungicides (carbendazim and chlorothalonil) in human lymphocytes with the comet assay. *Mutat Res*., **375**, 105–217.

- LeBel C. P., Bondy S. C., (1992). Oxidative damage and cerebellar aging. *Prog. Neurobiol*. **38**, 601–609.

- Lebel M and Leder, P. A., (1998). deletion within the murine Werner syndrome helicase induces sensitivity to inhibitors of topoisomerase and loss of cellular proliferative capacity. *Proc. Natl. Acad. Sci. USA*, **95**, 13097–13102.

- Lebel M, Spillare E.A, Harris, C.C, and Leder, P., (1999). The Werner syndrome gene product co-purifies with the DNA replication complex and interacts with PCNA and topoisomerase I. *J. Biol. Chem*, **274**, 37795–37799.

- Lee M.P, Brown S.D, Chen A and Hsieh T.S., (1993). DNA Topoisomerase I is essential in Drosophila melanogaster. *Proc. Natl. Acad. Sci. USA.* **90**, 6656–6660.

- Lee, C. K., Weindruch, R. and Prolla T. A., (2000). Gene-expression profile of the ageing brain in mice. *Nat. Genet*. **25**, 294–297.

- Leist M, Jaattela M., (2001). Four deaths and a funeral: from caspases to alternative mechanisms. *Nat Rev Mol Cell Biol*, **2**, 589-98.

- Lesuisse C, Martin L.J., (2002). Immature and mature cortical neurons engage different apoptotic mechanisms involving caspase-3 and the mitogenactivated protein kinase pathway. *J Cereb Blood Flow Metab* **22**, 935-50.

- Lewis LK, Resnick MA., (2000). Tying up loose ends: nonhomologous endjoining in Saccharomyces cerevisiae. *Mutat Res*, **451**, 71 –89.

- Li, W. and Wang, J.C., (1998). Mammalian DNA topoisomerase IIIalpha is essential in early embryogenesis *Proc. Natl Acad. Sci. USA*, **95**, 1010–1013.

- Lu T, Pan Y, Kao SY, Li C, Kohane I, Chan J., (2004). Gene regulation and DNA damage in the ageing human brain. *Nature*, **429**, 883–91.

- Maccioni, R.B., Munoz, J.P., Barbeito, L., (2001). The molecular bases of Alzheimer's disease and other neurodegenerative disorders. *Arch. Med. Res*. **32**, 367-381.

- Maftahi M, Han CS, Langston LD, Hope JC, Zigouras N, Freyer GA., (1999). The top3(+) gene is essential in *Schizosaccharomyces pombe* and the lethality associated with its loss is caused by Rad12 helicase activity. *Nucleic Acids Res.* **27**, 4715–4724.

- Mandavilli B. S., Rao, K. S., (1996). Accumulation of DNA damage in aging neurons occurs through a mechanism other than apoptosis, *J. Neurochem*. **67**, 1559–1565.

- Mandavilli BS, Rao KS., (1996). Neurons in the cerebral cortex are most susceptible to DNA-damage in aging rat brain. *Biochem Mol Biol Int*, **40**, 507–14.

- Mandraju, R.K., Kannapiran P., Kondapi, A. K., (2008). Distinct roles of topoisomerase II isoforms: DNA damage accelerating α, double strand break repair promoting β. *Arch. Biochem. Biophys*., **470**, 27–34.

- Marina V. Aksenova, Michael Y. Aksenov, Charles F. Mactutus and Rosemarie M. Booze., (2005). Cell Culture Models of Oxidative Stress and Injury in the Central Nervous System. *Current Neurovascular Research.* **2**, 73-89

- Marina V. Aksenova, Michael Y. Aksenov, William R. Markesbery, and Allan Butterfield D., (1999). Aging in a Dish: Age-Dependent Changes of Neuronal Survival, Protein Oxidation, and Creatine Kinase BB Expression in Long-Term Hippocampal Cell Culture. *Journal of Neuroscience Research* **58**, 308–317.

- Martin G.M., (1978). Genetic syndrome in man with potential relevance to the pathobiology of aging. *Birth Defects Orig. Artic. Ser.* **14**, 5–39.

- Martin G.M, Oshima J, Gray M.D and Poot M., (1999). What geriatricians should know about the Werner syndrome. *J. Am. Geriatr. Soc.* **47**, 1136–1144.

- Martin, G. M., Smith, A. C., Ketterer, D. J., Ogburn, C. E., and Disteche, C. M., (1985). "Increased chromosomal aberrations in first metaphases of cells isolated from the kidneys of aged mice." *Isr J Med Sci.* **21**(3), 296-301.

- Mason D. X., Jackson T. J., Lin A. W., (2004). Molecular signature of oncogenic ras-induced senescence. *Oncogene.*, **23**, 9238-46.

- Mattson M.P., (1997). Cellular actions of beta-amyloid precursor protein and its soluble and fibrillogenic derivatives. *Physiol Rev,* **77**, 1081-132.

- Mattson, M.P., (1992). Calcium as sculptor and destroyer of neural circuitry. *Exp. Gerontol.* **27**, 29–49.

- Mehlhorn RJ., (2003). Oxidants and antioxidants in aging. In: *Physiological Basis of Aging and Geriatrics* (3rd ed.), edited by Timiras PS. Boca Raton, FL: CRC, 61-83.

- Melov, S., Schneider, J.A., Coskun, P.E., Bennett, D.A., Wallace, D.C., (1999). Mitochondrial DNA rearrangements in aging human brain and in situ PCR of mtDNA. *Neurobiol. Aging*, 20, 565- 571.

- Merino A, Madden KR, Lane WS., (1993). Champoux JJ, Reinberg D. DNA topoisomerase I is involved in both repression and activation of transcription. Nature 365, 227–232.

- Micheau O, Tschopp J., (2003). Induction of TNF receptor I-mediated apoptosis via two sequential signalling complexes. *Cell*, **114**, 181-90.

- Milgram NW, Head E, Zicker SC, Ikeda-Douglas C, Murphey H, Muggenberg BA, Siwak CT, Tapp PD, Lowry SR, Cotman CW., (2004). Long-term treatment with antioxidants and a program of behavioral enrichment reduces age-dependent impairment in discrimination and reversal learning in beagle dogs. *Exp Gerontol*, **39**, 753-65.

- Milligan J.F and Uhlenbeck O.C., (1989). Synthesis of small RNAs using T7 RNA polymerase, *Methods Enzymol.* **180**, 51–62.

- Mondragon A. & DiGate R., (1999). The structure of *Escherichia coli* DNA topoisomerase III. *Struct. Fold Des*. **7**, 1373–1383.

- Morham S.G, Kluckman K.D, Voulomanos N and Smithies O., (1996). Targeted disruption of the mouse topoisomerase I gene by camptothecin selection. *Mol. Cell. Biol.* **16**, 6804–6809.

- Morris E.J and Geller H.M., (1996). Induction of neuronal apoptosis by camptothecin, an inhibitor of DNA topoisomerase-I: evidence for cell cycle independent toxicity, *J Cell Biol.* **134**, 757–770.

- Morrison JH, Hof PR., (2002). Selective vulnerability of corticocortical and hippocampal circuits in aging and Alzheimer's disease. *Prog Brain Res*, **136**, 467–86.

- Mosmann T., (1983). Rapid colorimetric assay for cellular growth and survival: application to proliferation and cytotoxicity assays, *J. Immunol. Methods.* **65**, 55-63.

- Nur-E-Kamala, S. Meinersb, I. Ahmedb, A. Azarovab and Chao-po Linb., (2007). Role of DNA topoisomerase IIβ in neurite outgrowth, Brain Research. **1154**, 50 – 60.

- Ohki E.C, Tilkinsa M.L, Ciccaroneb V.C and Pricea P.J., (2001). Improving the transfection efficiency of post-mitotic neurons. *J. Neuroscience Methods.* **112** , 95-99

- Onodera, R., Seki, M., Ui, A., Satoh, Y., Miyajima, A., Onoda, F., and Enomoto, T., (2002). Functional and physical interaction between Sgs1 and Top3 and Sgs1-independent function of Top3 in DNA recombination repair. Genes Genet. Syst, **77**, 11–21.

- Oppenheim RW., (1991). Cell death during development of the nervous system. Annu Rev *Neurosci*, **14**, 453-501.

- Orgel LE., (1963). The maintenance of the accuracy of protein synthesis and its relevance to aging. *Proceedings of the National Academy of Science USA*, **49**, 517-521.

- Orgel LE., (1970). The maintenance of the accuracy of protein synthesis and its relevance to aging: a correction. *Proceedings of the National Academy of Science USA* **67**, 1476.

- Orgel, L.E., (1973). Ageing of clones of mammalian cells. *Nature* **243**, 441-445.

- Pandey, S. and E. Wang., (1995). Cells en route to apoptosis are characterized by the upregulation of c-fos, c-myc, c-jun, cdc2, and RB phophorylation, resembling events of early cell-cycle traverse. *J. Cell. Biochem.*,58, 135–150.

- Pastor, N., Cortes, F., (2002). DNA Topoisomerase activities in Chinese hamster radiosensitive mutants after X-ray treatment. *Cell Biol. Int.* **26**, 547–555.

- Pawelec G, Rehbein A, Haehnel K, Merl A, Adibzadeh M.Human., (1997). T-cell clones in long-term culture as a model of immunosenescence. Immunol Rev. **160**, 31–42.

- Peterson CA., (1995). Cell culture systems as tools for studying age-related changes in skeletal muscle. *J Gerontol A Biol Med Sci.* **50**, 142–144.

- Pfeiffer, P., Vielmetter, W., (1988). Joining of non-homologous DNA doublestrand breaks *in vitro*, *Nucl. Acids Res*. **16**, 907–924.

- Plaschkes, F.W. Silverman and E. Priel., (2005). DNA topoisomerase I in the mouse central nervous system: Age and sex dependence. *J Comp Neurol* **493**, 357-369.

- Polymeropoulos MH, Lavedan C, Leroy E, Ide SE, Dehejia A, Dutra A, Pike B, Root H, Rubenstein J, Boyer R, Stenroos ES, Chandrasekharappa S, Athanassiadou A, Papapetropoulos T, Johnson WG, Lazzarini AM, Duvoisin RC, Di Iorio G, Golbe LI, Nussbaum RL., (1997). Mutation in the alpha-synuclein gene identified in families with Parkinson'sdisease. *Science.* **276**, 2045-7.

- Porter S.E and Champoux J. J., (1989). The basis for camptothecin enhancement of DNA breakage by eukaryotic topoisomerase I, *Nucleic Acids Res*. **17**, 8521–8532.
- Rao K.S., (2003). DNA-repair and brain aging: the importance of base excision repair and DNA-polymerase β, *Proc. Indian Natl. Sci. Acad*.-B, **69**, 141–156.
- Rao K.S., (2007). DNA repair in aging rat neurons. *Neuroscience*. **145**, 1330-1340.
- Rao MS, Mattson MP., (2001). Stem cells and aging: expanding the possibilities. *Mech Ageing Dev*, **122**, 713-34.
- Rao, K.S., (1997). DNA-damage and DNA-repair in aging brain, *Indian J. Med. Res.* **106**, 423–437.
- Raza M., Deshpande L.S., Blair R. E., Carter D. S., Sombati S., DeLorenzo R. J., (2007). Aging is associated with elevated intracellular calcium levels and altered calcium homeostatic mechanisms in hippocampal neurons; *Neurosci Lett.* 418, 77–81.
- Richardson, A., (1985). in: R.S. Sohal, L.S. Birnbaum and R.G. Cutler Eds.., Molecular Biology of Aging: Gene Stability and Gene Expression, *Raven Press, New York*, **29**, 229–242.
- Robert M. Brosh, Jr. and Vilhelm A. Bohr., (2002). Roles of the Werner syndrome protein in pathways required for maintenance of genome stability. *Experimental Gerontology*. **37** (4), 491-506
- Rubin H., (1997). Cell aging in vivo and in vitro. *Mech Ageing Dev.* **98**, 1–35.
- Sarkar, G. and M.E. Bolander., (1995). Telomeres, telomerase, and cancer, *Science*, **268**, 1115–1117.
- Schmitz C, Axmacher B, Zunker U, Korr H., (1999). Age-related changes of DNA repair and mitochondrial DNA synthesis in the mouse brain. *Acta Neuropathol*, **97,** 71–81.

- Schochet, S.S., Jr., (1998). Neuropathology of aging. *Neurol. Clin*, **16**, 569- 580.

- Seeberg E, Eide L, Bjoras M., (1995). The base excision repair pathway. *Trends Biochem Sci.* **20**(10), 391–397.

- Shackelford D. A., Tobaru T., Zhang S., Zivin J. A., (1999). Changes in expression of the DNA repair protein complex DNA-dependent protein kinase after ischemia and reperfusion. *J Neurosci*. **19**, 4727–38.

- Skaper S. D., Floreani M., Negro A., Facci L., Giusti P., (1998). Neurotrophins rescue cerebellar granule neurons from oxidative stress-mediated apoptotic death: selective involvement of phosphatidylinositol 3-kinase and the mitogen-activated protein kinase pathway. *J Neurochem*. **70**, 1859-68.

- Stefanis L, Park D. S, Wilma J and Lloyd A., (1999). Caspase-Dependent and -Independent Death of Camptothecin- Treated Embryonic Cortical Neurons, *The Journal of Neuroscience*. **19**(15), 6235–6247.

- Sunaga K., Tanaka T., Tani S., Kawase M., (2002). Trifluoromethyl ketones show culture age-dependent inhibitory effects on low K(+)-induced apoptosis in cerebellar granule neurons. *In Vivo.*, **16**, 97-101.

- Szilard., (1959). On the nature of the Aging process. *Proc. Natl. Acad. Sci. USA*. **45**, pp. 30-45.

- Tajes M, Yeste-Velasco M, Zhu X, Chou S. P., Smith M. A., Pallàs M., Camins A., Casadesús G., (2009). Activation of Akt by lithium: pro-survival pathways in aging. *Mech Ageing Dev.*, **130**, 253-61.

- Tajes Orduña M, Pelegrí Gabalda C, Vilaplana Hortensi J, Pallàs Lliberia M, Camins Espuny A., (2009). An evaluation of the neuroprotective effects of melatonin in an in vitro experimental model of age-induced neuronal apoptosis. *J Pineal Res.* **46**(3), 262-7.

- Terman A., (2001) Garbage catastrophe theory of aging: imperfect removal of oxidative damage?. *Redox Re.* **6**, 15–26

- Thibault O., Hadley R., Landfield P. W., (2001). Elevated Postsynaptic [Ca2+]i and L-Type Calcium Channel Activity in Aged Hippocampal Neurons: Relationship to Impaired Synaptic Plasticity. *J Neurosci*., **21**, 9744-9756.

- Thibault O., Landfield P. W., (1996). Increase in single L-type calcium channels in hippocampal neurons during aging. *Science*. **272**, 1017–1020.

- Thrash, A.T. Bankier, B.G. Barrell and R. Sternglanz., (1985). Cloning, characterization, and sequence of the yeast DNA topoisomerase gene, *Proc. Natl. Acad. Sci. USA.* **82**, 4374-4378.

- Toescu E. C., Verkhratsky A., (2000). Neuronal ageing in long-term cultures: alterations of Ca2+ homeostasis. *Neuroreport.* **11**, 3725-9.

- Towbin H., Staehelin T., Gordon J., (1979). Electrophoretic transfer of proteins from polyacrylamide gels to nitrocellulose sheets: procedure and some applications. *Proc Natl Acad Sci*, U S A, **76**, 4350–4354.

- Trushina E, McMurray C., (2007). Oxidative stress and mitochondrial dysfunction in neurodegenerative diseases. *Neuroscience*. **145**,1233-1248

- Tsutsui K., Hosoya O., Sano K., Tokunaga A., (2001). Immunohistochemical analyses of DNA topoisomerase II isoforms in developing rat cerebellum, *J. Comp. Neurol.* **431**, 228–239.

- Uemura T and Yanagida M., (1984). Isolation of type I and II DNA Topoisomerase mutants from fission yeast: single and double mutants show different phenotypes in cell growth and chromatin organization, *EMBO J*.**3**, 1737–1744.

- Valente EM, Abou-Sleiman PM, Caputo V, Muqit MM, Harvey K, Gispert S, Ali Z, Del Turco D, Bentivoglio AR, Healy DG, Albanese A, Nussbaum R, Gonzalez-Maldonado R, Deller T, Salvi S, Cortelli P, Gilks WP,Latchman DS, Harvey RJ, Dallapiccola B, Auburger G, Wood NW., (2004). Hereditary early-onset Parkinson's disease caused by mutations in PINK1. *Science*, **304**, 1158-60.

- Veng L. M., Browning M. D., (2002). Regionally selective alterations in expression of the [alpha]1D subunit (Cav1.3) of L-type calcium channels in the hippocampus of aged rats. *Mol Brain Res*. **107**, 120–127.

- Victor, M., Ropper, A.H., (2001). (Eds.), Principles of Neurology, **7** ed.. McGraw-Hill, New York.

- Vijg J, Busuttil RA, Bahar R, Dolle ME., (2005). Aging and genome maintenance. *Ann N Y Acad Sci*, **1055**, 35–47.

- Vijg, J., (2000). "Somatic mutations and aging: a re-evaluation." *Mutat Res.* **447**(1), 117-135.

- von Zglinicki, T., Burkle, A., Kirkwood, T.B., (2001). Stress, DNA damage and ageing-an integrative approach. *Exp. Gerontol*, **36**, 1049-1062.

- Vosberg H.P., (1985). DNA topoisomerases: enzymes that control DNA conformation. *Curr. Top. Microbiol. Immunol.* **114**, 19–102.

- Vyjayanti V.N, and Rao K.S, (2006). DNA double strand break repair in brain: Reduced NHEJ activity in aging rat neurons. *Neuroscience Letters* **393**, 18-22.

- Walford RI., (1962). Auto-immunity and aging. *J Gerontol***.17**, 281.

- Wang J.C., (1996). DNA topoisomerases. *Annu Rev Biochem.* **65**, 635–692.

- Wang J.C., (1998). Moving one DNA double helix through another by a type II DNA topoisomerase: the story of a simple molecular machine. *Q. Rev. Biophys.* **31**, 107–144.

- Wang J.C., (1987). Recent studies of DNA topoisomerases. *Biochim. Biophys.Acta* **909**, 1–9.

- Wang J.C., (2002). Cellular roles of DNA topoisomerases. *Nat. Rev.Mol. Cell Biol*, **3**, 430–440.

- Wang X., Zaidi A., Pal R., Garrett A. S., Braceras R., Chen X. W., Michaelis M. L., Michaelis E. K., (2009). Genomic and biochemical approaches in the discovery of mechanisms for selective neuronal vulnerability to oxidative stress. *BMC Neurosci*., **19**, 10-12.

- Wang, J. C., (1996). DNA topoisomerases. *Annu. Rev. Biochem*, **65**, 635–692.

- Watanabe M., Tsutsui K., Tsutsui K., Inoue Y., (1994). Differential expressions of the topoisomerase II alpha and II beta mRNAs in developing rat brain. *Neurosci Res*.**19**, 51-7.

- Weidenheim KM, Dickson DW, Rapin I., (2009). Neuropathology of Cockayne syndrome: Evidence for impaired development, premature aging, and neurodegeneration. *Mech Ageing Dev*. **130**, 619-36.

- Weissman L, de Souza-Pinto NC, Stevnsner T, Bohr VA., (2007). DNA repair, mitochondria, and neurodegeneration. Neuroscience; [Epub ahead of print]

- Wickelgren, I., (1996). For the cortex, neuron loss may be less than thought. *Science*, **273**, 48-50.

- Wilson DM 3rd, McNeill DR., (2007). Base excision repair and the central nervous system. *Neuroscience*. 145, Issue 4, 1187-1200.

- Wistrom C, Villeponteau P., (1990). Long-term growth of diploid human fibroblasts in low serum media. *Exp Gerontol.* **25**, 97–105.

- Woessner, R.D., Chung, T.D.Y., Drake, F.H., (1991). Proliferation and cell cycle dependent differences in expression of the 170 and 180 KDa forms of Topoisomerase II. Cell Growth Differ. **2**, 209–214.

- Wu H.Y, Shyy S.H, Wang J.C and Liu L.F., (1988). Transcription generates positively and negatively supercoiled domains in the template. *Cell*. **53**, 433–440.

- Wu, L., and Hickson, I. D., (2002). The Bloom's syndrome helicase stimulates the activity of human topoisomerase III. *Nucleic Acids Res.* **30**, 4823–4829.

- Wu, L., Davies, S. L., North, P. S., Goulaouic, H., Riou, J. F., Turley, H., Gatter, K. C., and Hickson, I. D., (2000). The Bloom's syndrome gene product interacts with topoisomerase III. *J. Biol. Chem*, **275**, 9636–9644.

- Xiong J., Camello P. J., Verkhratsky A., Toescu E. C., (2004). Mitochondrial polarisation status and [Ca2+]i signalling in rat cerebellar granule neurones aged in vitro. *Neurobiol Aging.* **25**, 349-59.

- Yao C. J., Lin C. W., Lin-Shiau S. Y., (1999). Roles of thapsigargin-sensitive Ca2+ stores in the survival of developing cultured neurons. *J Neurochem*. **73**, 457-65.

- Zimprich A, Biskup S, Leitner P, Lichtner P, Farrer M, Lincoln S, Kachergus J, Hulihan M, Uitti RJ, Calne DB, Stoessl AJ, Pfeiffer RF, Patenge N, Carbajal IC, Vieregge P, Asmus F, Muller-Myhsok B, Dickson DW, Meitinger T, Strom TM, Wszolek ZK, Gasser T., (2004). Mutations in LRRK2 cause autosomal-dominant parkinsonism with pleomorphic pathology. *Neuron*, **44**, 601-7.

Publications:

- **M. Uday Bhanu**, Anand K. Kondapi., (2010). Neurotoxic activity of a Topoisomerase-I inhibitor, camptothecin, in cultured cerebellar granule neurons. *Neurotoxicology* (2010), doi:10.1016/j.neuro.2010.06.008.

- **M. Uday Bhanu,** R.K. Mandraju, C. Bhaskar, Anand Kumar Kondapi. Cultured Cerebellar Granule Neurons as an *in vitro* aging model: Topoisomerase II beta as an additional biomarker in DNA repair and aging. (Accepted for publication in Toxicology *in vitro*).

- P. Jhansi Lakshmi, B.V.S. Suneel Kumar, Ravi Shasi Nayana, M. Srinivas Mohan, Ramababu Bolligarla, Samar K. Das, **M. Uday Bhanu,** Anand K. Kondapi, Muttineni Ravikumar., (2009). Design, sythesis & discovery of novel non-peptide inhibitor of caspase-3 using ligand based and structure based virtual screening approach. *Bioorganic & Medicinal Chemistry*. Vol **17**, Issue 16, 15 Aug 2009.

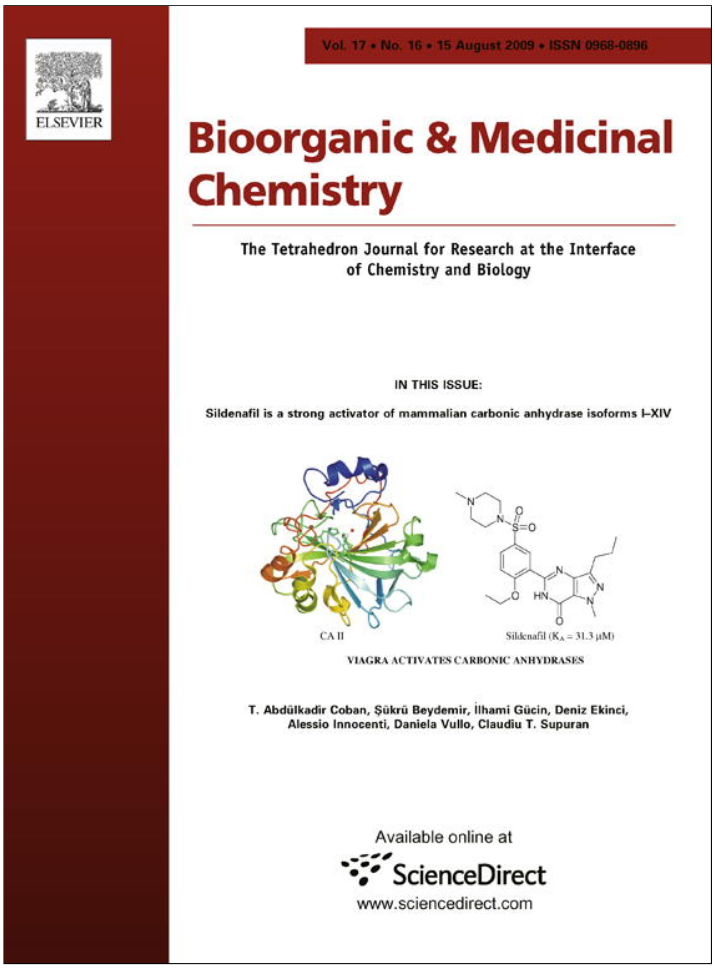

Bioorganic & Medicinal Chemistry 17 (2009) 6040–6047

Contents lists available at ScienceDirect

Bioorganic & Medicinal Chemistry

journal homepage: www.elsevier.com/locate/bmc

Design, synthesis, and discovery of novel non-peptide inhibitor of Caspase-3 using ligand based and structure based virtual screening approach

P. Jhansi Lakshmi [a], B. V. S. Suneel Kumar [b], Ravi Shasi Nayana [b], M. Srinivas Mohan [a], Ramababu Bolligarla [c], Samar K. Das [c], M. Uday Bhanu [d], Anand K. Kondapi [d], Muttineni Ravikumar [b,*]

[a] Department of Chemistry, Osmania University College for Women, Koti, Hyderabad 5000095, India
[b] BioCampus, GVKBIO Sciences Private Limited, S-1, Phase-1, TIE, Balanagar, Hyderabad 500037, India
[c] School of Chemistry, University of Hyderabad, Hyderabad 500046, India
[d] Department of Biotechnology, University of Hyderabad, Hyderabad 500046, India

ARTICLE INFO

Article history:
Received 14 February 2009
Revised 22 June 2009
Accepted 23 June 2009
Available online 7 July 2009

Keywords:
Caspase-3
Virtual screening
Pharmacophore
Docking
Apoptosis

ABSTRACT

Caspase-3 belonging to a family of cysteine proteases is main executioner of apoptotic cascade pathway. The inhibitors of this protein are useful in the treatment of cardiomyopathy and neurodegenerative diseases. For the discovery of novel Caspase-3 non-peptide inhibitors from Maybridge database, ligand based and structure based virtual screening methods were used. Quantitative 3D pharmacophore models were generated using 25 known inhibitors of Caspase-3 and it was used as initial screen to retrieve the hits from the database. These compounds with high estimated activity were analyzed for drug like properties and docking studies were performed, to study the interaction between new hits and active site. One of the hits (AW01208), with good predictions was selected for synthesis and biological screening. This compound showed an inhibition activity against Caspase-3 in SKNH cell lines.

1. Introduction

Caspases are a family of cysteine proteases responsible for promoting cell death (Apoptosis).[1] Caspase-3 (apopain), is situated at a key junction in the apoptosis, mediating apoptotic cascade from the intrinsic and extrinsic activation pathways. Apoptosis has been observed in a large number of pathological conditions, including ischemia-reperfusion injury (stroke and myocardial infarction), cardiomyopathy, neurodegeneration (Alzheimer's disease, Parkinson's disease, Huntington's disease, and ALS), sepsis, type I diabetes, and allograft rejection.[2,3] Two different classes of caspases involved in apoptosis, the initiator caspases and the executioner caspases. The initiator caspases, which include Caspase-2, -8, -9, and -10, are located at the top of the signalling cascade; their primary function is to activate the executioner caspases, Caspase-3, -6, and -7.

The executioner caspases are responsible for the physiological (e.g., cleavage of the DNA repair enzyme poly (ADP-ribose) polymerase-1, nuclear laminins, and cytoskeleton proteins) and morphological changes (DNA strand breaks, nuclear membrane damage, and membrane blebbing) that occur in apoptosis. Most of the caspases are activated by cleavage at a specific aspartate site by assembly of their active subunit forms. Activation of Caspase-9 requires the release of cytochrome *c* from mitochondria to cytosol where the caspase resides. Caspase-3 is activated by the upstream Caspase-8 and Caspase-9 and since it serves as a convergence point for different signalling pathways.[4,5]

Several Merck Caspase-3 inhibitors are currently in preclinical trials. M-826, a small reversible Caspase-3 inhibitor, blocked brain tissue damage in an animal model of hypoxia–ischemia when injected 2 h after ligation[6] and another merck Caspase-3 specific inhibitor M-791 decreased lymphocyte apoptosis in thymus and spleen of mice subjected to sepsis induced by cecal ligation-puncture and rescued 80–90% of animals from lethal septic shock.[7,8]

In our present study, we used computational approach to identify the potent and selective Caspase-3 inhibitors. Three-dimensional (3D) pharmacophore models were generated using the known set of Caspase-3 inhibitors, to reveal the chemical features required for its activity. Best pharmacophore (Hypo 1) is validated with docking and structure based pharmacophore studies. These models were used to rapidly screen compounds from Maybridge database, for the identification of a series of novel and highly potent Caspase-3 inhibitors. Ten molecules were selected from virtual screening using pharmacophore as query and these molecules are selected for synthesis and in vitro screening studies based on the docking scores, predicted binding location and their drug like properties.

* Corresponding author. Tel.: +91 9989889074.
E-mail address: ravambio@gmail.com (M. Ravikumar).

0968-0896/$ - see front matter © 2009 Elsevier Ltd. All rights reserved.
doi:10.1016/j.bmc.2009.06.069

2. Methods

2.1. Molecular modelling

We have collected 97 human Caspase-3 inhibitors with activity data (IC_{50}) spanning over 6 orders of magnitude (from 0.1 nM to 27,900 nM)[9–15] from research articles. Activity measured was at same assay method for all the compounds used in this study. Activity values are uniformed to nM. The 3D structures of all molecules were constructed by using Cerius2[16] and further these molecules are subjected to energy minimization using the steepest descent algorithm with a convergence gradient value of 0.001 kcal/mol. The Geometry optimization was carried out with the MOPAC 6 packages using semi empirical AM1 Hamiltonian method.[17]

2.2. Pharmacophore generation

Pharmacophore models were generated for known inhibitors of Caspase-3 using Catalyst package.[18] Chemical-featured quantitative pharmacophore can be generated automatically using the HypoGen module within Catalyst, provided that structure–activity relationship data of a well-balanced set of compounds is available.

All compounds used in the study were subjected to best method option of conformational search using Monte Carlo-like algorithm together with poling[19] to generate a maximum of 250 conformers. Our models emphasized a conformational diversity within the constraint of a 20 kcal/mol energy threshold above the estimated global minimum based on use of the CHARMM force field and using poling algorithm.[20,21] The molecules associated with their conformation models were then submitted to Catalyst hypotheses generation.

The dataset was divided into training set and test set, considering both structural diversity and wide coverage of the activity range (shown in Scaffold 1–5, in Supplementary data). The compounds with activity with <10 nM were considered as highly actives (+++), compounds with an activity range of 10–100 nM as moderate actives (++) and activity of >1000 nM as least actives (+).

In hypotheses generation, the structure and activity correlations in the training set were rigorously examined. HypoGen identifies features that are common to the active compounds but excludes common features for the inactive compounds within conformationally allowable regions of space. Ten hypotheses were generated for every HypoGen run from which the ones with the highest correlation values were chosen. The pharmacophore models were validated using cost analysis and test set activity prediction.

The best pharmacophore (Hypo 1) having high correlation coefficient (r), lowest total cost, and lower RMSD value was chosen to estimate the activity of test set (Details of Cost parameters mentioned in Supplementary data).

2.3. Docking studies

X-ray crystal structure of Caspase-3 (PDB ID 1pau with a resolution of 2.50 Å) was used for docking studies. Preparation of the protein for docking included removal of ligand and solvent coupled with addition of hydrogen atoms. All selected inhibitors were docked into the active site of the target protein using Glide (version 8.0, Schrödinger, Inc.) in standard precision mode (Glide SP).[22,23] The binding region was defined by a 12 A^0_12 A^0_12 A^0 box centred on the centroid of the crystallographic ligand to confine the centroid of the docked ligand. No scaling factors were applied to the Van der Waals radii. Default settings were used for all the remaining parameters. The top 20 poses were generated for each ligand. The docking poses were then energy minimized with Macro model in the OPLS2001 force field[24] with flexible ligand and rigid receptor. Best pose was selected on the basis of Glide score and the interactions formed between the ligands and active site amino acids.

2.4. Virtual screening

To find the novel non-peptide inhibitors of Caspase-3, virtual screening was conducted on Maybridge database[25] containing about 50,000 compounds along with their conformations. Best pharmacophore model (Hypo 1) comprising of four chemical features was used as a query to retrieve the leads from the database. Fast flexible search method was used for database searching to retrieve new lead molecules.

2.5. Experimental

In silico studies led to the identification of top 10 lead compounds with Caspase-3 inhibitor activity. The synthesis of AW01208 (3,4-dichloro-*N*-{3-[4-(2-chloro-6-fluoro-benzyl)-piperazin-1-yl]-propyl}-benzamide) is described in-detail in Scheme 1. Spectral data such as NMR, IR, and LC–MS of AW01208 was given in Scheme 2 (Supplementary data). After synthesis, the lead compound AW1208 (3,4-dichloro-*N*-{3-[4-(2-chloro-6-fluoro-benzyl)-piperazin-1-yl]-propyl}-benzamide) was used to carry out in vitro bioassay studies using spectroflourimetric techniques to assess the Caspase-3 inhibition ability of the synthesized compound. All chemicals and reagents were purchased from Aldrich Chemical Co. unless and otherwise indicated, and used without further purification. All reactions were carried out under an inert nitrogen atmosphere with dry solvents using anhydrous conditions unless otherwise stated. The ^1H NMR spectra of compounds were recorded on Bruker DRX-400 spectrometer using $Si(CH_3)_4$ [TMS] as an internal standard. Samples were dissolved in an appropriate deuterated solvent ($CDCl_3$). Proton chemical shifts are reported as parts per million (δ) relative to tetramethylsilane (Me_4Si; 0.00 ppm), ^{13}C NMR spectra are reported as δ relative to deuterated chloroform ($CDCl_3$, 77.0 ppm). Solution mass spectrum (LCMS) of compound AW01208 was obtained on a LCMS-2010A Shimadzu spectrometer using ESI mode of ionisation. Infrared (IR) spectra were recorded on KBr pellets with a JASCO FT/IR-5300 spectrometer in the region of 400–4000 cm^{-1}

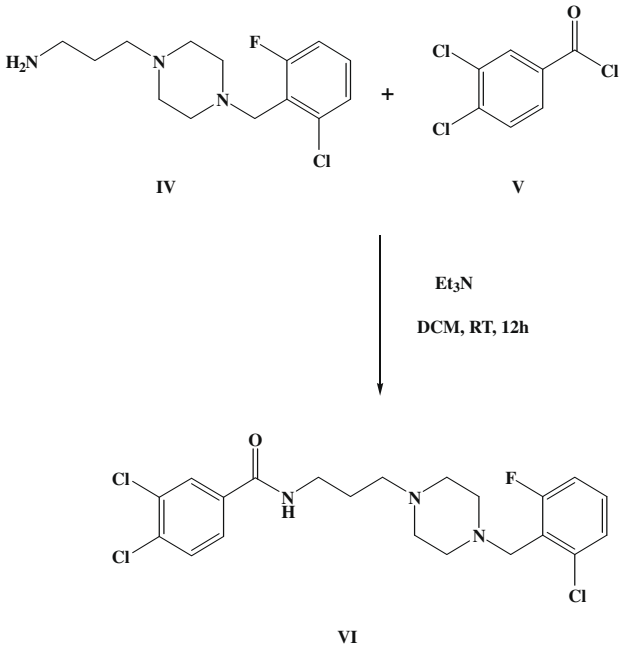

2.5.1. Synthesis of (3-bromopropyl) carbamic acid benzyl ester (II)

The compound was prepared according to the literature.[26]

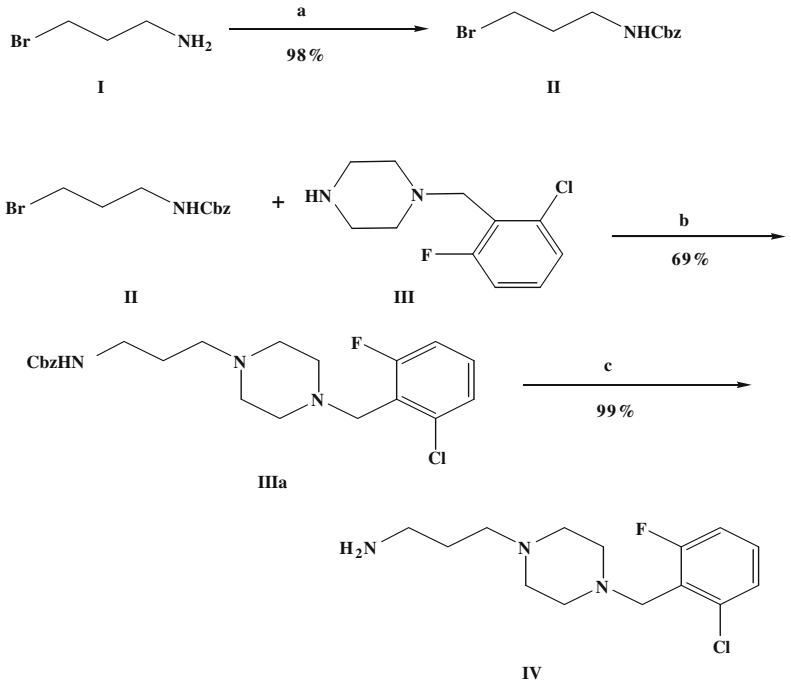

Scheme 1. Reagents and conditions: (a) benzylchloroformate; (b) K_2CO_3, MeCN, 80 °C; (c) iodotrimethysilane, MeCN.

2.5.2. Synthesis of {[3-(4-(2-chloro, 6-fluoro benzyl piperazin-1-yl)] propyl} carbamic acid benzyl ester (IIIa)

The free base (**III**) form of (**IIIa**) (0.450 g) and the alkyl bromide (0.650 g) (1.1 equiv) and K_2CO_3 (0.78) (2 equiv) were heated to reflux in 20.0 mL CH_3CN solvent for 4 h under nitrogen atmosphere. The mixtures were cooled at room temperature. Then evaporated the solvent and the residue dissolved in water and extracted with ethyl acetate. The organic extract was dried (Na_2SO_4) filtered and solvent evaporated in vacuo to give the product as clear oil. Column chromatography (100% ethyl acetate, R_f 0.4). NMR data: ^{1}H NMR (400 MHz, δ ppm) ($CDCl_3$): 1.62–1.68 (m, 2H), 2.40–2.58 (br d, 10H), 3.26 (q, 2H, J = 4.6 Hz), 3.70 (s, 2H), 5.09 (s, 2H), 5.89 (s, 1H), 6.95–6.99 (m, 1H), 7.18 (s, 2H), 7.28–7.30 (m, 5H).

2.5.3. Synthesis of {[3-(4-(2-chloro, 6-fluoro benzyl piperazin-1-yl)] propylamide (IV)

Iodotrimethylsilane (0.278 mL, 1.94 mmol) was added to a solution of compound (**IIIa**) (0.278 g, 1.94 mmol) in acetonitrile (5 mL). The reaction mixture was stirred for 15 min at room temperature, quenched with methanol (3 mL) and stirred for an additional 10 min. Volatiles are removed in vacuo; the residue was dissolved in 3 N HCl (10 mL) and extracted with ether (6.0 mL). The aqueous portion was neutralized to pH 9–10 with aqueous NH_4OH. Extraction with $CHCl_3$ (5.0 mL) and drying (Na_2SO_4) followed by evaporation yielded the product as a clear viscous oil that was used in the next step without further purification. NMR and IR data: ^{1}H NMR (400 MHz, δ ppm) ($CDCl_3$): 1.60–1.66 (m, 2H), 2.38 (t, 2H, J = 7.4 Hz), 2.46 (br s, 4H), 2.60 (br s, 4H), 2.74 (t, 2H, J = 6.8 Hz), 3.73 (s, 2H), 6.93–6.70 (m, 1H), 7.17–7.19 (m, 2H). ^{13}C NMR δ 30.29, 40.79, 52.30, 52.61, 53.23, 56.41, 113.9, 123.7, 125.37, 129.05, 136.63, 160.86. IR (NaCl plate, neat) 697, 1134, 1260, 1538, 1694, 2946, 3332 cm^{-1}.

2.5.4. Synthesis of 3,4-dichloro-*N*-{3-[4-(2-chloro-6-fluoro-benzyl)-piperazin-1-yl]-propyl}-benzamide (VI)

A mixture of amine (**IV**) (0.15 mL) (1 equiv), triethylamine and 5.0 mL dry DCM was stirred under nitrogen gas for 10 min, then the acid chloride (**V**) (0.080 g) (1.1 equiv) was added and stirred continuously for 12 h. The solvent was removed under reduced pressure and mixture was stirred with water. Later extracted into ethyl acetate and the organic layer washed with water and brine solution then with water and dried with Na_2SO_4. The solvent was evaporated by rotary vapour and separated by the column chromatography by using 4% methanol + 96% $CHCl_3$ mixture. A clear oily liquid compound was obtained. NMR data: ^{1}H NMR (400 MHz, δ ppm) ($CDCl_3$): 1.92 (s, 2H), 2.76 (br d, 8H), 3.48 (s, 2H), 3.69 (s, 2H), 4.04 (br s, 2H), 6.93 (d, 1H), 7.15 (s, 1H), 7.39 (d, 1H), 7.72 (d, 1H), 7.99 (s, 1H), 8.40 (s, 1H). Mass spectra given in SI, LCMS Data: Molecular ion peak obtained at 458 with few other fragment peaks.

2.6. Biological screening

Caspase-3 inhibition studies were estimated by using a Spectrofluorometric method[27,28] by measuring the accumulation of a flourogenic product. The activities of the compound were evaluated in SKNSH cell lines as a cell-based model of apoptosis. The compound inhibited Caspase-3 activity in a concentration dependent manner.

Inhibition studies were carried out using Caspase-3 Assay kit (BD Pharmingen™). The kit is designed to measure Caspase-3 cleaving activity, an early marker of cells undergoing apoptosis. Doxorubicin induced apoptotic extracts were used as Caspase-3 and 7 sources. Ac-DEVD-AMC is a synthetic tetra peptide flourogenic substrate (MW = 675 Da; purity $\geq$ 98%) that was used to identify and quantitate Caspase-3 activity in apoptotic cell lysates.

Caspase-3 cleaves the tetra peptide between D and AMC, releasing AMC. The enzymatic activity of Caspase-3 and 7 was determined by measuring the accumulation of the flourogenic product 7-amino-4-methyl coumarin (AMC) using an excitation wavelength of 380 nm and an emission wavelength range of 420–460 nm. Apoptotic cell lysates containing active Caspase-3 yield a considerable emission as compared to non-apoptotic cell lysates. The Caspase-3 and 7 were first assayed to determine the optimal

concentration for each experiment. Optimal concentrations were based in the linear range of the enzyme activation curves.

The Caspase-3 protein inhibitor compound was tested with the standard compounds as a control for caspase activity. The non-peptide inhibitor was dissolved in DMSO, and a serial dilution was performed before screening in order to obtain desired concentrations. The compound synthesized was analyzed for Caspase-3 inhibitory activity with doxorubicin induced extract for Caspase-3 source.

3. Results and discussion

3.1. Pharmacophore generation

Pharmacophore models are developed in HypoGen module in Catalyst software. All dataset compounds were divided into a training set of 25 compounds and a representative test set of 72 compounds. HypoGen attempts to construct the simplest hypotheses that best correlates the activities (experimental vs predicted).

Ten statically best pharmacophore models were generated and these models were considered for further analysis. The Null cost (no correlation cost) for 10 hypotheses was 173.02, the fixed cost (ideal cost) of the run was 100.12 and the configuration cost was 14.90. A difference of 59.45 bits obtained between fixed and null costs is a sign of highly predictive nature of hypotheses. All 10 hypotheses generated showed high correlation coefficient between experimental and predicted IC_{50} values, in the range of 0.93–0.86 and moreover, these are having cost difference greater than 45 bits between the cost of each hypothesis and the null cost. It indicates that all the hypotheses are having true correlation between 75% and 90%. The cost values, correlation coefficients (r), RMSD, and pharmacophore features are listed in Table 1. The best pharmacophore (Hypo 1) consisted of one H-bond acceptor (HBA), one H-bond donor (HBD), and two hydrophobic (HY) features shown in Figure 1. This model is having high correlation coefficient (r) of 0.93, lowest total cost (59.45), and least RMSD value (0.98) and it was chosen to further validate its predictive power by estimating the activity of test set.

For the highly active compound (62) all the features are perfectly mapped to the features of Hypo 1 and had a fit score of 9.19, shown in Figure 2a. Whereas, for the least active compound (92) only three features of Hypo 1 were mapped properly and had fit value of 4.98, shown in Figure 2b. In compound 62, HBA feature is mapped to oxygen atom of carbonyl group present in amide moiety. The HBD feature mapped to the NH group which is attached to the 5th position of 4-oxo pentanoic acid. Among the two hydrophobic groups, one was mapped to the tertiary butyl group substituted at 5th position on pyrazine ring of the compound and another on *n*-pentane chain.

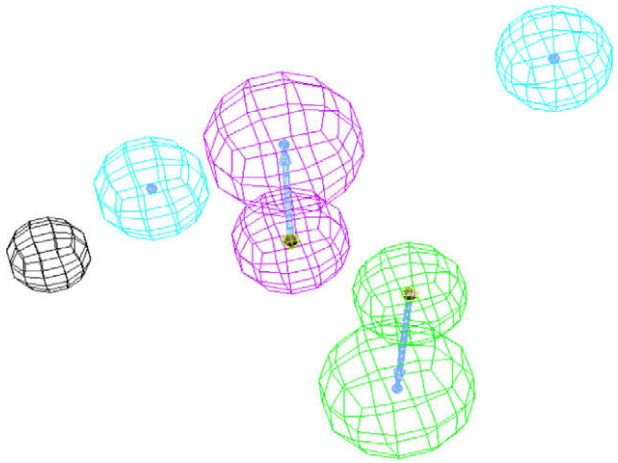

Figure 1. The best hypothesis model Hypo 1 produced by the HypoGen module in Catalyst 4.11 software. Pharmacophore features are color-coded with green, blue, and red contours representing the hydrogen-bond acceptor feature (A), hydrophobic feature (Z), hydrogen bond donor, respectively. Distance between pharmacophore features are reported in angstroms (Å).

The experimental and predicted activities of training set are listed in Scaffold 1–5 (in Supplementary data). In training set, among the 7 highly active compounds, all are predicted as highly active (+++). Out of 8 moderately active compounds (++), only three compounds was predicted as high active (+++), and the rest were predicted on the target. Out of 10 least active compounds, all compounds were predicted as least active (+).

The prediction power of Hypo 1 was evaluated by using 72 test set containing chemically diverse compounds. The experimental and predicted activities of test set are listed in str1–5 (in Supplementary data). Among the 9 highly active '+++' compounds in the test set, pharmacophore model was able to predict 8 compounds correctly and only one compound predicted as moderate active. Out of 47 compounds present in moderately active '++' range, 39 compounds predicted as '++', but 7 compounds predicted as high active and one compound inactive. Out of 16 least actives only 3 compounds predicted as '++'.

For the highly active compound (97) all the features are perfectly mapped to the 3 features of Hypo 1, shown in Figure 2a. Whereas, for the least active compound (11) mapped three features of Hypo 1 were mapped properly, shown in Figure 3b.

The generated pharmacophore model has predicted the activity of these test set compounds with correlation of 0.88 (shown in Graph 1). The over all correlation between the experimental and predicted activity was about 0.88 and hence from this analysis, Hypo 1 was able to distinguish actives from the inactives.

Table 1
Results of pharmacophore hypothesis generated using training set against Caspase-3 inhibitors

Hypo no.	Total cost	Cost-difference	Error cost	RMS	Correlation	Features
1	113.57	59.45	96.24	0.98	0.93	A,D,H,H
2	115.78	57.24	97.96	1.05	0.92	A,D,H,H
3	118.02	55.00	100.76	1.15	0.90	A,D,H,H
4	118.11	54.91	101.51	1.18	0.89	A,D,H,H
5	120.20	52.82	103.23	1.23	0.88	A,D,H,H
6	121.09	51.93	104.96	1.29	0.87	A,D,H,H
7	121.31	51.71	104.55	1.27	0.87	A,D,H,H
8	121.80	51.22	105.40	1.30	0.87	A,D,H,H
9	122.15	50.87	105.25	1.30	0.87	A,D,H,H
10	122.16	50.86	105.84	1.31	0.86	A,D,H,H

All cost values are in bits.
A = hydrogen bond acceptor, D = hydrogen bond donor, H = hydrophobic.
Cost details of ten pharmacophores: Fixed cost: 100.12, Configuration cost 14.90 and Null cost 173.02.

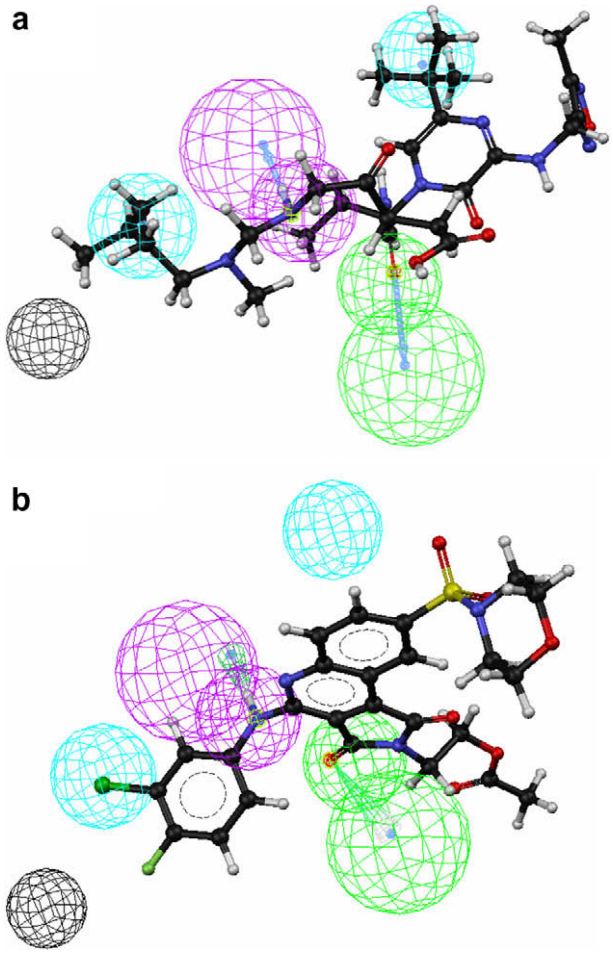

Figure 2. Pharmacophore mapping of the most active and least compound (1 from the training set) on the best hypothesis model Hypo 1 (a). Pharmacophore mapping of the highest active compound on the best hypothesis model Hypo 1 from the training set model number 62. (b) Pharmacophore mapping of the least active compound on the best hypothesis model Hypo 1 from the training set model number 92.

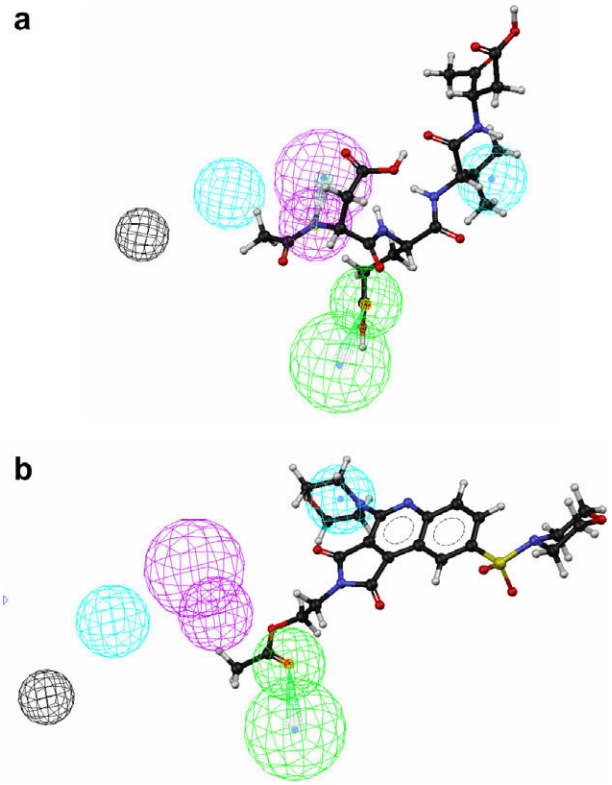

Figure 3. Pharmacophore mapping of the most active and least compound (1 from the test set) on the best hypothesis model Hypo 1 (a). Pharmacophore mapping of the highest active compound on the best hypothesis model Hypo 1 from the test set model number 77. (b) Pharmacophore mapping of the least active compound on the best hypothesis model Hypo 1 from the test set model number 91.

3.2. Docking studies

Initial docking calculations were performed for these 97 known inhibitors to analyze the important interactions between protein and the ligand to generate a structural model for virtual ligand docking (VLS).

All docking calculations were performed using the 'Standard Precision' (SP) mode of GLIDE program and with OPLS-AA 2001 force field. All the compounds in the study were docked in the active site of receptor and calculated the binding interactions. The estimated docking scores (G Score) by the algorithm for these compounds are listed in Table 2. These studies provided insight into interactions that may be important for inhibitor activity by comparing docking simulations of each inhibitor in the Caspase-3.

The docked conformations determined by Glide with the best docking energy for the high active compounds are in the range of −11.35 and for the low active compounds are having in the range of −5.49. In Figure 4a, showing the Glide generated binding pose of highly active compound (62) inside the active of Caspase-3. As depicted from the figure, the compound is showing four hydrogen bond interactions with the atoms active amino acids. The two important hydrogen bond contacts with Arg207, the first hydrogen bond is formed by the backbone CO and NH of the compound (CO···HN, 2.13 Å) and the second hydrogen bond is formed by side chain NH of Arg207 and CO group of the compound (NH···OC, 2.74 Å). Other two crucial hydrogen bond interactions are formed between the compound and the receptor is: NH of indole ring present in Try 214 with CO group of compound (NH···OC, 3.25 Å), backbone NH of Ser209 with carbonyl oxygen of the ligand (NH···OC, 2.62 Å).

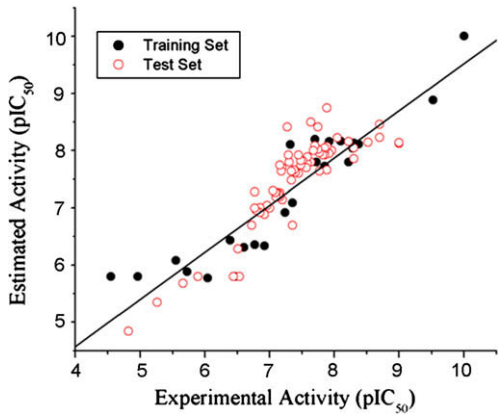

Graph 1. Correlation graph between experimental (pIC_{50}) and Hypo 1-estimated activities (pIC_{50}) of training and test set.

All dataset molecules were docked into the active site of Caspase-3, and the correlation was calculated between Glide score and the pIC_{50} by linear regression analysis method. An acceptable correlation coefficient (r) of 0.78 was obtained between experimental pIC_{50} and docking energy (Graph 2).

Table 2
Experimental activity (pIC_{50}) and dock scores obtained by Glide SP of dataset molecules

Compound number	Experimental activity (pIC_{50})	Dock score
sdmol 62	10.000	−11.351
sdmol 20	9.523	−9.037
sdmol 80	9.000	−9.338
sdmol 77	9.000	−8.139
sdmol 82	8.699	−9.822
sdmol 78	8.699	−8.634
sdmol 17	8.523	−8.428
sdmol 11	8.377	−7.868
sdmol 72	8.301	−8.101
sdmol 19	8.301	−8.576
sdmol 15	8.301	−8.952
sdmol 16	8.284	−7.964
sdmol 68	8.222	−8.762
sdmol 60	8.222	−7.410
sdmol 39	8.097	−8.576
sdmol 59	8.046	−7.921
sdmol 58	7.959	−7.096
sdmol 73	7.921	−7.817
sdmol 36	7.921	−7.841
sdmol 61	7.886	−7.416
sdmol 57	7.886	−7.503
sdmol 47	7.886	−6.921
sdmol 71	7.854	−7.341
sdmol 70	7.854	−7.527
sdmol 48	7.854	−7.568
sdmol 44	7.854	−8.354
sdmol 43	7.854	−7.916
sdmol 56	7.824	−7.720
sdmol 64	7.770	−8.030
sdmol 55	7.770	−6.914
sdmol 81	7.745	−7.238
sdmol 34	7.745	−7.365
sdmol 69	7.721	−7.021
sdmol 74	7.699	−7.677
sdmol 67	7.699	−6.484
sdmol 51	7.678	−6.122
sdmol 83	7.638	−6.221
sdmol 46	7.638	−6.272
sdmol 54	7.585	−6.531
sdmol 35	7.585	−7.996
sdmol 85	7.569	−6.208
sdmol 76	7.523	−6.443
sdmol 3	7.509	−6.576
sdmol 97	7.481	−6.771
sdmol 96	7.481	−7.109
sdmol 45	7.481	−5.576
sdmol 86	7.444	−6.094
sdmol 28	7.444	−5.576
sdmol 84	7.398	−6.576
sdmol 53	7.377	−5.576
sdmol 14	7.357	−6.345
sdmol 10	7.357	−6.389
sdmol 79	7.337	−7.072
sdmol 38	7.337	−7.322
sdmol 23	7.319	−5.576
sdmol 65	7.301	−5.576
sdmol 37	7.292	−5.576
sdmol 21	7.276	−7.506
sdmol 95	7.237	−7.263
sdmol 41	7.201	−6.000
sdmol 42	7.194	−6.049
sdmol 63	7.180	−7.031
sdmol 8	7.155	−7.350
sdmol 75	7.155	−6.728
sdmol 66	7.155	−6.855
sdmol 30	7.149	−6.427
sdmol 24	7.143	−6.426
sdmol 40	7.108	−6.300
sdmol 22	7.097	−7.169
sdmol 32	7.086	−6.576
sdmol 25	7.056	−7.223
sdmol 49	7.000	−6.511
sdmol 52	6.959	−6.614
sdmol 50	6.921	−6.342
sdmol 1	6.921	−6.751
sdmol 31	6.854	−6.855
sdmol 26	6.854	−5.246
sdmol 33	6.796	−5.522
sdmol 5	6.770	−6.220
sdmol 18	6.770	−5.278
sdmol 12	6.770	−6.549
sdmol 29	6.721	−6.188
sdmol 89	6.602	−7.464
sdmol 88	6.532	−7.217
sdmol 27	6.509	−6.018
sdmol 93	6.456	−6.031
sdmol 94	6.441	−6.295
sdmol 9	6.387	−6.187
sdmol 4	6.041	−6.076
sdmol 90	5.889	−5.491
sdmol 7	5.721	−5.679
sdmol 6	5.658	−5.540
sdmol 2	5.553	−5.180
sdmol 13	5.260	−5.702
sdmol 87	4.959	−6.546
sdmol 91	4.814	−4.625

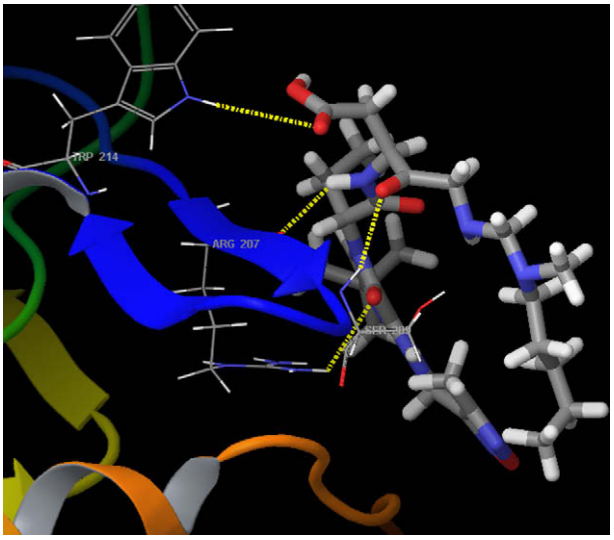

Figure 4. Docked conformation of the most active compound 62 in the active site. Broken lines represent hydrogen bonds.

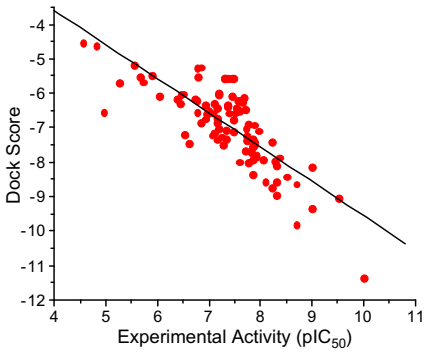

Graph 2. Correlation graph between experimental activity (pIC_{50}) and docking score.

3.3. Virtual screening

The main aim of our study is to identify the non-peptide inhibitors against Caspase-3 for the database. For conducting virtual

screening we used Maybridge database containing 50,000 compounds. Best hypothesis (hypo 1) used as a query, to retrieve the novel and potent candidates from the database. Two thousand five hundred compounds were retrieved as hits and these compounds were further screened for drug like properties using Lipinski rule[29] of 5 as a filter. The remaining molecules were overlaid with the 3D-pharmacophore by using the 'Best Fit' option and the top 200 scored hits were analysed for binding patterns using docking studies. Ten compounds having interactions with important amino acids: Arg207, Try 214, and Ser209 of Caspase-3, were selected for synthesis and biological testing to measure the Caspase-3 inhibitory activity. The binding pose of the AW01208 inside the active site of the Caspase-3 was shown in Figure 5b. The compound is having strong hydrogen bond with the active site amino acid Arg207 (backbone CO with amide NH of the compound with 2.013 Å). We have finished the synthesis and screening for the hit 1 (AW01208) shown in Figure 5a and the synthesis and the inhibitory activity of the hit 1 was evaluated as reported in Section 2.5.

3.4. Biological screening

The first graph with concentration on *x*-axis and fluorescence intensity on *y*-axis in Figure 6 shows induction of non-apoptotic control in SKNH cells shown by increase in fluorescence intensity in comparison to the standard inhibitor used. Further increased concentrations from 0.5 μM to 5 μM of Doxorubicin indicates increased slope values (an average value of 5 experiments in duplicates) with individual concentrations thereby indicating increased levels of apoptosis in the SKNH cell lines further evidenced by increase in fluorescence intensity with strong emission at higher concentrations of Doxorubicin (5 μM).

Plot of fluorescence intensity with respect to variable wavelengths shown in Figure 7. The results showed the maximum fluorescence intensity from 420 to 430 nm for Doxorubicin at 1 μM and 5 μM.

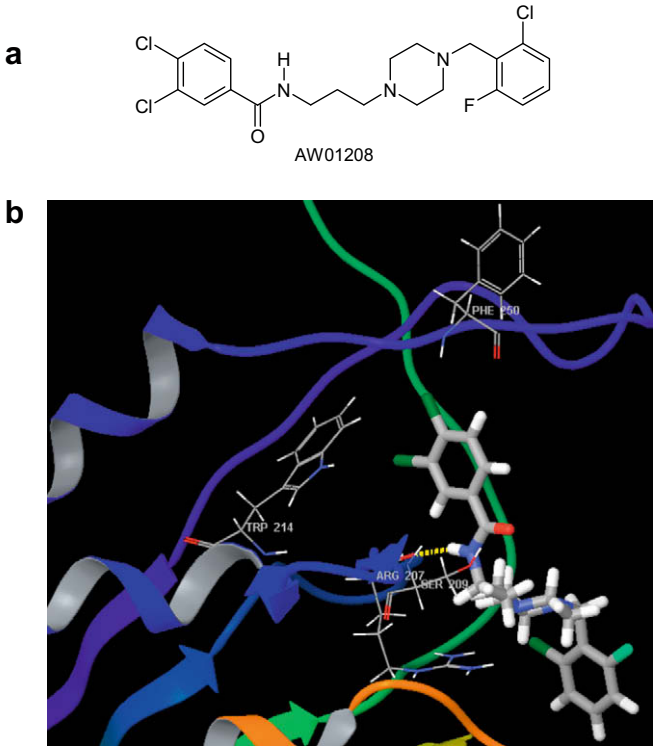

Figure 5. (a) 2D-structure of the virtual screening hit, (b) best docked conformation of the AW01208 in the active site. Broken lines represent hydrogen bonds. Hydrogen bond distances are presented in angstroms (Å).

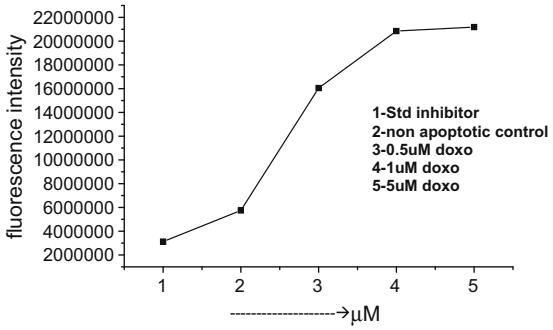

Figure 6. Doxorubicin induced apoptosis in SKNSH cell lines.

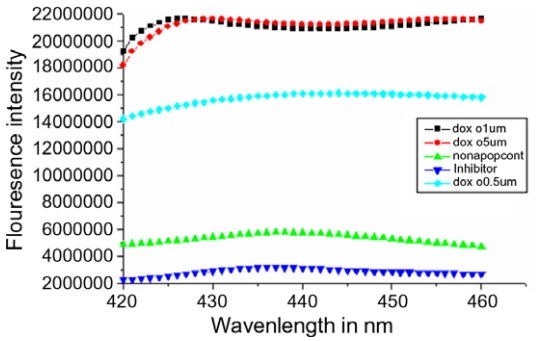

Figure 7. Doxorubicin induced apoptosis in SKNSH cell lines as measured by Caspase-3 activity.

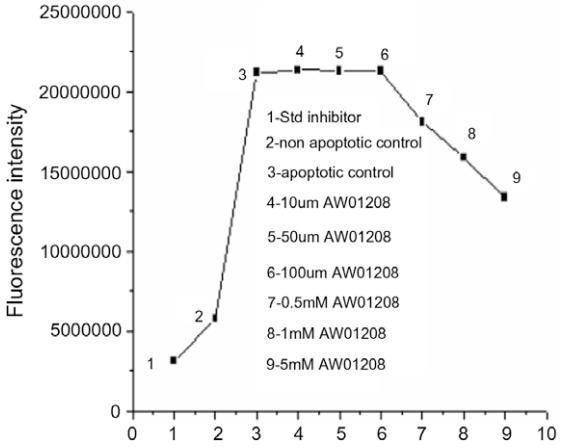

Figure 8. Caspase 3 inhibition by compound AW01208 at various concentrations.

Plot of concentration and fluorescence intensity shown in Figure 8. The various concentrations of the compound AW01208 was taken and fluorescence intensity was studied, the AW01208 showed maximum fluorescence for 10 μM, 50 μM, and 100 μM solutions. The fluorescence was decreasing for increase in concentrations, that is, for 0.5 μM, 1 mM, and 5 mM.

Plot of fluorescence and wavelength shown in Figure 9. The fluorescence of inhibitor compound and standard inhibitor was studied in the range 420–460 nm. The standard inhibitor showed maximum fluorescence at 430–440 nm and the synthesized inhibitor AW01208 of 0.5 μM concentration exhibited maximum fluorescence at 440 nm. The inhibitory effect of Caspase-3 is better

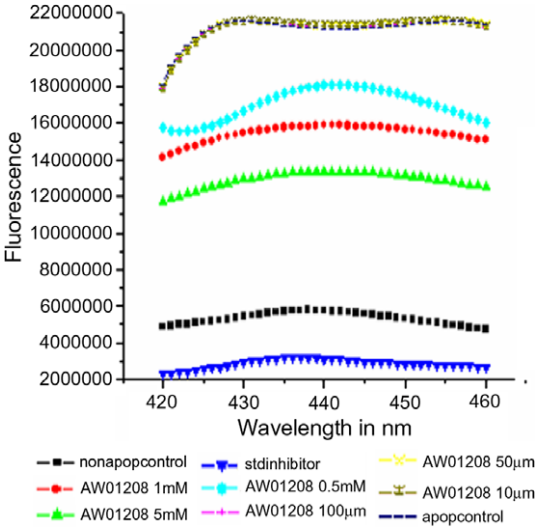

Figure 9. Apoptosis inhibition by AW01208.

evidenced by the decrease in fluorescence intensity when the concentration of the compound is 5 mM which is approximately 50% decrease in intensity with respect to the strong fluorescence emitted by the apoptotic controlled cells but did not show any inhibition at 10 μM. The fluorescence intensity was decreased with increase in concentrations of the lead compound AW01208. It is evident from the graph in Figure 9 that the decrease in fluorescence intensity observed for compound AW01208 at 5 mM concentration and inhibitory effect is approximately 50% when compared to the apoptotic controlled cells. Similar experiments were carried out with Caspase-7 protein and the lead compound AW01208 did not showed much inhibition effect with Caspase-7 protein and hence the experimental results are further not discussed here. From the above biological studies it is evident that the compound AW01208 is a specific inhibitor for Caspase-3 and not for Caspase-7.

The above data obtained shows that the compound AW1208 determined by in silico studies and synthesized in the lab is highly selective. Caspase-3 inhibition was effective then Caspase-7, due to the fact that the receptor sites of Caspase-3 and 7 differ from each other.

4. Conclusion

We have generated ligand based pharmacophore model using 25 diversed compounds. The model consisted of one H-bond acceptor (HBA), one H-bond donor (HBD), and two hydrophobic (HY) features. Further docking studies were performed on the known inhibitors and these results indicated that the amino acids Arg207, Ser209, and Trp214 present in the active site of caspase-3 are important for ligand binding. Using both ligand and structure based models virtual screening was performed against Maybridge database to find the novel non-peptide inhibitors. From this study, we identified compound (AW1208) as a non-peptide inhibitor against Caspase-3.

Supplementary data

Supplementary data associated with this article can be found, in the online version, at doi:10.1016/j.bmc.2009.06.069.

References and notes

1. Jacobson, M. D.; Weil, M.; Raff, M. C. *Cell* **1997**, *88*, 347.
2. Porter, A. G.; Janicke, R. U. *Cell Death Differ.* **1999**, *6*, 99.
3. Nuttall, M. E.; Lee, D.; McLaughlin, B.; Erhardt, J. A. *Drug Discovery Today* **2001**, *6*, 85.
4. Reed, J. C. *Nat. Rev. Drug Disc.* **2002**, *2*, 111.
5. Rodriguez, I.; Matsuura, K.; Ody, C.; Nagata, S.; Vassalli, P. *J. Exp. Med.* **1996**, *184*, 2067.
6. Slee, E. A.; Adrain, C.; Martin, S. J. *J. Biol. Chem* **2000**, *276*, 7320.
7. Denault, J.-B.; Salvesen, G. S. *Chem. Rev.* **2002**, *12*, 4489.
8. Salvesen, G. S.; Dixit, V. M. *Cell* **1997**, *91*, 443–446.
9. Han, B. H.; Xu, D.; Choi, J.; Han, Y.; Xanthoudakis, S.; Roy, S.; Tam, J.; Vaillancourt, J.; Colucci, J.; Siman, R.; Giroux, A.; Robertson, G. S.; Zamboni, R. *J. Biol. Chem.* **2002**, *277*, 30128.
10. Hotchkiss, R. S.; Chang, K. C.; Swanson, P. E.; Tinsley, K. W.; Hui, J. J.; Klender, P.; Xanthoudakis, S.; Roy, S.; Black, C.; Grimm, E.; Aspiotis, R.; Han, Y.; Nicholson, D. W.; Karl, I. E. *Nat. Immunol.* **2000**, *1*, 496–501.
11. Yongxin, H.; Andrem, G.; John, C.; Christopher, I. B.; Daniel, J. M.; Sophie, R.; Steve, X.; John, V.; Dita, M. R.; John, T.; Paul, T.; Donald, W. N.; Robert, J. Z. *Bioorg. Med. Chem. Lett.* **2005**, *15*, 1173.
12. Lee, D.; Long, S. A.; Adams, J. L.; Chan, G.; Vaidya, K. S.; Francis, T. A.; Kikly, K.; Winkler, J. D.; Sung, C. M.; Debouck, C.; Richardson, S.; Levy, M. A.; DeWolf, W. E., Jr.; Keller, P. M.; Tomaszek, T.; Head, M. S.; Ryan, M. D.; Haltiwanger, R. C.; Liang, P. H.; Janson, C. A.; McDevitt, P. J.; Johanson, K.; Concha, N. O.; Chan, W.; Abdel-Meguid, S. S.; Badger, A. M.; Lark, M. W.; Nadeau, D. P.; Suva, L. J.; Gowen, M.; Nuttall, M. E. *J. Biol. Chem.* **2000**, *275*, 16007.
13. Wang, Y.; Guan, L.; Jia, S.; Tseng, B.; Drewe, J.; Cai, S. X. *Bioorg. Med. Chem. Lett.* **2005**, *15*, 1379.
14. Grimm, E. L.; Roy, B.; Aspiotis, R.; Bayly, C. I.; Nicholson, D. W.; Rasper, D. M.; Renaud, J.; Roy, S.; Tam, J.; Tawa, P.; Vaillancourt, J. P.; Xanthoudakis, S.; Zamboni, R. J. *Bioorg. Med. Chem.* **2004**, *12*, 845.
15. Kravchenko, D. V.; Kuzovkova, Y. A.; Kysil, V. M.; Tkachenko, S. E.; Maliarchouk, S.; Okun, I. M.; Balakin, K. V.; Ivachtchenko, A. V. *J. Med. Chem.* **2005**, *48*, 3680.
16. Cerius2 4.11; Accelrys: San Diego, CA, 2005, www.accelrys.com.
17. Stewart, J. J. *J. Comput. Aided Mol. Des.* **1990**, *4*, 1–103.
18. Catalyst 4.11; Accelrys: San Diego, CA, 2005, www.accelrys.com.
19. Smellie, A.; Teig, S. L.; Towbin, P. *J. Comput. Chem.* **1995**, *16*, 171.
20. Smellie, A.; Kahn, S. D.; Teig, S. L. *J. Chem. Inf. Comput. Sci.* **1995**, *35*, 285.
21. Smellie, A.; Kahn, S. D.; Teig, S. L. *J. Chem. Inf. Comput. Sci.* **1995**, *35*, 295.
22. Friesner, R. A.; Banks, J. L.; Murphy, R. B.; Halgren, T. A.; Klicic, J. J.; Mainz, D. T.; Repasky, M. P.; Knoll, E. H.; Shelley, M.; Perry, J. K.; Shaw, D. E.; Francis, P.; Shenkin, P. S. *J. Med. Chem.* **2004**, *47*, 1739.
23. Halgren, T. A.; Murphy, R. B.; Friesner, R. A.; Beard, H. S.; Frye, L. L.; Pollard, W. T.; Banks, J. L. *J. Med. Chem.* **2004**, *47*, 1750.
24. Jorgensen, W. L.; Maxwell, D.; Tirado, R. J. *J. Am. Chem. Soc.* **1996**, *118*, 11225.
25. Maybridge Chemical Company (England); http://www.chem.ac.ru/Chemistry/Databases/MAYBRIDGE.en.html.
26. Michael, J. R.; Stephen, M. H.; Andrej, K.; Robbin, B.; Andrew, T.; Amy, H. N. *J. Med. Chem.* **2001**, *44*, 3175.
27. Chen, Y. H.; Zhang, Y. H.; Zhang, H. J.; Liu, D. Z.; Gu, M.; Li, J. Y.; Wu, F.; Zhu, X. Z.; Li, J.; Nan, F. J. *J. Med. Chem.* **2006**, *49*, 1613.
28. Wenhua, C.; Jun, Z.; Chenbo, Z.; Justin, R.; Zhude, T.; Yunxiang, C.; David, E. R.; Micheal, J. W.; Robert, H. M. *J. Med. Chem.* **2005**, *48*, 7637.
29. Lipinski, C. A. *Adv. Drug Delivery Rev.* **1997**, *23*, 3.

NeuroToxicology xxx (2010) xxx–xxx

Contents lists available at ScienceDirect

NeuroToxicology

Neurotoxic activity of a Topoisomerase-I inhibitor, camptothecin, in cultured cerebellar granule neurons

M. Uday Bhanu [b], Anand K. Kondapi [a,b,*]

[a] Department of Biotechnology, School of Life Sciences, University of Hyderabad, Gachibowli, Hyderabad 500046, AP, India
[b] Department of Biochemistry, School of Life Sciences, University of Hyderabad, Gachibowli, Hyderabad 500046, AP, India

ARTICLE INFO

Article history:
Received 4 March 2010
Accepted 18 June 2010
Available online xxx

Keywords:
Neurotoxic activity
Cerebellar granule neurons (CGNs)
Neurite outgrowth
Topoisomerase-I (Topo-I)
siRNA
Camptothecin (Cpt)

ABSTRACT

DNA Topoisomerase-I (Topo-I) is an enzyme involved in DNA rearrangements, transcription and replication and is a potential target for cancer chemotherapy. Camptothecin is one of the chemotherapeutic agents inhibiting the catalytic activity of Topo-I through the formation of single-strand protein–DNA cross-links. Here, we show that camptothecin is toxic to primary cerebellar granule neurons (CGNs), and camptothecin-induced toxicity is not solely due to the inhibition of Topo-I. An analysis of the effect of camptothecin on CGNs in culture showed that camptothecin inhibits the viability of CGNs. The observed inhibition of cell viability is through the induction of a pro-apoptotic pathway that leads to neuronal degeneration. Furthermore, results show that camptothecin inhibits both protein synthesis and the neuritic outgrowth of CGNs. To determine if the observed neurotoxicity was due to inhibition of Topo-I alone, siRNA-mediated Topo-I-downregulated CGNs were analyzed for cell viability, apoptosis, protein synthesis and neurite outgrowth. The results of these experiments demonstrate that Topo-I downregulation affects only neurite outgrowth and has no significant effect on viability, apoptosis and protein synthesis in granule neurons. In conclusion, camptothecin-induced neurotoxicity may be due to the induction of protein–DNA cross-links and other unknown drug-related interactions rather than the inhibition of Topo-I activity alone.

1. Introduction

DNA Topoisomerases are a class of enzymes involved in the regulation of DNA supercoiling that play a crucial role in DNA transcription, replication and recombination; however, the exact mechanism is not understood. During DNA replication, the two strands of DNA are completely delinked by Topoisomerases, and the translocating RNA polymerase generates supercoiling tension in the DNA that is released during transcription (Wu et al., 1988; Wang, 1998). DNA Topoisomerases resolve the entangled DNA intermediates by transiently cleaving one or two DNA strands and passing the strand through the nick of another intact strand(s). Subsequently, the enzymes rejoin the DNA break and complete one round of the catalytic cycle (Vosberg, 1985; Wang, 1987, 1996; Champoux, 2001). Based on their catalytic mechanism, Topoisomerases have been categorized into four subfamilies: type IA, IB, IIA and IIB.

All higher eukaryotes contain at least one type I Topoisomerase enzyme that plays a major role in supporting fork movement during replication and in facilitating relaxation of transcription-related supercoils. Topo-I is indispensable during processes leading to cell development and cell division (Lee et al., 1993). Inactivation of Topo-I affects the rate of transcription in *Saccharomyces cerevisiae* (Di Mauro et al., 1993). Experiments with yeast Topo-I mutants show that Topo-I is not indispensable for cell growth (Thrash et al., 1985; Uemura and Yanagida, 1984). However, in *Drosophila melanogaster*, Topo-I is essential for development after the blastocyst stage (Lee et al., 1993).

Topo-I is a crucial enzyme for cell growth and embryo development (Morham et al., 1996). Mammalian Topo-I belongs to the type IB subfamily. It plays key roles in DNA replication, transcription, and recombination. The members of the type IB subfamily share no sequence or structural homology with other known Topoisomerases (Caron and Wang, 1994) and are functionally distinct from the members of the type IA subfamily. The activity level of Topo-I is age- and gender-dependent, and this activity increases from birth to maturity and then decreases, more significantly in males, with senescence. This shows a possible role for Topoisomerase-I activity and regulation in various brain functions (Plaschkes et al., 2005).

(S)-(+)-camptothecin (Camptothecin, Cat. No. C9911, Sigma), a specific Topo-I inhibitor, traps covalent intermediates of single-strand protein–DNA cross-links, thereby damaging the genome (Kang et al., 2004). Camptothecin seems to act by stabilizing the

* Corresponding author. Tel.: +91 40 23134571; fax: +91 40 23010145.
E-mail addresses: akondapi@yahoo.com, akksl@uohyd.ernet.in (A.K. Kondapi).

0161-813X/$ – see front matter © 2010 Elsevier Inc. All rights reserved.
doi:10.1016/j.neuro.2010.06.008

Topo-I-DNA covalent intermediate, which significantly slows the reclosure step of the nicking-closing reaction (Hsiang et al., 1985; Porter and Champoux, 1989). Camptothecin is an S-phase-specific anti-cancer agent that inhibits the activity of the Topo-I enzyme. Irreversible DNA double-strand breaks are produced during DNA synthesis in the presence of camptothecin, suggesting that this agent should not be toxic to non-dividing cells, such as neurons. Unexpectedly, camptothecin is found to induce significant, dose-dependent cell death of postmitotic rat cortical neurons in vitro, whereas astrocytes are more resistant (Morris and Geller, 1996). Although many studies link Topo-I to important cellular functions, the precise role of the enzyme in these processes remains obscure.

Granule neurons are the most abundant type of neuron in the brain. The granule neurons are ideal for neurotoxic studies because they exist in high numbers, have a homogeneous population and can be transfected with ease.

In the present study, we have analyzed the neurotoxic activity of the Topo-I inhibitor camptothecin in cultured CGNs and analyzed the role of Topo-I in drug-mediated neurotoxicity compared to siRNA-mediated downregulation of the enzyme.

2. Methods

2.1. Culture and cell viability assay (MTT) of rat cerebellar granule neurons

Postnatal day 6–8 Wistar rat pups were obtained from the University Animal House Facility (University of Hyderabad, India). Primary cultures of rat CGNs were obtained from dissociated cerebellum as described previously (Cambray-Deakin, 1995). The cells were plated in poly-L-lysine-coated 24-well dishes in 0.5 ml of medium per well at a density of ~200,000 cells per well. The growth medium consisted of MEM Eagle's with Earle's BSS, 2 mM glutamine (0.292 g/L), 10% fetal bovine serum (Lifetech), 6 mg/ml glucose, 25 mM KCl, 10 U/ml penicillin, and 10 μg/ml streptomycin-containing DNase-I (0.05%). To eliminate non-neuronal cells, 1 μM arabinosylcytosine (SIGMA, USA), a mitotic inhibitor, was added to the cultures 12 h later. Over 95% of the cells cultured using this method were granule cells and were identified both by their small size (diameter 8–12 μm) and by their rounded body shape with bipolar neurites. All experiments were conducted 1 day after plating when neurons were arborizing (dendrites and axons). At 24 h after plating, the neurons were treated with Topo-I siRNA (0.1 μM–1 μM) using lipofectamine-2000 (Invitrogen, Cat. No. 11668) as transfection agent and with camptothecin (1–100 μM, Sigma, Cat. No. C9911, Sigma); a non-silencing Topo-I siRNA (0.5 μM, scrambled) was used as a control. The effect of varying concentrations of Topo-I siRNA and camptothecin on the viability of the granule neurons in culture after 16 h of treatment was determined by colorimetric quantification of MTT (3-(4,5-dimethylthiazol-2-yl)-2,5-diphenyl tetrazolium bromide, Sigma) with an assay that was described previously (Mosmann, 1983). After the treatment, the cultured CGNs in poly-L-lysine-coated 24-well plates were incubated with 500 μl of 0.5 mg/ml MTT in fresh medium at 37 °C for 4 h. The plates were then centrifuged at 1500 rpm for 20 min at 37 °C, and the medium was carefully removed. Dimethyl sulfoxide (DMSO, 500 μl) was then added to each well to dissolve the formazan crystals. The DMSO-dissolved formazan crystals were read immediately at 540 nm with DMSO as blank on a spectrophotometer.

2.2. siRNA synthesis

We used double-strand siRNA oligos for transient down-regulation of Topo-I in rat CGNs. Lipofectamine 2000 (Invitrogen) was used for transfecting the double-strand siRNA oligos. One day after plating, the cultures were used for transfection, as standardized in our lab (Mandraju et al., 2008). Double-strand siRNA oligos were synthesized as described earlier (Donze and Picard, 2002). For this protocol, desalted DNA oligonucleotides were obtained from Sigma (India). The oligonucleotide-directed production of small RNA transcripts with T7 RNA polymerase has been implemented as described (Milligan and Uhlenbeck, 1989). For each transcription reaction, 1 nM of each oligonucleotide was annealed in 50 μl of TE buffer (10 mM Tris–HCl, pH 8.0, and 1 mM EDTA) by heating at 95 °C; after 2 min, the heating block was switched off and allowed to slowly cool to obtain double-stranded DNA. Transcription was performed in 50 μl of transcription mix: 1 × T7 transcription buffer (40 mM Tris–HCl, pH 7.9; 6 mM $MgCl_2$; 10 mM dithiothreitol (DTT); 10 mM NaCl and 2 mM spermidine), 1 mM nucleotide triphosphates (NTPs), 0.1 U yeast pyrophosphatase (Sigma), 40 U Rnase OUT (Life Technologies) and 100 U T7 RNA polymerase (Invitrogen), which contained 200 pM of the double-stranded DNA (dsDNA) as a template. After incubation at 37 °C for 2 h, 1 U RNase-free DNase (Genetix) was added at 37 °C for 15 min. Sense and antisense 21-nucelotides (nt) RNAs generated in separate reactions were annealed by mixing both crude transcription reactions and heating at 95 °C for 5 min, followed by 1 h at 37 °C to obtain T7 RNA polymerase-synthesized small interfering double-stranded RNA (T7 siRNA). The mixture (100 μl) was then adjusted with 0.2 M sodium acetate, pH 5.2 and precipitated with 2.5 volumes of ethanol. After centrifugation, the pellet was washed once with 70% ethanol, dried and resuspended in 50 μl of water.

2.2.1. siRNA oligos

The following oligos were used to synthesize siRNA: Topo-I sense strand-5′GCGGATTTCCGATTGAATGTT3′, Topo-I anti-sense strand-5′CATTCAAT CGGAAATCCGCTT3′, scrambled sense-5′TTCGCGGATCGATTGAATGTT3′ and scrambled anti-sense-5′CATTCAATCGATCCGCGAATT3′.

2.2.2. siRNA transfection

Cultured granule neuron cells (2×10^6 million) were transfected using lipofectamine-2000 (Invitrogen) with 0.5 μM of non-silencing Topo-I siRNA (scrambled) and silencing Topo-I siRNA separately. For the immunofluorescence studies, the CGNs were co-transfected with the green fluorescent-expressing pEGFP-N2 plasmid along with siRNA. Earlier studies on neuronal transfection of DNA vectors using LIPOFECT-AMINE 2000™ demonstrated that neuronal transfection was approximately 20–25% with the cortical neurons and 25–30% with the hippocampal neurons (Ohki et al., 2001); we could achieve similar transfection efficiency with the pEGFP-N2 plasmid in CGNs in vitro.

2.3. Western blot analysis

Cells were harvested by scraping the cells into a solution (25 mM Tris–HCl pH 7.4, 137 mM NaCl, 3 mM KCl) and centrifuging at 300 × g for 7 min at 4 °C. The cell pellet was homogenized in 0.2 ml homogenization buffer (20 mM Tris–HCl pH 7.5, 0.1 mM β-mercaptoethanol, 1 mM $MgCl_2$, 0.1 mM EDTA, 5% glycerol, 0.1% triton X-100, 0.5 mM KCl, 0.5 mM PMSF and 1 μg/μl pepstatin and leupeptin) for 10 min on ice followed by sonication for 15–20 s. The protein concentrations in the cell lysates were measured by the Bradford method (Bradford, 1976). Twenty micrograms of total protein/lane were separated on 10% sodium dodecyl sulfate (SDS) gels and then transferred to nitrocellulose membranes (Towbin et al., 1979). The membranes were blocked with 5% non-fat dry milk in TBS-containing 0.05% Tween 20 for 1 h and then incubated overnight at 4 °C with corresponding protein-specific antibodies at an 1:1000 dilution (anti-Topo-I monoclonal antibodies (Mab), Sigma; and anti β-actin polyclonal antibodies (Pab), BD biosciences). Subsequently, the blots were washed and incubated with

Please cite this article in press as: Uday Bhanu M, Kondapi AK. Neurotoxic activity of a Topoisomerase-I inhibitor, camptothecin, in cultured cerebellar granule neurons. Neurotoxicology (2010), doi:10.1016/j.neuro.2010.06.008

secondary anti-mouse IgG and anti-rabbit IgG alkaline phosphatase (ALP, Upstate) conjugated antibodies (1:2000 dilution), respectively. The blots were developed using a NBT (nitro-blue tetrazolium chloride) – BCIP (5-bromo-4-chloro-3′-indolyphosphate *p*-toluidine salt) substrate in freshly prepared alkaline phosphatase buffer (100 mM Tris-pH 9.5, 5 mM $MgCl_2$, 100 mM NaCl). Western blots were quantified using the NIH IMAGE program. All studies were performed a minimum of three times using independent cultures.

2.4. Reverse transcription PCR (RT-PCR)

Total RNA was extracted from 0.5 μM Topo-I siRNA-transfected or 10 μM camptothecin-treated granule neurons using TRI-REAGENT (Sigma, USA). Aliquots of 5 μg were then subjected to reverse transcription using an oligo deoxy-thymidine (dT) primer and an Enhanced Avian First Strand Synthesis Kit (eAMV-RT, SIGMA). Equal aliquots were then used for PCR with primers for rat β-actin and Topo-I. Cycling conditions were optimized for each primer, and PCR products were run on a 1.2% agarose gel stained with ethidium bromide. Gels were digitally photographed, and densitometric analysis was performed using Image J software (NIH, USA), a java-based image analysis program (NIH, USA) available on the internet. Values were expressed as ratios with respect to β-actin.

The following primers were used for PCR: Topo-I FP-5′CTCTA GTCCACCACGAATTAAAGAC3′, RP-5′TACTTCTTCTGCTT TGGGACT-CAG 3′, β-actin FP-5′CTGACAGGATGCAGAAGGAG3′ and RP-5′GATAGAGCCACCAATCC ACA3′.

2.5. Annexin-V assay by flow cytometer

Annexin-V staining of apoptotic cells was used to compare whether downregulation of Topo-I with siRNA or treatment with camptothecin induces cell death. Sixteen hours after transfection with the appropriate siRNA constructs and camptothecin concentrations, apoptosis was measured in terms of Annexin-V staining (Vybrant Apoptosis Assay Kit#3, Invitrogen, USA) followed by fluorescence activated cell sorter (FACS) analysis (BD biosciences). For the cytotoxicity assay, 2×10^6 freshly trypsinized 0.5 μM Topo-I siRNA-transfected or 10 μM camptothecin-treated granule neurons were used. The collected target cells were then washed in PBS, resuspended in 1× Annexin binding buffer and stained with Annexin-V-FITC for 5 min at room temperature in the dark. The staining solution was removed, and the cells were resuspended in cold PBS on ice for FACS. Quantification of cytotoxicity was determined by the percentage of apoptotic target cells scored by FACS analysis.

2.6. Caspase-3 assay

Caspase-3 activity was measured through cleavage of a colorless substrate specific for caspase-3 (Ac-DEVD-AMC), which releases the chromophore 7-amino-4-methylcoumarin (AMC). Assays were carried out according to the manufacturer's instructions (Caspase-3 assay kit, BD Pharmingen, San Jose, CA, USA). To evaluate the activity of caspase-3, cell lysates were prepared in lysis buffer after their respective treatment with 10 μM camptothecin and Topo-I siRNA. Assays were performed by incubating 50 μg of protein from the cell lysate per sample in 1 ml of protease assay buffer (40 mM HEPES (pH 7.5), 20% glycerol, 4 mM DTT) that contained 10 μl of 1 μg/μl caspase-3 substrate (Ac-DEVD-AMC, 2 mM). Lysates were incubated at 37 °C for 1 h. Samples were measured for the AMC that was liberated from Ac-DEVD-AMC using a spectrofluorometer with an excitation wavelength of 380 nm and an emission wavelength range of 420–460 nm.

2.7. S^{35}-methionine in vitro labeling

S^{35}-methionine is a commonly used isotope for radio labeling of proteins. Topo-I siRNA-transfected CGNs or camptothecin-treated CGNs (2×10^6 cells) were incubated for 16 h with 10 μCi S^{35}-methionine in methionine-free DMEM medium (Gibco) for 4 h in a 5% CO_2 incubator; afterwards, the cells were suspended in a protein lysis buffer (20 mM Tris–HCl (pH 7.5), 0.1 mM β-mercaptoethanol, 1 mM $MgCl_2$, 0.1 mM EDTA, 5% glycerol, 0.1% triton X-100, 0.5 mM KCl, 0.5 mM PMSF and 1 μg/μl pepstatin and leupeptin), and 100 μg of total protein extract was subjected to 10% polyacrylamide gel electrophoresis (PAGE) and stained with Coomassie. The dried gels were exposed to X-ray film for 4 days and developed. The protein equivalent of S^{35}-methionine incorporation into proteins was measured using 25 μg of treated cell extracts, aliquoted on a filter and dried, followed by counting in a toluene-containing scintillation liquid using a LKB Beta counter. The data are represented as counts per minute (cpm).

2.8. Immunofluorescence

CGNs were dissociated and cultured, as described above, in 6-well plates containing poly-L-lysine-coated cover slips at a density of 2×10^6 cells/well. After 24 h in culture, the cells were co-transfected with siRNA and a pEGFP-N2 plasmid (a gift from Prof. N. Siva Kumar, University of Hyderabad, India) using lipofectamine 2000, or treated with 10 μM camptothecin separately, as required. After a 16 h treatment, the neurons were fixed with a 4% paraformaldehyde mixture that contained 0.025% triton X-100 for 15 min at room temperature, blocked with PBS-containing 5% bovine serum and incubated with monoclonal anti-Topo-I (1:100 dilution, Sigma, USA) and polyclonal anti-neurofilament (NF, 1:100 dilution). Subsequently, the cells were washed 3–4 times with PBS and incubated with fluorescent-tagged anti-mouse IgG-Cy3 and anti-rabbit IgG-Cy5 (Chem Bio) at 1:250 dilutions. These cultures on cover slips were mounted onto a glass slide and viewed under a Leica Fluorescence Confocal Microscope (Leach Instruments, Heidelberg, Germany). The excitation/emission wavelengths used were 400 nm/510 nm for GFP (green), 548 nm/562 nm for Cy3 (blue) and 650/700 for Cy5 (red).

2.9. Morphometric analysis

To evaluate neurite length, cells were co-transfected with 0.5 μM Topo-I siRNA and a pEGFP-N2 plasmid and were cultured for 16 h. In a separate dish, cells were treated with 10 μM camptothecin for 16 h. After 16 h, cells were fixed and immunolabeled with anti-Topo-I and anti-NF antibodies, as described in Section 2.8. Based on the GFP (green) and NF (red) positive cells, individual processes were traced manually and measured with Image J software. The total neurite length per neuron was determined and measured as the sum of the lengths of all the neurites of the neurons in culture. The average total neurite length was determined from a sample of at least 50 neurons per group from two independent experiments. The neurite lengths were compared for the Topo-I siRNA and control cells. Values are expressed as the mean ± standard error. Statistical differences were evaluated with an independent parametric *t*-test.

2.10. Data analysis

All experiments were repeated three times individually, unless otherwise specified. Differences between groups were assessed with an One Way Analysis of Variance (ANOVA) followed by a Student–Newman–Keuls test using Sigma Plot 11.0 for Windows, and *p*-value less than 0.05 ($p < 0.05$) were considered statistically significant. Data are expressed as the mean ± standard deviation.

Please cite this article in press as: Uday Bhanu M, Kondapi AK. Neurotoxic activity of a Topoisomerase-I inhibitor, camptothecin, in cultured cerebellar granule neurons. Neurotoxicology (2010), doi:10.1016/j.neuro.2010.06.008

3. Results

3.1. siRNA-mediated transient downregulation of Topoisomerase-I

CGNs transfected with Topo-I siRNA and camptothecin for 16 h were analyzed to determine protein and mRNA levels with immunoblotting and semi-quantitative RT-PCR, respectively, using Topo-I-specific monoclonal antibodies and PCR primers, as described above (Section 2). The immunoblotting analysis and RT-PCR studies show a nearly 80% decrease in Topo-I in 0.5 μM Topo-I siRNA-transfected CGNs. Camptothecin (10 μM) showed no marked effect on the Topo-I mRNA and protein levels (Fig. 1). Fluorescence confocal images (Fig. 6) confirm the efficient down-regulation of Topo-I with siRNA, whereas no significant change was observed in control and camptothecin-treated CGNs.

3.2. Effect of Topo-I siRNA and camptothecin on the viability of CGNs

The effect of Topo-I siRNA and camptothecin on the viability of CGNs in culture was tested using a MTT assay, as described in Section 2. Increasing concentrations of camptothecin and Topo-I-siRNA were used to test the viability of CGNs (Fig. 2). Camptothecin showed cytotoxicity starting at 1 μM and decreased the viability of the CGNs by more than 50% at 10 μM. Topo-I siRNA showed only a 20% decrease in the viability of the CGNs at 0.5 μM, which is a concentration corresponding to more than 80% downregulation of Topo-I (Fig. 1), and there was no change in viability at higher siRNA concentrations. These results show that siRNA-mediated down-regulation of Topo-I was achieved under these conditions.

3.3. Comparison of apoptosis in Topo-I siRNA-transfected and camptothecin-treated CGNs

Camptothecin is known to induce caspase-3-dependent death of cortical neurons (Stefanis et al., 1999; Keramaris et al., 2000), which plays a central role in the execution-phase of cellular apoptosis. As a measure of apoptosis, caspase-3 activity was assessed by the extent

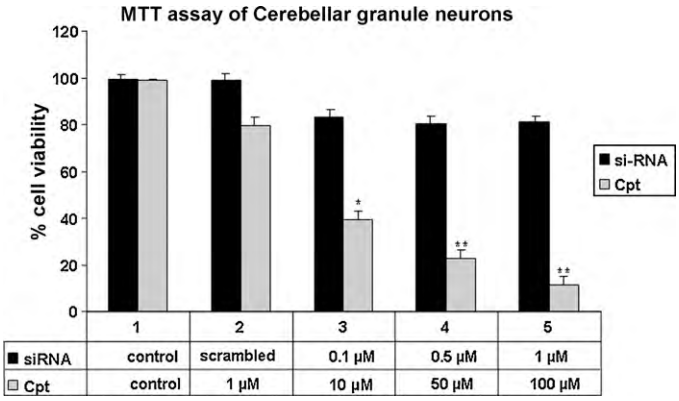

Fig. 2. MTT assay for viability of CGNs. A colorimetric-based MTT assay was performed to examine the survival of CGNs under siRNA transfection or camptothecin treatments using 1-day-old CGNs in culture. The data are represented in terms of % cell viability of CGNs at the indicated concentrations of siRNA or camptothecin. The bar graph clearly shows a decrease in CGN viability with increasing camptothecin concentrations, whereas there was no significant change with increasing concentrations of Topo-I siRNA. Data are presented as the mean ± SD in three independent experiments; $^{*}p < 0.05$ and $^{**}p < 0.01$ as compared to the normal control.

of the cleavage of the fluorogenic substrate Ac-DEVD-AMC by neuronal lysates prepared after transfection with Topo-I siRNA and camptothecin treatments. As shown in Fig. 3, there is elevation in caspase-3 activity in camptothecin-treated cell extracts, while Topo-I siRNA-transfected extracts did not show any marked increase. We used FACS analysis of Annexin-V as an additional measure of apoptosis because one of the earliest indications of apoptosis is the translocation of the membrane phospholipid phosphatidylserine (PS) from the inner to the outer leaflet of the plasma membrane to which Annexin-V binds (Vermes et al., 1995).

FACS analysis of the FITC-labeled apoptotic cell population showed a marked increase of about 20% in 10 μM camptothecin, whereas 0.5 μM Topo-I siRNA-transfected CGNs did not show any

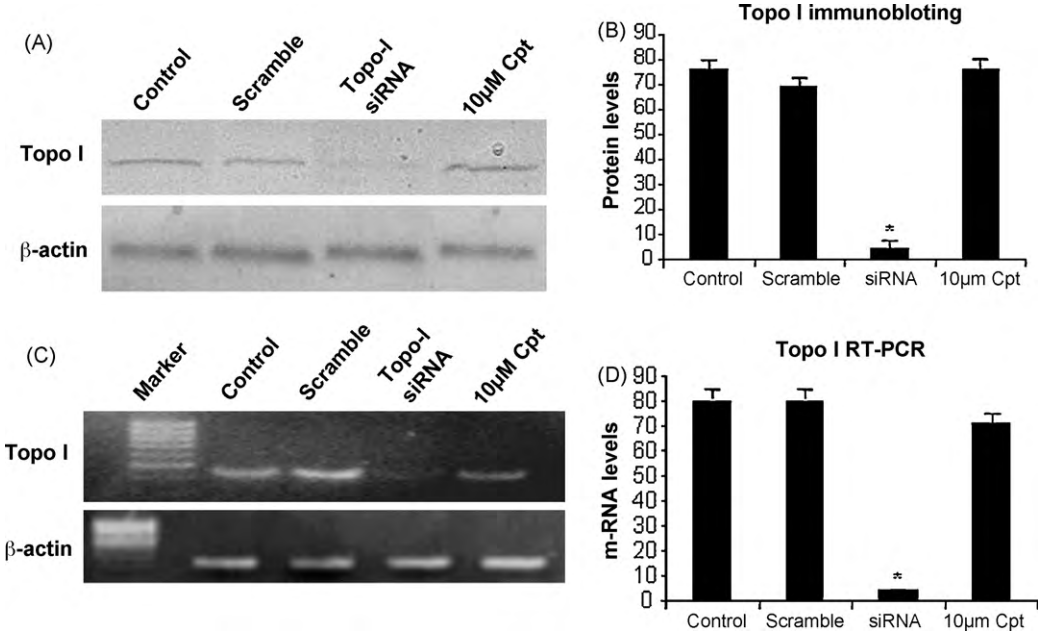

Fig. 1. Protein and mRNA levels of Topo-I in siRNA-transfected and camptothecin-treated CGNs. Following 16 h of siRNA transfection or camptothecin (Cpt, 10 μM) treatment, cultured CGNs were used for protein and RNA isolation and were subjected to immunoblotting and semi-quantitative RT-PCR. Panel A shows the immunoblot of a ~100 kD Topo-I protein with a 43 kD β-actin as an endogenous control; Panel B represents the corresponding densitometric graph. Panel C shows the amplification of Topo-I and β-actin m-RNA by PCR followed by separation on a 1% agarose gel with the corresponding densitometric data in Panel D. The results clearly show a significant decrease in Topo-I protein and mRNA levels (~80%), which suggests there was efficient downregulation of Topo-I using siRNA, while camptothecin induced no significant decrease in these levels. Data are presented as the mean ± SD in three independent experiments; $^{*}p < 0.05$.

Please cite this article in press as: Uday Bhanu M, Kondapi AK. Neurotoxic activity of a Topoisomerase-I inhibitor, camptothecin, in cultured cerebellar granule neurons. Neurotoxicology (2010), doi:10.1016/j.neuro.2010.06.008

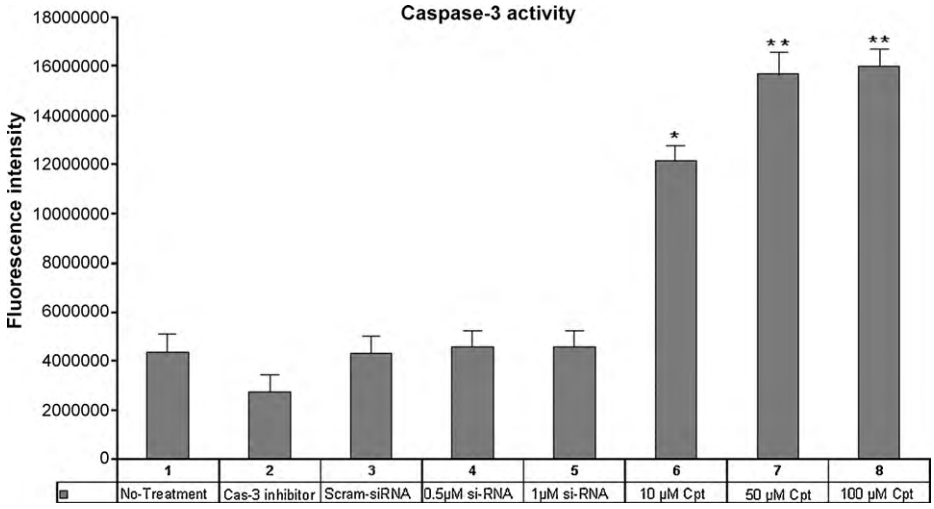

Fig. 3. Caspase-3 activity in CGN extracts. Caspase-3 activity was measured using a fluorogenic (Ac-DEVD-AMC) substrate in the extracts of siRNA-transfected or camptothecin-treated CGNs. The data are presented in terms of caspase-3 activity in different siRNA-transfected or camptothecin-treated CGN extracts. The bar graph clearly shows elevation of caspase-3 activity with increasing concentrations of camptothecin, while Topo-I siRNA showed no significant elevation of caspase-3 activity. Data are represented as the mean ± SD in three independent experiments; $^{*}p < 0.05$ and $^{**}p < 0.01$ as compared to the normal control.

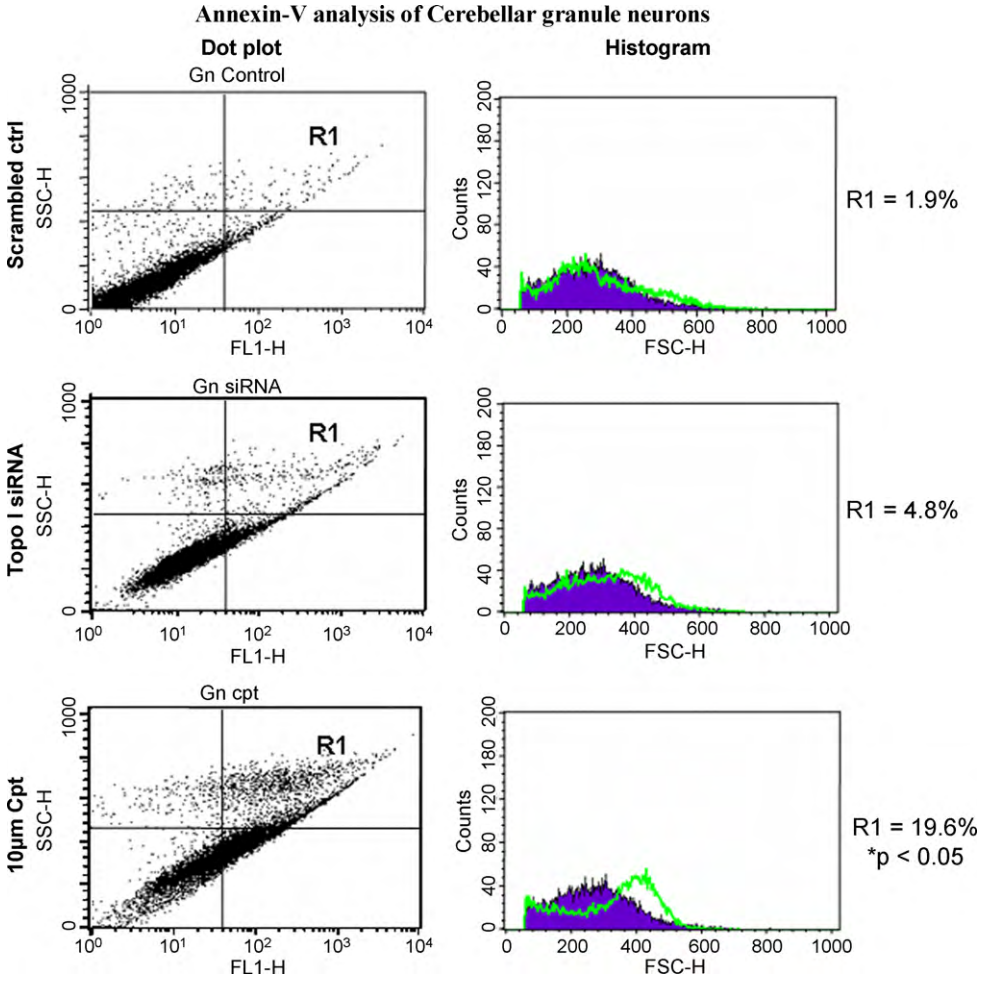

Fig. 4. Flow cytometric analysis of FITC Annexin-V staining. Cultured CGNs were subjected to 16 h of transfection with 0.5 μM silencing and non-silencing (scrambled) Topo-I siRNA or treatment with 10 μM camptothecin. CGNs were then incubated with FITC Annexin-V (Vybrant Apoptosis Assay Kit#3, Invitrogen, USA) and were analyzed for Annexin-V positive cells using a flow cytometer (BD biosciences). Data are presented in the contour diagram of Annexin-V-labeled cells. The upper right quadrant in the dot plot shows a significant increase (~20%) in Annexin-V positive cells in camptothecin-treated CGNs, while Topo-I siRNA-transfected CGNs only showed a small increase (~5%) in annexin-V positive cells. Data are the mean ± SD in three independent experiments; $^{*}p < 0.05$ as compared to the control.

Please cite this article in press as: Uday Bhanu M, Kondapi AK. Neurotoxic activity of a Topoisomerase-I inhibitor, camptothecin, in cultured cerebellar granule neurons. Neurotoxicology (2010), doi:10.1016/j.neuro.2010.06.008

significant increase (~5%) in Annexin-V positive cells (FITC) (Fig. 4). This result further confirms that it is camptothecin, not Topo-I siRNA, that induces a high degree of apoptosis in CGNs. These results suggest that the increase in apoptosis is not due to the cells devoid of Topo-I, but rather the induction of pro-apoptotic factors by the protein–DNA–camptothecin cross-link-mediated signaling or the single-stranded DNA break intermediates.

3.4. Comparison of overall protein expression in Topo-I siRNA-transfected and camptothecin-treated CGNs

The effect of Topo-I downregulation on overall protein expression in siRNA- and camptothecin-treated granule neurons was studied using the in vitro S^{35}-methionine incorporation assay described in Section 2. The autoradiogram (Fig. 5B) and S^{35} radiolabel counts (Fig. 5C) show decreased S^{35}-methionine incorporation in the protein extracts of camptothecin but not in Topo-I siRNA-transfected samples. This result suggests that Topo-I has no significant role in regulation of protein expression. This effect induced by camptothecin may be due to factors such as DNA strand breaks that may be involved in induction of apoptosis, proteolysis and DNA fragmentation.

3.5. Neurite outgrowth in Topo-I siRNA-transfected and camptothecin-treated CGNs

The degree of maturation of neurite growth was examined (arborization status of neurons) and traced based on the pEGFP-N2 (GFP-green) and anti-neurofilament (NF-red) positive cells in Topo-I siRNA-transfected CGNs and NF (red) positive cells in

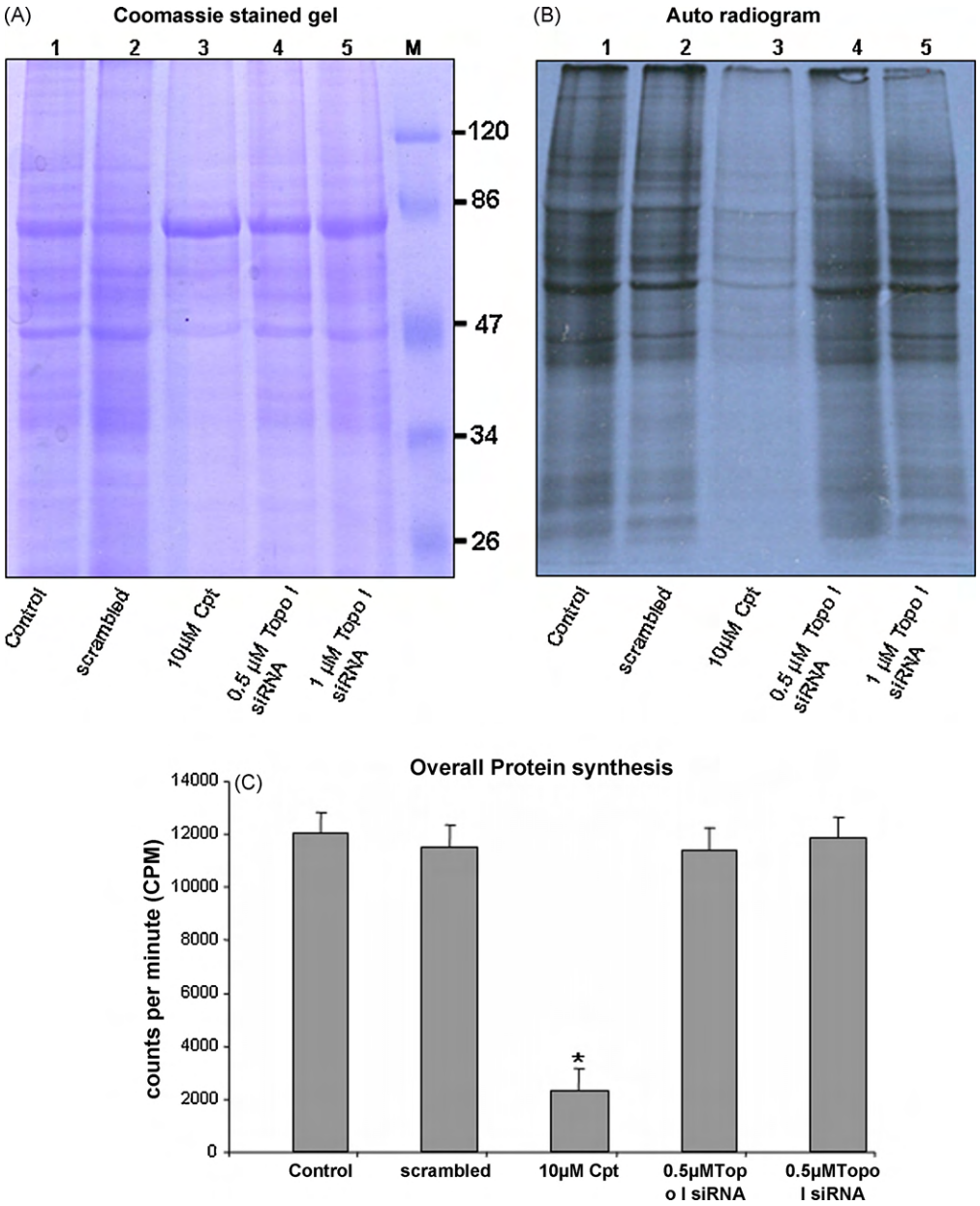

Fig. 5. S^{35}-methionine incorporation. Protein synthesis in siRNA- or camptothecin-treated CGNs was assayed by incorporation of radiolabeled S^{35}-methionine. Panel A represents Coomassie-stained 100 μg total protein extracts separated on 10% SDS PAGE, as detailed. Panel B represents the autoradiogram of the corresponding Coomassie gel. Panel C represents the bar graph of the S^{35}-methionine incorporation that was measured using a liquid scintillation counter; 25 μg of siRNA- and camptothecin-treated CGN cell extracts were assayed for S^{35}-methionine incorporation using a toluene-based liquid scintillation counter as radiation counts per minute (CPM). The data clearly show a significant decrease in S^{35}-methionine incorporation into 10 μM camptothecin-treated CGNs, whereas Topo-I siRNA showed no significant change in comparison with control cells. Data are presented as the mean ± SD in three independent experiments; $^{*}p < 0.05$ as compared to the normal control.

Please cite this article in press as: Uday Bhanu M, Kondapi AK. Neurotoxic activity of a Topoisomerase-I inhibitor, camptothecin, in cultured cerebellar granule neurons. Neurotoxicology (2010), doi:10.1016/j.neuro.2010.06.008

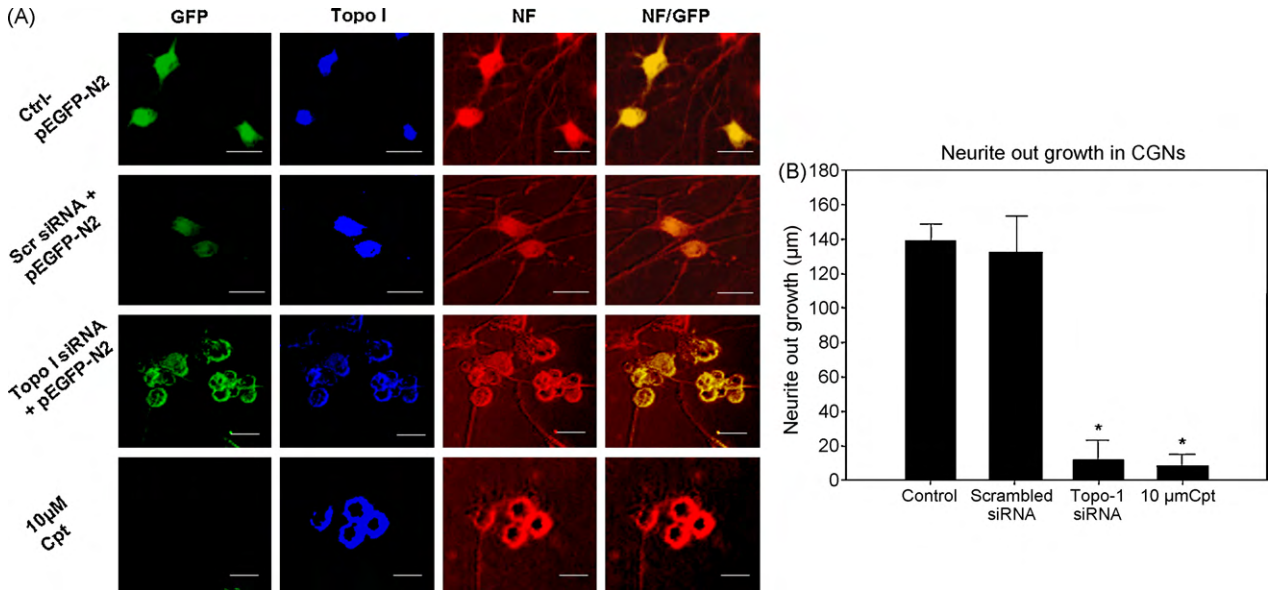

Fig. 6. Morphometric analysis of CGNs. Figure represents fluorescent confocal images of pEGFP-N2 (GFP-green), Topo-I (Cy3-blue) and neurofilament (NF) (Cy5-red) staining in treated CGNs as indicated. Individual neuritic processes were traced manually and measured with Image J, a java-based image analysis program (NIH, USA); GFP-green and anti-neurofilament (NF-red) positive cells were traced in Topo-I siRNA + pEGFP-N2-transfected CGNs, and NF (red) positive cells were traced in camptothecin-treated cultures. Panel A represents the confocal images, and Panel B represents the bar graph of the average total neurite length, which was determined from a sample of at least 50 neurons per dish from two independent experiments. The results clearly demonstrate a significant change in neuronal arborization in Topo-I siRNA-transfected CGNs. Data are presented as the mean ± SD; $^{*}p < 0.05$ as compared to control. Scale bar-15 μm (For interpretation of the references to colour in this figure legend, the reader is referred to the web version of this article.).

camptothecin-treated cultures, as described above. The results show that 0.5 μM Topo-I siRNA + pEGFP-N2 transfected CGNs failed to arborize normally when compared to control and scrambled siRNA-treated cells. Camptothecin-treated (10 μM) granule neurons showed enhanced aggregation followed by clumping and altered morphological features of apoptosis without any extended processes (Fig. 6A). Further analysis of the length of the neurite using Image J software showed a significant decrease in neurite outgrowth (Fig. 6B) in both siRNA-downregulated cells and camptothecin-treated cells. The observed effect in the presence of camptothecin could be due to the clumping of cells (Fig. 6A) or to the death of cells due to apoptosis. In the case of siRNA-downregulated cells, the observed effect on neurite outgrowth could be due to a deficiency in Topo-I enzymatic activity, which implicates the role of Topo-I in neurite outgrowth; however, the exact mechanism needs to be elucidated.

4. Discussion

The present study shows that Topo-I downregulation alone does not induce any apoptotic factors; however, camptothecin, a Topo-I specific inhibitor, promotes the formation of Topo-I DNA cleavage complexes, which may induce apoptosis in cells. The viability of CGNs in 0.5 μM Topo-I siRNA-transfected neurons showed only a ~20% decrease, whereas camptothecin showed more than a 50% decrease in viability at 10 μM. The observed marginal decrease in ~20% of Topo-I siRNA-treated granule neurons was not associated with elevated levels of caspase 3 and Annexin-V positive cells. However, camptothecin-treated neurons had elevated levels of pro-apoptotic markers. This result suggests that camptothecin induces apoptotic death, whereas the downregulation of Topo-I marginally decreases neuronal survival (<20%) in a non-apoptotic pathway. Our results thus demonstrate that camptothecin is neurotoxic, affecting neuronal survival through induction of a pro-apoptotic pathway, whereas transient downregulation of Topo-I with siRNA showed no significant effect on cell viability and activation of pro-apoptotic markers.

Neuronal development includes the birth and differentiation of neurons from stem cell precursors. High rates of transcription and protein synthesis are required for neuronal development, differentiation and information processing. Neurons are metabolically very active and hence carry out a high level of protein synthesis. We have used the incorporation of radiolabeled S^{35}-methionine to assess the effect of camptothecin and Topo-I siRNA on overall protein synthesis. Topo-I siRNA-transfected CGNs showed no significant effect on total protein synthesis compared to camptothecin-treated neurons. However, the decrease in protein synthesis in camptothecin-treated cerebellar granule neurons might be attributed to its apoptotic induction and DNA damage (data not shown here). This result establishes that Topo-I itself has no significant role in DNA transcription and translation.

Directional neurite extension from the soma depends on precise cytoskeletal and adhesion dynamics that are induced by sensing attractive and extracellular cues, such as chemokines and extracellular matrix proteins (ECMs) (Dityatev and Schachner, 2003; Kleene and Schachner, 2004). Although a large amount of information is available on the extracellular mechanisms, the intracellular mechanisms have only recently been addressed. The camptothecin and Topo-I siRNA-transfected CGNs failed to extend their neuritic processes; this result suggests a role for Topo-I in neuritogenesis. There is a significant effect on the arborization status of neurons related to neuritic growth in Topo-I siRNA-transfected and camptothecin-treated granule neurons. This effect of camptothecin on neuritic growth can be attributed to neurotoxicity and protein depletion, whereas the Topo-I siRNA-mediated downregulation suggests a significant role for Topo-I in processes related to neuritic growth and development, including controlling the genes involved at the transcriptional level. Present observation is similar to that of Topoisomerase-II, which shows no effect on expression of housekeeping genes but has a role in neuronal development and maturation (neuritic growth and cone formation) (Tsutsui et al., 2001; Nur-E-Kamala et al., 2007).

Please cite this article in press as: Uday Bhanu M, Kondapi AK. Neurotoxic activity of a Topoisomerase-I inhibitor, camptothecin, in cultured cerebellar granule neurons. Neurotoxicology (2010), doi:10.1016/j.neuro.2010.06.008

5. Conclusions

Camptothecin exhibits neurotoxicity due to induction of apoptotic cell death of cultured CGNs. Because the siRNA-mediated downregulation of Topo-I did not exhibit any toxicity and apoptosis, the observed neurotoxicity of camptothecin implicates the role of the DNA single-strand break intermediates formed in the presence of camptothecin. Further, siRNA-mediated down-regulation of Topo-I implicates a role for Topo-I in neuritic outgrowth and development without involving itself in active protein synthesis and neuronal survival.

Conflict of interest statement

The authors declare that there are no conflicts of interest.

Acknowledgments

This research work is funded under the Department of Science and Technology, Government of India sponsored research project. MUB is a UGC-CSIR SRF. Infrastructure developed under Universities Grants Commission Centre for Advance Studies, was used for the work.

Appendix A. Supplementary data

Supplementary data associated with this article can be found, in the online version, at doi:10.1016/j.neuro.2010.06.008.

References

Bradford MM. A rapid and sensitive method for quantitation of microgram quantities of protein utilizing the principle of protein-dye-binding. Anal Biochem 1976;72:248–54.
Cambray-Deakin MA. Cerebellar granule cells. In: Cohen J, Wilkin GP, editors. Neural cell culture a practical approach. OIRL Press; 19953–14.
Caron PR, Wang JC. Alignment of primary sequences of DNA topoisomerases. Adv Pharmacol 1994;29:271–97.
Champoux JJ. DNA topoisomerases: structure, function, and mechanism. Annu Rev Biochem 2001;70:369–413.
Di Mauro E, Camilloni G, Verdone L, Caserta M. DNA Topoisomerase I controls the kinetics of promoter activation and DNA topology in Saccharomyces cerevisiae. Mol Cell Biol 1993;13:6702–10.
Dityatev A, Schachner M. Extracellular matrix molecules and synaptic plasticity. Nat Rev Neurosci 2003;4:456–68.
Donze O, Picard D. RNA interference in mammalian cells using siRNAs synthesized with T7 RNA polymerase. Nucl Acids Res 2002;30: pp. 46.
Hsiang YH, Hertzberg R, Hecht S, Liu LF. Camptothecin induces protein-linked DNA breaks via mammalian DNA Topoisomerase-I. J Biol Chem 1985;260:14873–8.
Kang MR, Muller MT, Chung IK. Telomeric DNA damage by topoisomerase I. A possible mechanism for cell killing by camptothecin. J Biol Chem 2004;279:12535–41.
Keramaris E, Stefanis L, MacLaurin J, Harada N, Takaku K, Ishikawa T, et al. Involvement of caspase 3 in apoptotic death of cortical neurons evoked by DNA damage. Mol Cell Neurosci (4):2000;368–79.
Kleene R, Schachner M. Glycans and neural cell interactions. Nat Rev Neurosci 2004;5:195–208.
Lee MP, Brown SD, Chen A, Hsieh TS. DNA Topoisomerase I is essential in Drosophila melanogaster. Proc Natl Acad Sci U S A 1993;90:6656–60.
Mandraju RK, Kannapiran P, Kondapi AK. Distinct roles of Topoisomerase II isoforms: DNA damage accelerating α, double strand break repair promoting β. Arch Biochem Biophys 2008;470:27–34.
Milligan JF, Uhlenbeck OC. Synthesis of small RNAs using T7 RNA polymerase. Methods Enzymol 1989;180:51–62.
Morham SG, Kluckman KD, Voulomanos N, Smithies O. Targeted disruption of the mouse topoisomerase I gene by camptothecin selection. Mol Cell Biol 1996;16:6804–9.
Morris EJ, Geller HM. Induction of neuronal apoptosis by camptothecin, an inhibitor of DNA topoisomerase-I: evidence for cell cycle independent toxicity. J Cell Biol 1996;134:757–70.
Mosmann T. Rapid colorimetric assay for cellular growth and survival: application to proliferation and cytotoxicity assays. J Immunol Methods 1983;65:55–63.
Nur-E-Kamala A, Meinersb S, Ahmedb I, Azarovab A, Chao-po Linb. et al. Role of DNA topoisomerase IIβ in neurite outgrowth. Brain Res 2007;1154:50–60.
Ohki EC, Tilkinsa ML, Ciccaroneb VC, Pricea PJ. Improving the transfection efficiency of post-mitotic neurons. J Neurosci Methods 2001;112:95–9.
Plaschkes I, Silverman FW, Priel E. DNA topoisomerase I in the mouse central nervous system: age and sex dependence. J Comp Neurol 2005;493:357–69.
Porter SE, Champoux JJ. The basis for camptothecin enhancement of DNA breakage by eukaryotic topoisomerase I. Nucleic Acids Res 1989;17:8521–32.
Stefanis L, Park DS, Wilma J, Lloyd A, et al. Caspase-dependent and -independent death of camptothecin-treated embryonic cortical neurons. J Neurosci 1999;19(15):6235–47.
Thrash C, Bankier AT, Barrell BG, Sternglanz R. Cloning, characterization, and sequence of the yeast DNA topoisomerase gene. Proc Natl Acad Sci U S A 1985;82:4374–8.
Towbin H, Staehelin T, Gordon JA. Electrophoretic transfer of proteins from polyacrylamide gels to nitrocellulose sheets. Proced Some Appl 1979;76:4350–4.
Tsutsui K, Tsutsui K, Sano K, Kikuchi A, Tokunaga A. Involvement of DNA Topoisomerase IIβ in neuronal differentiation. J Biol Chem 2001;276:5769–78.
Uemura T, Yanagida M. Isolation of type I and II DNA Topoisomerase mutants from fission yeast: single and double mutants show different phenotypes in cell growth and chromatin organization. EMBO J 1984;3:1737–44.
Vosberg HP. DNA topoisomerases: enzymes that control DNA conformation. Curr Top Microbiol Immunol 1985;114:19–102.
Vermes I, Haanen C, Steffens-Nakken H, Reutellingsperger C. A novel assay for apoptosis Flow cytometric detection of phosphatidylserine expression on early apoptotic cells using fluorescein labelled Annexin V. J Immunol Methods 1995;184:39–51.
Wang JC. Moving one DNA double helix through another by a type II DNA topoisomerase: the story of a simple molecular machine. Q Rev Biophys 1998;31:107–44.
Wang JC. DNA topoisomerases. Annu Rev Biochem 1996;65:635–92.
Wang JC. Recent studies of DNA topoisomerases. Biochim Biophys Acta 1987;909:1–9.
Wu HY, Shyy SH, Wang JC, Liu LF. Transcription generates positively and negatively supercoiled domains in the template. Cell 1988;53:433–40.

Please cite this article in press as: Uday Bhanu M, Kondapi AK. Neurotoxic activity of a Topoisomerase-I inhibitor, camptothecin, in cultured cerebellar granule neurons. Neurotoxicology (2010), doi:10.1016/j.neuro.2010.06.008